



THE UNIVERSITY *of* EDINBURGH

## Edinburgh Research Explorer

# Testing alternative tectonic models for the Permian-Pleistocene tectonic development of the Kyrenia Range, N Cyprus: Implications for E Mediterranean Tethyan palaeogeography

### Citation for published version:

Robertson, AHF, Parlak, O & Taslı, K 2024, 'Testing alternative tectonic models for the Permian-Pleistocene tectonic development of the Kyrenia Range, N Cyprus: Implications for E Mediterranean Tethyan palaeogeography', *Gondwana Research*, vol. 132, pp. 343-379. <https://doi.org/10.1016/j.gr.2024.05.003>

### Digital Object Identifier (DOI):

[10.1016/j.gr.2024.05.003](https://doi.org/10.1016/j.gr.2024.05.003)

### Link:

[Link to publication record in Edinburgh Research Explorer](#)

### Document Version:

Publisher's PDF, also known as Version of record

### Published In:

Gondwana Research

### Publisher Rights Statement:

2024 The Author(s). Published by Elsevier B.V. on behalf of International Association for Gondwana Research.

### General rights

Copyright for the publications made accessible via the Edinburgh Research Explorer is retained by the author(s) and / or other copyright owners and it is a condition of accessing these publications that users recognise and abide by the legal requirements associated with these rights.

### Take down policy

The University of Edinburgh has made every reasonable effort to ensure that Edinburgh Research Explorer content complies with UK legislation. If you believe that the public display of this file breaches copyright please contact [openaccess@ed.ac.uk](mailto:openaccess@ed.ac.uk) providing details, and we will remove access to the work immediately and investigate your claim.





# Testing alternative tectonic models for the Permian-Pleistocene tectonic development of the Kyrenia Range, N Cyprus: Implications for E Mediterranean Tethyan palaeogeography

Alastair H.F. Robertson<sup>a,\*</sup>, Osman Parlak<sup>b</sup>, Kemal Taslı<sup>c</sup>

<sup>a</sup> School of GeoSciences, University of Edinburgh, EH9 3JW Edinburgh, UK

<sup>b</sup> Çukurova Üniversitesi, Jeoloji Mühendisliği Bölümü, 01330 Balcalı, Adana, Türkiye

<sup>c</sup> Mersin Üniversitesi, Jeoloji Mühendisliği Bölümü, 33100 Mersin, Türkiye

## ARTICLE INFO

### Article history:

Received 14 December 2023

Revised 5 April 2024

Accepted 4 May 2024

Available online 10 May 2024

Handling Editor: A. Festa

### Keywords:

Kyrenia Range  
Eastern Mediterranean  
Tectonic models  
Subduction  
Collision  
Regional synthesis

## ABSTRACT

Three published alternative tectonic models of the Permian-Pleistocene development of the Kyrenia Range, N Cyprus are tested, supported by new field, geochemical and micropalaeontological evidence: 1. The Kyrenia Range represents the northern continental margin of the S Neotethys, close to its present relative position. The range initiated as a Permian-Cretaceous rift/passive margin, switching to a N-facing active margin during Late Cretaceous-Neogene; 2. The Range was located along the N African continental margin until the Neogene when northward subduction transferred it to the southern margin of the Eurasian plate; 3. The Range is a far-travelled allochthon that was emplaced to near its present position, probably during the Eocene.

In the light of regional comparisons, especially with southern Turkey, the combined evidence mainly supports tectonic model 1. Sedimentary and palaeontological data show that the restored stratigraphy of the Kyrenia Range indicates Late Permian initial rifting and Early-Middle Triassic advanced rifting, followed by Jurassic-Early Cretaceous passive margin subsidence. Small exposures of ophiolite-related melange located between the Mesozoic carbonate platform and the overlying latest Cretaceous-Palaeogene deep-water volcanic-sedimentary succession include evidence of HP/LT metamorphism, pointing to Late Cretaceous subduction. MORB/boninites, diabase-gabbro and extensive harzburgitic serpentinite originated as a SSZ ophiolite, together with a possible high-grade metamorphic sole (garnet amphibolite) and an accretionary prism (E-MORB/OIB; metachert). Microfossil evidence indicates exhumation of the melange and the underlying platform prior to Late Maastrichtian. A mass-transport complex formed within a compression-related foredeep during the Middle Eocene. Associated southward thrusting and folding culminated in emergence and subaerial erosion, generating a major unconformity, that was followed by subaerial and then marine deltaic deposits (Late Eocene-Oligocene). Following major Late Miocene southward thrusting, uplift of the Kyrenia Range took place during the Pleistocene, related to collision of the leading edge of the North African plate (Eratosthenes Seamount) with the Eurasian (Anatolian) plate.

© 2024 The Author(s). Published by Elsevier B.V. on behalf of International Association for Gondwana Research. This is an open access article under the CC BY license (<http://creativecommons.org/licenses/by/4.0/>).

## 1. Introduction

The Kyrenia Range is located in a key position within the sutured Tethyan ocean in the easternmost Mediterranean region, adjacent to Turkey to the north and to the Levant to the east (Fig. 1). The ocean is commonly referred to as the Southern Neotethys (S Neotethys) to distinguish it from more northerly Neoteth-

yan ocean basins that lie sutured within Anatolia. The S Neotethys is widely interpreted as a Mesozoic basin that rifted along the northern margin of Gondwana (N Africa) (e.g., Robertson and Dixon, 1984; Dercourt et al., 1986; Barrier et al., 2018). A Red Sea-type intra-continental rift is commonly inferred (Robertson et al., 1991a), although a back-arc rift above a S dipping subduction zone (from Palaeotethys) has also been proposed (Şengör and Yılmaz, 1981). The timing of continental break-up is commonly interpreted at Late Triassic-Early Jurassic (e.g., Garfunkel, 1998), although Permian break-up (Stampfli and Borel, 2002) and Early

\* Corresponding author.

E-mail address: [Alastair.Robertson@ed.ac.uk](mailto:Alastair.Robertson@ed.ac.uk) (A.H.F. Robertson).

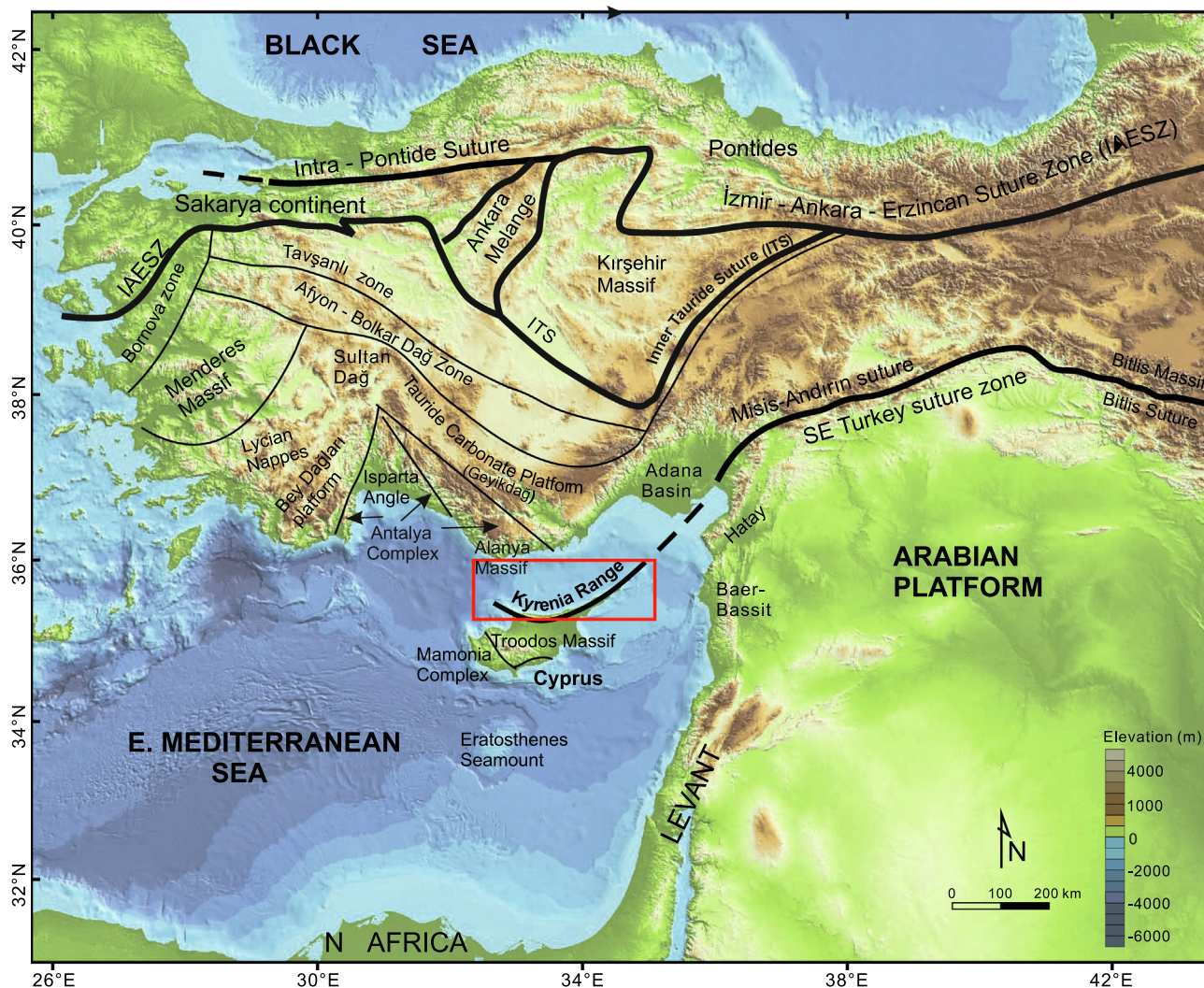


**Fig. 1.** Topography of Turkey showing the main tectonic zones and the location of the Kyrenia Range in the north of Cyprus (marked as a red box). Main data source for the tectonic zones of Turkey (MTA, 2011). (For interpretation of the references to colour in this figure legend, the reader is referred to the web version of this article.)

Cretaceous break-up (e.g., Ricou et al., 1986; Dilek and Rowland, 1993) have also been inferred. The ocean basin was bordered by subsiding passive margins during Late Triassic/Early Jurassic, up to and including Early Cretaceous time (Robertson et al., 2012a). It is widely accepted that oceanic crust formed above a subduction zone somewhere within the S Neotethys during the Late Cretaceous (e.g., Pearce et al., 1984). Opinions differ as to whether this subduction was located within the present N Africa-Tauride oceanic gap (Robertson, 2002; Parlak, 2016), or instead within the S Neotethys far to the northeast followed by subduction rollback into the Eastern Mediterranean region (Maffione et al., 2017). SSZ ophiolites were emplaced onto both the southerly (Arabian) continental margin and onto more northerly Tauride continental units during latest Cretaceous time. An alternative interpretation is that the Tethys in the Eastern Mediterranean region represents a small, elongate, pull-apart oceanic basin that opened related to left-lateral transform faulting adjacent to the North African continental margin (including Adria) (Le Pichon et al., 2019). In different interpretations, the S Neotethys sutured during latest Cretaceous, Eocene, Early Miocene, or Late Miocene. Evidence from SE Turkey (e.g., Boulton et al., 2006) and Iran (e.g., Darin and Umhoefer, 2022) favours Eocene initial collision followed by Early Miocene more advanced continental collision.

Three main tectonic models are currently proposed to explain the Late Palaeozoic-Recent development of the Kyrenia Range within its regional context (Fig. 2a-j).

1) The Kyrenia Range represents the northern continental margin of the S Neotethys; it began as a rift basin during the Permian-Triassic (Fig. 2a) and then became a passive margin during the Jurassic-Cretaceous; it then switched to an active margin related to northward subduction of the S Neotethys during the Late Cretaceous (Fig. 2b). Further northward subduction during the Early Cenozoic resulted in initial collision-related deformation during the Middle-Late Eocene (Fig. 2c), and more advanced collision during the Late Miocene (Fig. 2d); major surface uplift was delayed until the Pleistocene (McCay and Robertson, 2012; Palamakumbura et al., 2016; Palamakumbura and Robertson, 2016; Robertson et al., 2012a, 2014; Robertson and Kinnaird, 2016; Chen et al., 2019, 2022; Chen and Robertson, 2021).

2) The Kyrenia Range formed part of the north African rifted passive continental margin during the Permian-Cretaceous; the Troodos ophiolite was emplaced southwards onto the distal edge of this continental margin during Late Cretaceous time (Fig. 2e). The Kyrenia Range remained as part of the passive margin of north Africa during the Paleogene. The passive margin was destabilised, with uplift and associated down-margin mass transport during

### THREE ALTERNATIVE TECTONIC MODELS

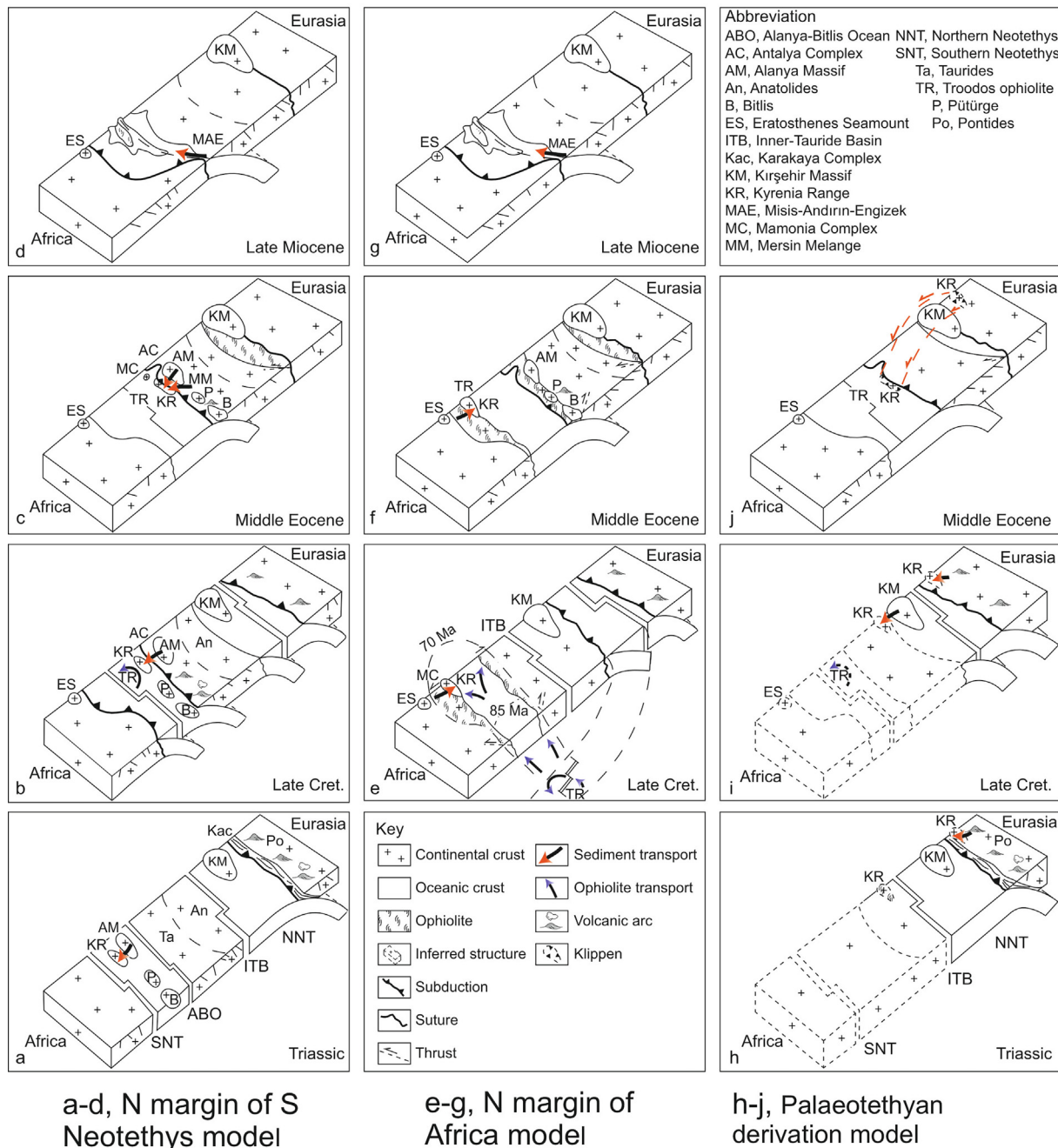


**Fig. 2.** Alternative tectonic models of the Kyrenia Range in the Eastern Mediterranean region. a-d, The Kyrenia Range is restored to the northern margin of Southern Neotethys (McCay and Robertson, 2012; Robertson et al., 2012a, 2014; Robertson and Woodcock, 1986), a, Triassic; b, Late Cretaceous; c, Middle Eocene; d, Late Miocene; e-g, The Kyrenia Range is restored as part of the distal, N Africa rifted continental margin (Maffione et al., 2017; McPhee and van Hinsbergen, 2019), e, Late Cretaceous; f, Middle Eocene; g, Late Miocene; h-j, The Kyrenia Range is restored as a far-travelled allochthon derived from Palaeotethys (S margin of Eurasia) or adjacent to this ocean basin (Glazer et al., 2021), h, Triassic; i, Late Cretaceous; j, Middle Eocene. In i and j, implied tectonic settings are shown although these are not specified by the authors of this interpretation. Modified from Chen et al. (2022).

the Eocene, related to far-field crustal deformation (Fig. 2f). Remaining S Neotethyan oceanic lithosphere subducted northwards during the Oligocene-Miocene, culminating in transfer of the Kyrenia Range during Late Miocene collision of the Eurasian plate and N African plate (Fig. 2g); this is, in turn, triggered major Late Miocene surface uplift of the Kyrenia Range (McPhee and van Hinsbergen, 2019; see also Maffione et al., 2017).

3) The Kyrenia Range as a whole is allochthonous and developed somewhere outside the confines of the present eastern

Mediterranean region. The main evidence used to support this model is the presence of relatively abundant detrital zircons of Late Palaeozoic, especially Carboniferous, age that occur within a Triassic calcschist intercalation and also within latest Cretaceous and Eocene sandstones within the Kyrenia Range (Glazer et al., 2021). A local provenance does not explain the abundance of Carboniferous grains that are instead characteristic of some units related to the Palaeotethyan suture zone of northern Turkey (Glazer et al., 2021). One option that was considered by Glazer et al. (2021) is

that the Kyrenia Range developed within, or adjacent, to Palaeotethys, to the north of the Taurides (Fig. 2h,i).

There are obviously fundamental differences between the above three tectonic models, especially for Permian to Paleogene time when the Kyrenia Range, alternatively was located near its present position south of the Taurides in model 1, far to the south along the North African continental margin in model 2, or located somewhere within reach of a supply of 'Palaeotethyan' Carboniferous zircons in model 3. Recently, the three alternative tectonic models were partially tested (Chen et al., 2022a,b) based on a combination of new and existing detrital zircon geochronological data from the Kyrenia Range, in the context of the geology of the Kyrenia Range and the adjacent region especially Turkey. However, several aspects remained unresolved that could best be addressed by obtaining some new data from key outcrops throughout the Kyrenia Range, as presented here.

The stratigraphy used here is based on traditional studies (e.g., Ducloz, 1972; Baroz, 1979; Robertson and Woodcock, 1986). More recently, a parallel stratigraphy was introduced using Turkish names (Hakyemez et al., 2002). Here, at first mention, we give the traditional name with the equivalent Turkish name in brackets (see Fig. 4). We utilise mainly Turkish names for settlements and geographical features as currently in use (see Fig. 3), with older names in brackets (at first mention).

The groups and formations that are mainly relevant here are as follows. The Mesozoic platform encompasses the Trypa (Tripa) Group, of which the Dikomo (Dikmen) Formation at the base is of particular interest. Ophiolite-related melange (no formal name) occurs above this. Above a regional unconformity, there is the Maastrichtian-Paleogene Lapithos (Lapta) Group, subdivided into four formations, namely the Kiparisso Vouno (Alevkaya Tepe) Formation, the Malounda (Mallidağ) Formation, the Ayios Nikolaos (Yamaçköy) Formation and the Kalograia-Ardana (Bahçeli-Ardahan) Formation, of which the first and last are important for this paper because they contain sandstones with dated detrital zircons. The Kiparisso Vouno Formation comprises hemipelagic marls, mudrocks and sandstone turbidites. The Eocene Kalograia-Ardana Formation is a mass-transport complex (traditional olistostrome) with a matrix of pelagic carbonates, marls, calciturbidites, sandstone turbidites and debris-flow deposits, the last mentioned including exotic blocks of Upper Palaeozoic shallow-

water carbonate rocks known as the Kantara Limestones. The succession continues with the Neogene Kythrea, or (Kithrea) Group, which is divided into 12 formations. The group begins with terrestrial alluvial fan to marine-deltaic conglomerates and sandstones (Bellapais Formation), deepening upwards into a variable succession of mainly marls and sandstones turbidites, volumetrically minor tuffs; lenticular Messinian gypsum deposits occur near the top of the continuous succession. Unconformably above there are three formations of the Pliocene-Pleistocene Mesaoria (Mesarya) Group, mainly composed of shelf-depth marine marls, passing upwards into minor sandstones and conglomerates representing regressive non-marine facies. Terraced fluvial conglomerates/sandstones and coastal littoral carbonates dominate the Pleistocene-Holocene (Fig. 4).

## 2. Regional setting and previous research

The regional tectonic setting of the Kyrenia Range in the north of Cyprus is shown in Fig. 1. The stratigraphy of the Kyrenia Range as a whole was outlined by Henson et al. (1949). The central and eastern ranges (Fig. 3) were mapped during the 1970s related to a United Nations development project (Ducloz, 1972). Also during the 1970s, much of the Kyrenia Range was independently mapped by Baroz (1979, 1980) related to his DSc studies. The first plate tectonic interpretation of the Kyrenia Range was given by Robertson and Woodcock (1986). Since then more specific aspects of the Kyrenia Range have been studied (e.g., Robertson et al., 2012b, 2014), leading to the stratigraphy shown in Fig. 4. The structure of the Kyrenia Range has been presented as numerous interpretative cross-sections of the range (Baroz, 1979), as cross-sections of the central and western range (Robertson and Kinnaird, 2016), and as a balanced cross-section of the central range (McPhee and van Hinsbergen, 2019).

## 3. Methods and materials

Specific outcrops along the length and breadth of the Kyrenia Range were visited with the aim of resolving some controversial issues (see above). For each relevant outcrop, local logs and local cross-sections were made and structural data were collected. Thin

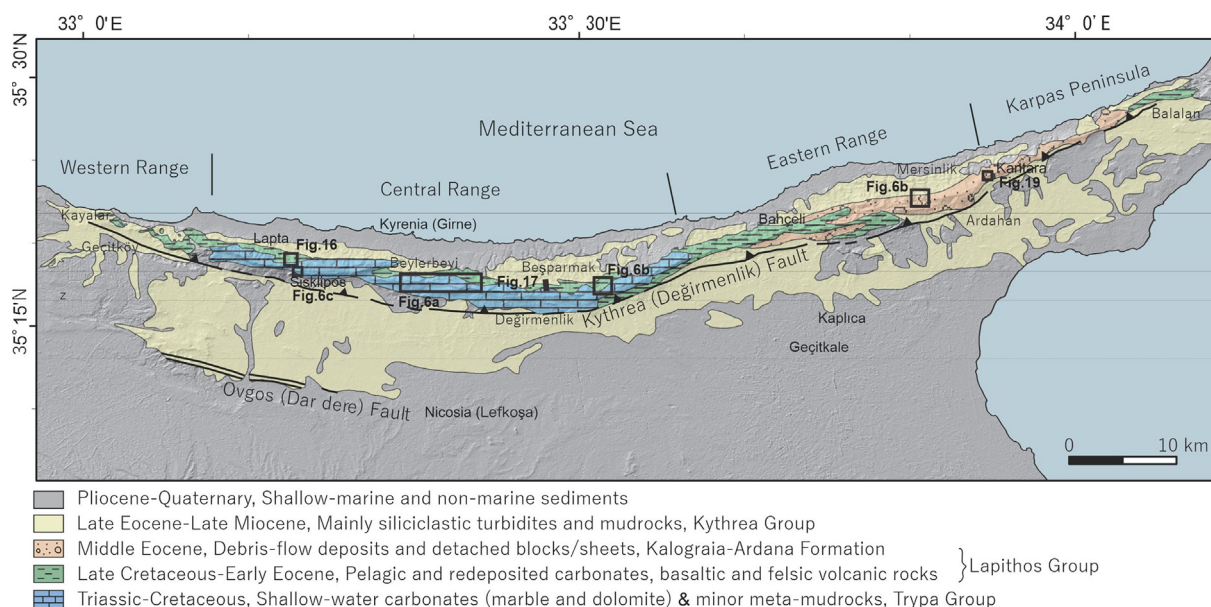
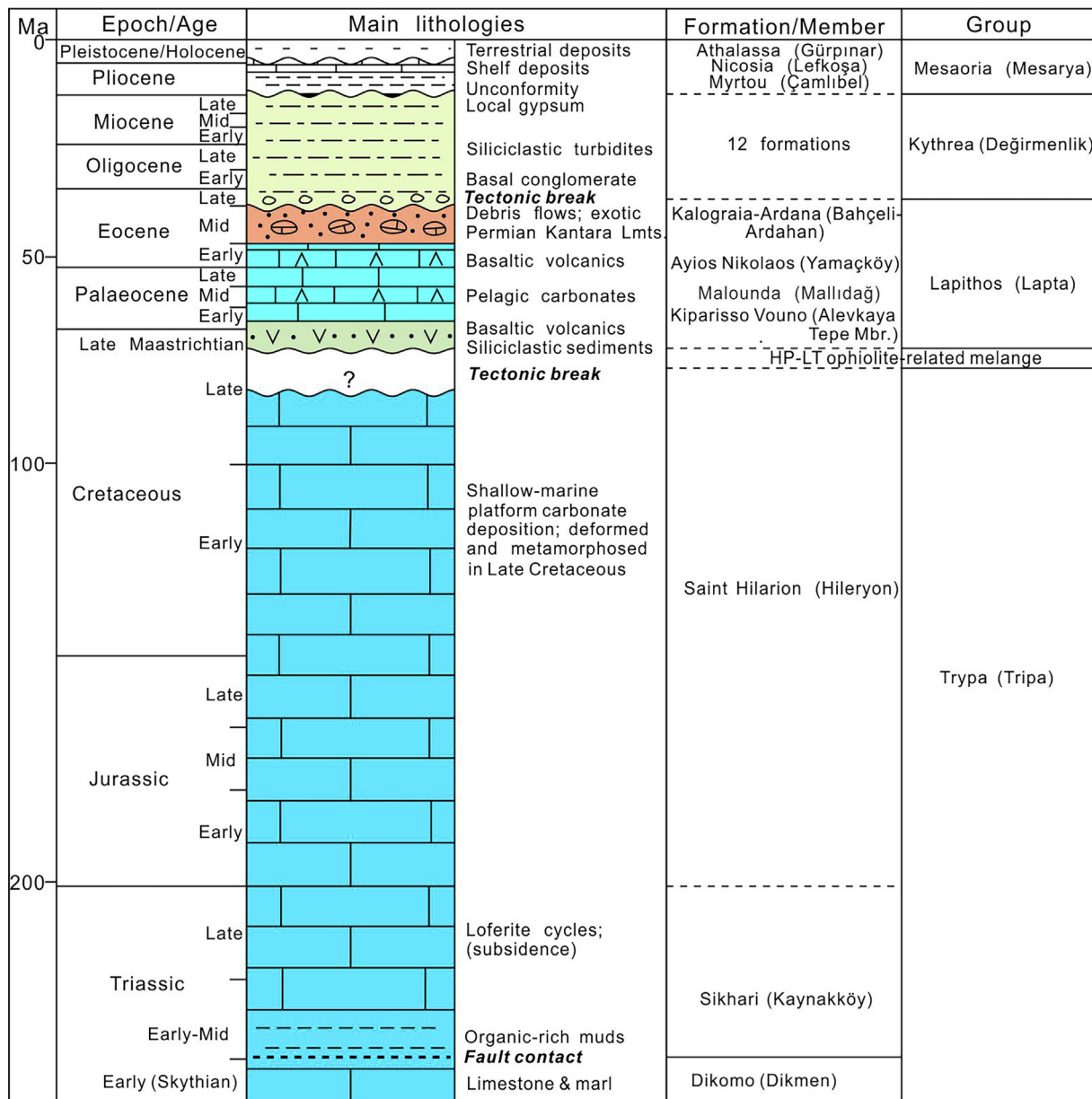


Fig. 3. Outline geological map of the Kyrenia Range (modified from Robertson et al., 2012a and Chen et al., 2022). The main places mentioned in the text are indicated.



**Fig. 4.** Simplified stratigraphy of the Kyrenia Range. Modified from Robertson et al. (2012a, 2014) and Chen et al. (2019). Compared to the previous stratigraphy, this version restores the Dikomo Formation to the stratigraphical base of the Trypa Group, beneath the Sikhari Formation. Also, small outcrops of metamorphic rocks that are interpreted as ophiolite-related melange are shown as a tectonic intercalation between the Trypa Group and the Lapithos Group.

sections of associated carbonate and siliciclastic sedimentary rocks were studied under the optical microscope (supplementing previous collections). Metamorphic lithologies from small exposures of melange were studied petrographically, and eight representative samples of meta-basalts were chemically analysed for major element, trace element and rare earth elements (REEs). The chemical analysis was carried out by ICP-MS at the ALSlab in Ireland. Major element concentrations were determined from a  $\text{LiBO}_2$  fusion by inductively coupled plasma mass spectrometry (ICP-AES) by using 2g of sample pulp. Trace element contents were determined from a  $\text{LiBO}_2$  fusion by ICP-MS by using 2g of sample pulp. In addition, limestones from several key locations were biostratigraphically dated using calcareous microfossils.

For this study, it was essential to take careful account of previous information, especially that based on mapping of large parts of the Kyrenia Range. As some of this information is not easily accessible (and in four languages), it is compiled as [Supplementary Data](#) (text), relating to four critical aspects: the oldest part of the stratigraphy

(Triassic), the meta-igneous and meta-sedimentary rocks within the tectonic melange beneath the Paleogene cover, the Mid-Late Eocene deformation, uplift and erosion, and the transgressive coarse clastic sedimentary cover of Late Eocene-Oligocene age.

Here, we use a combination of new and existing evidence to explore the three contrasting tectonic hypotheses (Fig. 2). To explore the alternatives, we extend these models to beyond the interpretations of the original authors. For example, we further consider the possibility, inherent in model 3 (Glazer et al., 2021), that the Kyrenia Range reached its present position by southward thrusting over the Taurides (to the north).

#### 4. Results and implications of alternative tectonic models

Below we focus on the following main aspects that are interpreted differently in the three tectonic models.

- The stratigraphy of the Kyrenia Range especially during the Triassic, which is relevant to regional correlations.
- Upper Cretaceous deformation and metamorphism, in view of the evidence of high pressure-low temperature (HP-LT) metamorphism (Glazer et al., 2021) that affects some lithologies beneath the latest Cretaceous-Paleogene sedimentary cover.
- The Paleogene development of the Kyrenia Range as an unstable, volcanically active basin.
- Eocene deposition and deformation affecting the Kyrenia Range.

- The exact timing of the Late Miocene thrusting that affected the Kyrenia Range, and also when the range first underwent strong surface uplift.

4.1. Triassic stratigraphy of the Kyrenia Range

The stratigraphy of the central and western ranges is well-documented as Mesozoic platform carbonates and Upper Cretaceous-Eocene deep-water carbonates and basaltic volcanics (Figs. 3, 4, 5a). The Upper Cretaceous-Paleogene lithologies of the

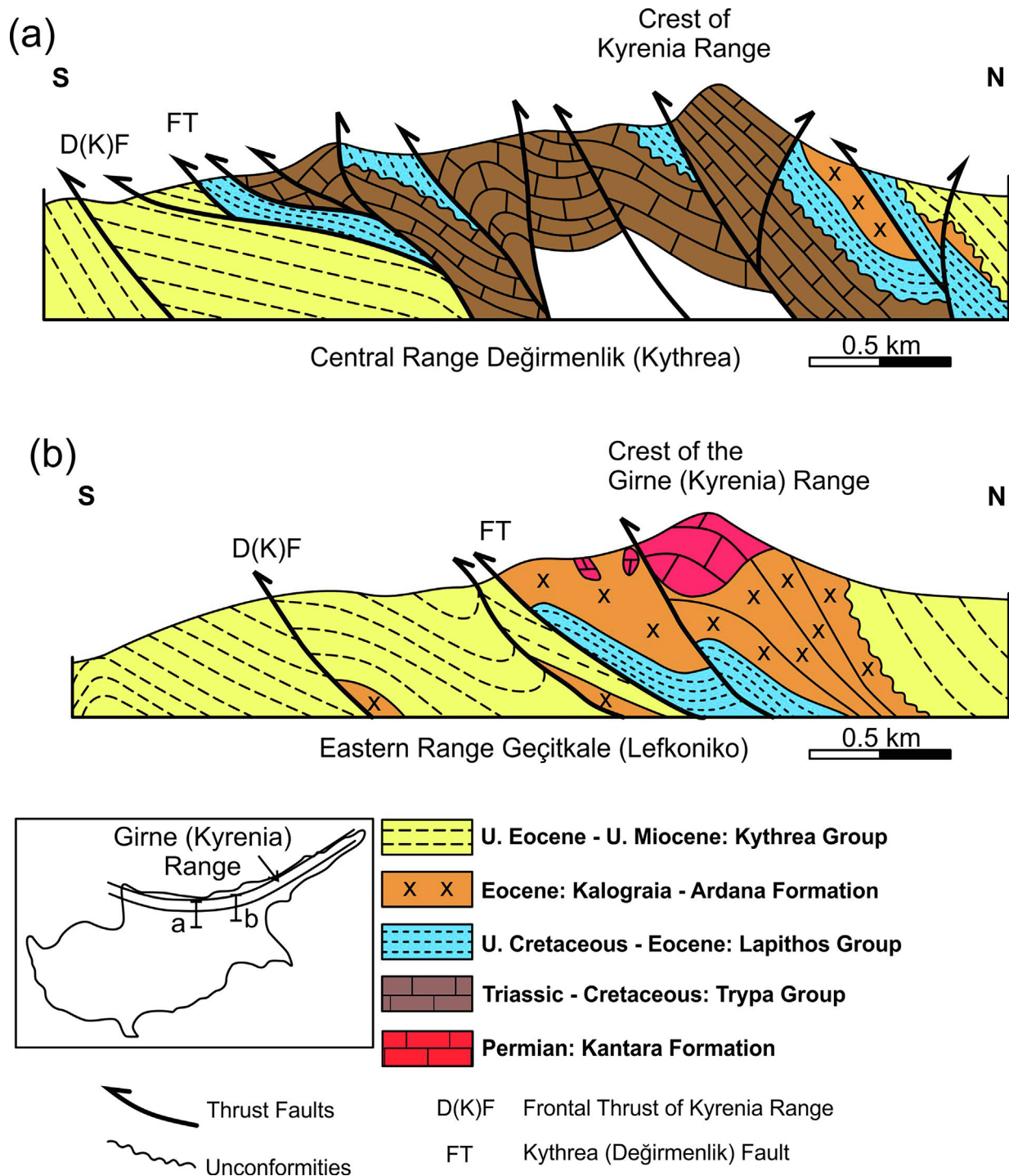
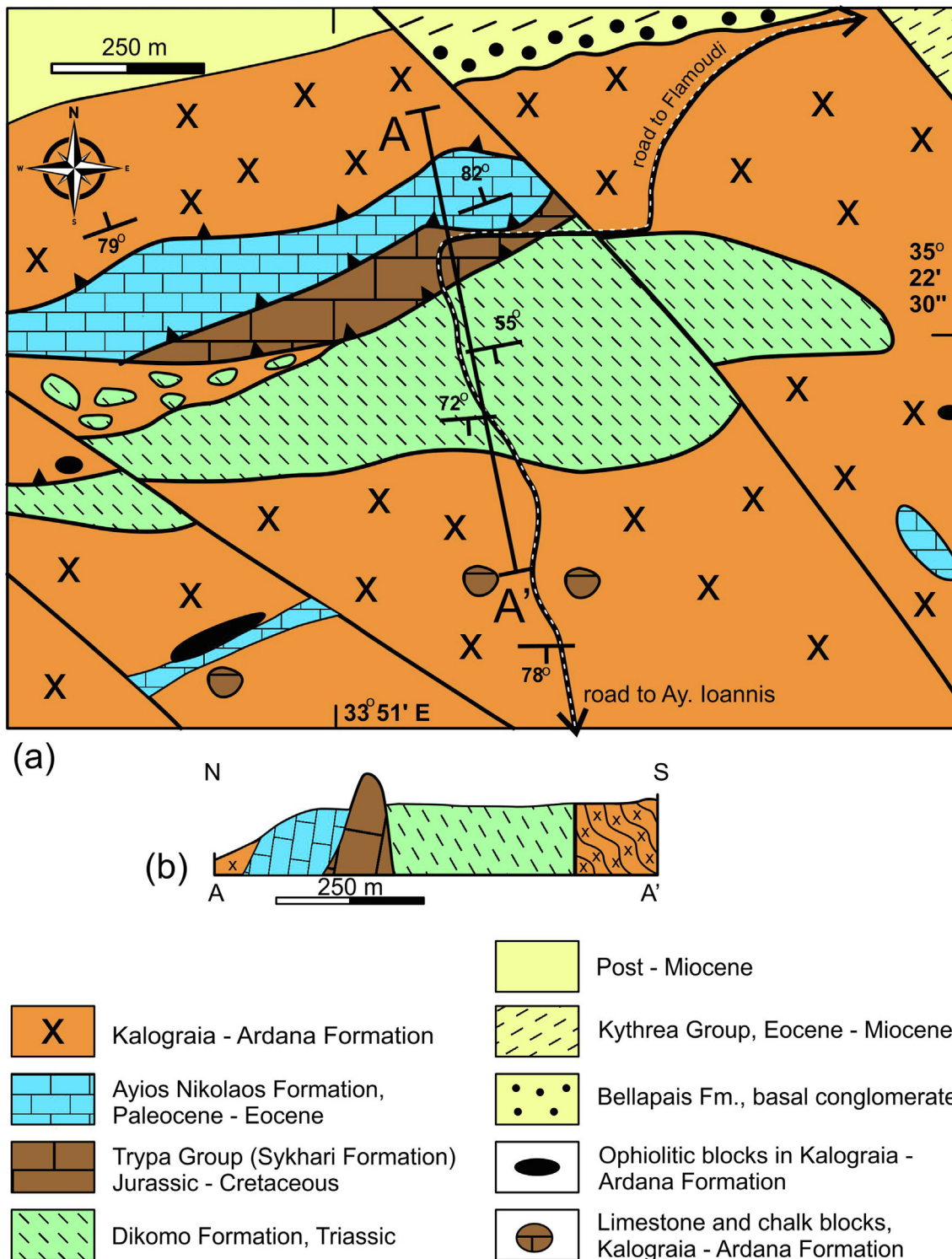


Fig. 5. Simplified cross-sections across the central and eastern Kyrenia Range. (a) A-A' Cross section passing near Değirmenlik (Kythrea); (b) B-B' Cross-section passing near Geçitkale (Lefkoniko). Modified from McCay and Robertson (2012).



**Fig. 6.** Geological map (a) and cross-section (b) of the largest outcrop of the Lower Triassic Dikomo Formation in the eastern Kyrenia Range (see Fig. 3). The outcrop is tectonically intercalated with Eocene mass-transport lithologies (Kalograia-Ardana Formation) and with a thrust slice of the Trypa-Lapithos group succession. Based on Ducloz (1972), Baroz (1979) and this study.

eastern Kyrenia Range and the Karpaz Peninsula are characterised by similar latest Cretaceous-Palaeocene volcanic-sedimentary units, together with a major Eocene mass-transport unit (olistostrome) (Baroz, 1979; Ducloz, 1972; Hakyemez et al., 2002; Robertson et al., 2012a; Robertson and Woodcock, 1986) (Figs. 3, 4, 5b).

The thrust-imblicated Triassic-Upper Miocene succession is well exposed in the central and western Kyrenia Range (Figs. 3, 4, 5a). The Triassic-Early Cretaceous lower part of this succession is interpreted as a rifted passive margin succession that was deformed, metamorphosed to greenschist facies and exhumed during the Late Cretaceous (pre-Maastrichtian) (Ducloz, 1972; Baroz,



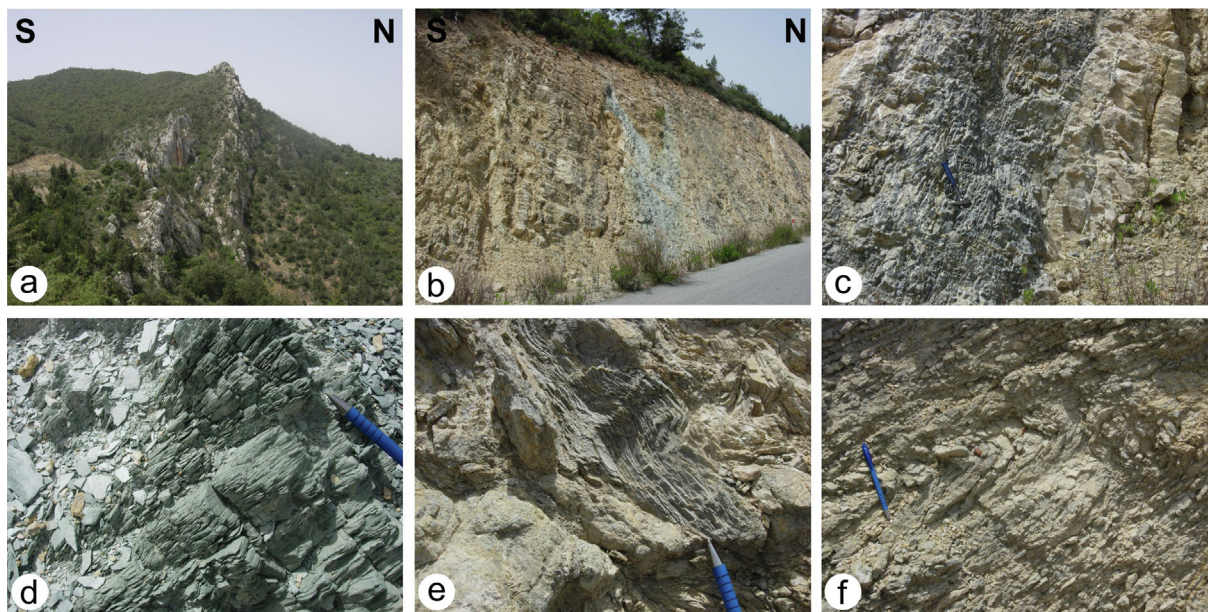


**Fig. 7.** Field photographs related to the Lower Triassic Dikomo Formation, eastern Kyrenia Range. a, Setting of the Dikomo Formation (D) intercalated with Mesozoic dolomitic platform carbonates (Sikhari Formation) and pelagic carbonates (Ayios Nikolaos Formation) to the north, and debris-flow deposits of the Kalograia-Ardana Formation to the south. The Dikomo Formation is c. 100 m thick. See Fig. 6a for location; b, Cyclical alternations (steeply dipping) of marble (limestone) and calc-schist (marl); the section shown is c. 70 m thick; See Fig. 6b for location; c, Medium-bedded meta-limestone, interbedded with dark, thin-bedded organic carbon-rich meta-carbonate rock, hammer for scale; d, Thin to medium-bedded meta-limestone with marl partings pen for scale; e, Greenish marl intercalation; pen for scale; f, Small-scale asymmetrical folds associated with shearing and duplexing (top-to-the south locally) of thin-bedded marble and calc-schist, pen for scale. Location of a-f, 2 km SSW of Mersinlik (Flamoudi) (GPS: 36S 0577682/3915805).

1979; Robertson and Woodcock, 1960; Robertson et al., 2012b). Additional small dismembered thrust sheets of mainly Upper Cretaceous volcanogenic rocks are locally exposed, mainly along the southern front of the western range (Moore, 1960; Huang et al., 2007; Chen and Robertson, 2021). These extrusive and tuffaceous units formed in a subduction-related setting, probably associated with a continental margin arc, based mainly on major and trace element geochemical data (see Chen and Robertson, 2021).

During this study, previously mapped outcrops of the oldest unit, the Triassic Dikomo Formation, >100 m thick (Fig. 4), were re-investigated in the eastern range (Fig. 3). The largest outcrop is tectonically intercalated between dark-coloured dolomitic lithologies of the Triassic Sikhari (Kaynakköy) Formation to the north, and an outcrop of the Eocene Kalograia-Ardana Formation (mass-transport unit) to the south and the north in different local areas (Fig. 6a,b, 7a). The Dikomo Formation consists of cyclical alternations of marble, meta-calcareous mudrock (calc-phyllite) (Fig. 7b-d). Some intervals are greenish or greyish and appear to be relatively rich in organic carbon (Fig. 7e). The outcrop has undergone heterogeneous deformation of variable scale and geometry, including variably developed axial-planar cleavage and top-south shear-related folding (Fig. 7f). Relatively competent marble is brecciated in places.

Very few fossils are preserved within the Dikomo Formation, although Hakyemez et al. (2002) report the bivalve *Claraia clarae* of Skythian (Early Triassic) age. Species of the genus *Claraia*, which is characteristic of the eastern Tethys, have relatively thick (and thus preservable) shells, and commonly lived in relatively deep-water oxygen-poor settings (He et al., 2014). Ducloz (1972) and Baroz (1979) interpreted the Dikomo Formation as the Triassic base of the platform succession (Trypa Group), taking account of its position beneath the intact dolomitic Sikhari Formation in some sections, although there is no known stratigraphical contact (see

Supplementary Data, text for details). The dolomitic Sikhari Formation lacks preserved fossils other than thick-shelled Megalodonts of non-specific Triassic-Early Jurassic age (Hakyemez et al., 2002). The Sikhari Formation includes black foliated calcschist from which Glazer et al. (2021) obtained a minimum age of 235 Ma for detrital zircons, suggesting a Middle Triassic maximum age of deposition. The Dikomo Formation can, therefore, be assumed to be Early Triassic and to have been originally overlain by the Sikhari Formation of mainly Middle-Late Triassic age.

The Dikomo Formation is similar to cyclical facies exposed within the metamorphic Alanya Massif to the north (undated) (Öztürk et al., 1995; see Robertson and Parlak, 2020), and is also similar to Lower Triassic well-dated unmetamorphosed successions throughout the Taurides generally, for example in the Tauride thrust sheets (Özgül, 1984a; Özgül, 1984b, 1997; Andrew and Robertson, 2002; Mackintosh and Robertson, 2012; McPhee et al., 2018) and in the Antalya Complex (nappes) (e.g., Poisson, 1977; Robertson and Woodcock, 1984). The Lower Triassic facies accumulated in a tectonically unstable rift setting characterised by fluctuating redox conditions (i.e., pinkish vs. dark grey meta-mudrocks). Shelf conditions became established during the Mid-Late Triassic (Sikhari Formation), followed by shallow-marine carbonate shelf deposition during the Early Jurassic-Cretaceous, near Alçiçek (Sisklipos).

In tectonic model 1, the Dikomo Formation accumulated along the rifted northern margin of the S Neotethys (Fig. 2a). Similar Triassic facies are widely exposed throughout the Taurides, as noted above. In tectonic model 2, the Dikomo Formation accumulated along the N African continental margin, which being still submerged does not expose evidence of its Triassic distal rift facies. Also, the Dikomo Formation does not show evidence of high-strain conditions, as might be expected if it was located near the base of a regional-scale thrust detachment, as in tectonic model 3.

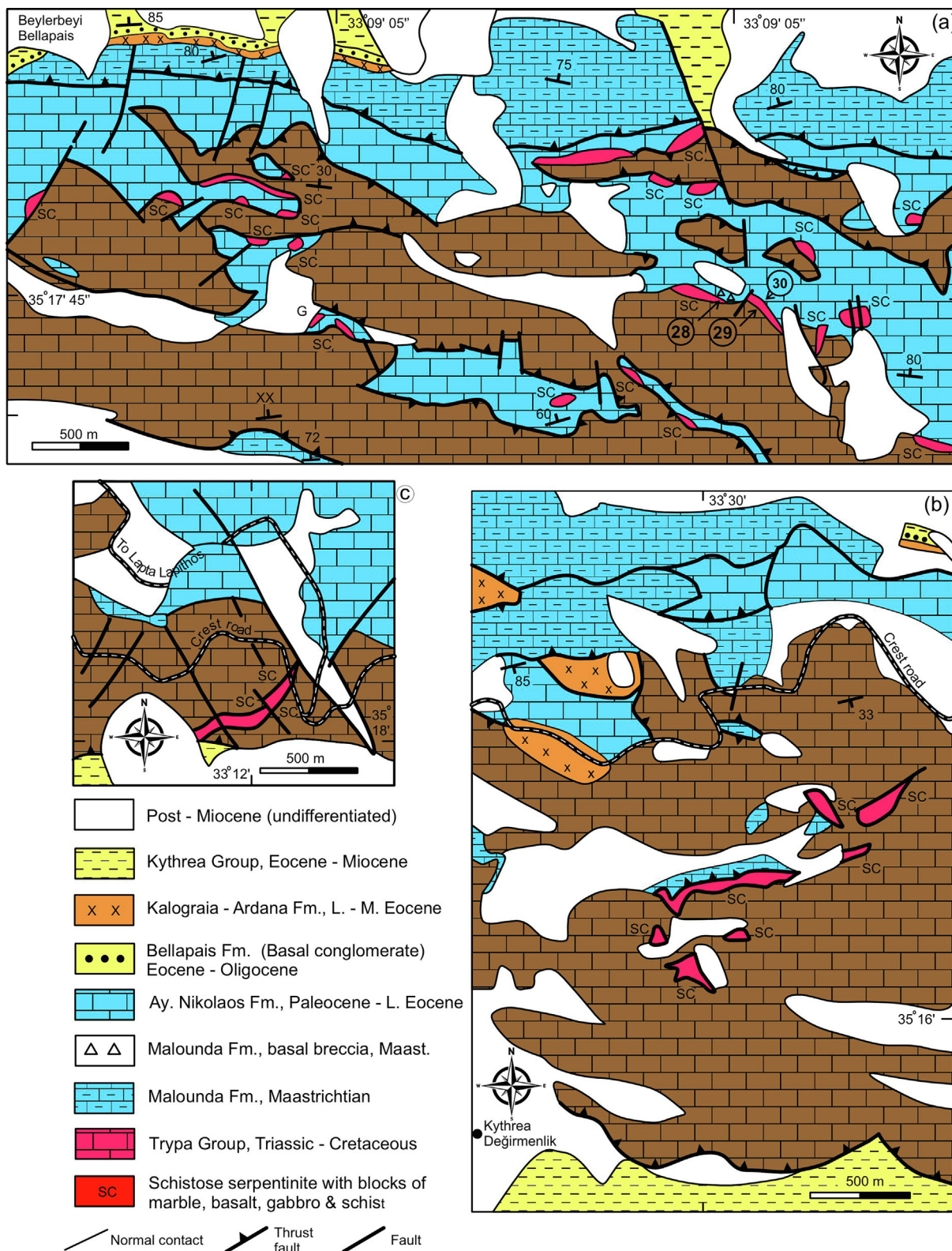


**Fig. 8.** Geological maps of the three main outcrops of Upper Cretaceous ophiolite-related melange, all located in the central range. a, SE of Beylerbeyi (Bellapais); b, NE of Değirmenlik (Kythrea). Note the occurrences of schistose serpentinite with blocks of mainly marble, metabasalt, metagabbro and metasedimentary rocks (Sc); c, SE of Lapta (Lapithos), near Alçiçek (Sisklipos); Based on [Ducloz \(1972\)](#), [Baroz \(1979\)](#), [Glazer et al. \(2021\)](#) and this study.

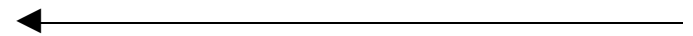
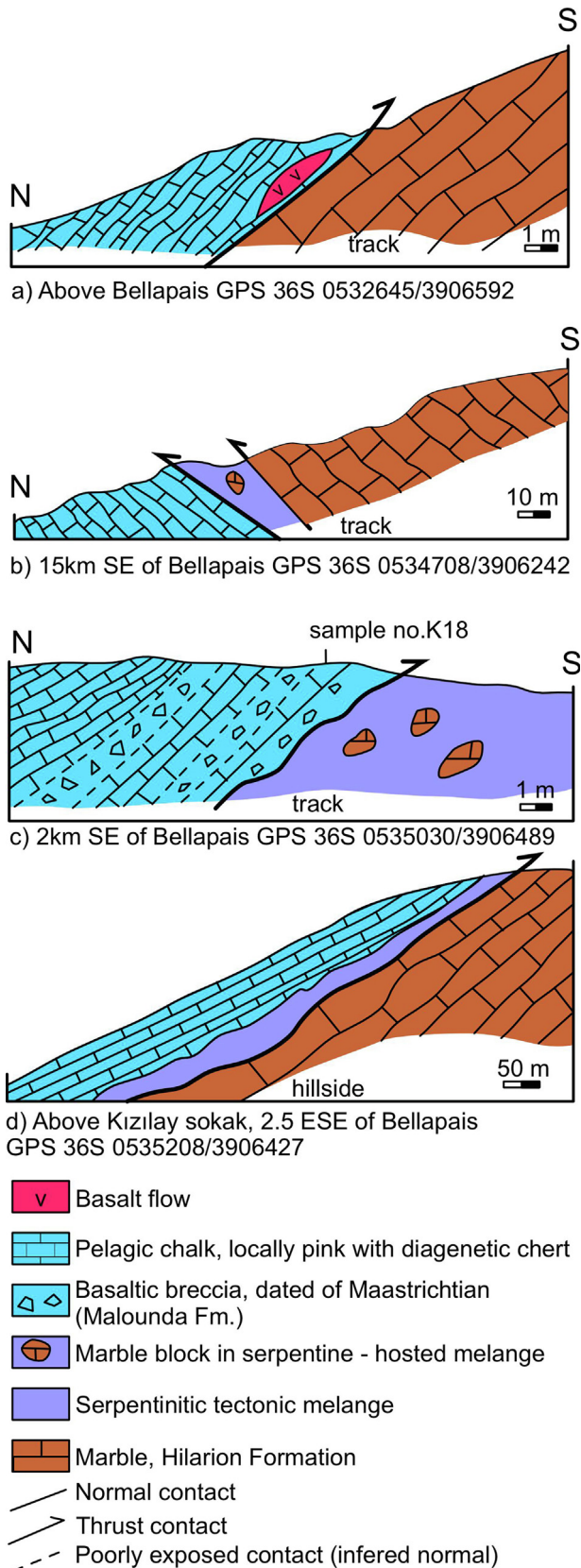


**Fig. 9.** Local cross-sections of the Upper Cretaceous ophiolite-related melange in relation to its adjacent units. a, Above Beylerbeyi (Bellapais), where (as in most exposures) the melange is absent; b, SE of Beylerbeyi (Bellapais), where the ophiolite-related melange is intercalated with Mesozoic platform carbonates and Palaeogene pelagic sediments and volcanics; c, SE of Beylerbeyi (Bellapais), where the ophiolite-related melange is overlain by basal carbonate-rock breccias of the Late Eocene-Oligocene Bellapais Formation. Where rarely observable the contact is an unconformity; d, ESE of Beylerbeyi (Bellapais), where sheared serpentinite is patchily exposed above the Mesozoic platform carbonates (Hilarion Formation). The contact with the overlying pelagic carbonates of the Lapithos Group is not exposed.

#### 4.2. Setting of Upper Cretaceous deformation and related metamorphism

Small exposures of metamorphic rocks are scattered throughout the central range including schist, marble, meta-chert, meta-lava, amphibolite and meta-serpentinite (see [Supplementary Data](#), text). These rocks were interpreted as fragments of a metamorphic basement to the Kyrenia Range ([Ducloz, 1972](#)). [Baroz \(1979\)](#) mapped them as small thrust slices between the Trypa and Lapithos groups ([Fig. 4](#)). [Glazer et al. \(2021\)](#) considered the metamorphics to be tectonic wedges within the Trypa and Lapithos groups.

[Glazer et al. \(2021\)](#) referred to the assemblage of closely juxtaposed rock types as ophiolitic melange mainly because of the association of meta-serpentinite, meta-gabbro/meta-diabase/lava and meta-chert. Blue amphibole including crossite in both meta-basic rocks and meta-chert suggested metamorphism at  $< 450$  °C. Phenigite geobarometry further suggested burial pressures of 10–15 kbar. A sample of metabasic rock included zircons of Mesoproterozoic to Late Neoproterozoic age ( $>555 \pm 9$  Ma). Precambrian ages were determined for detrital zircon grains within a metachert. However, the metamorphic lithologies are otherwise undated.

Three exposures of melange were studied along the range ([Fig. 8a-c](#)). Some other previously mapped exposures have been destroyed by recent quarrying of the range front (e.g., W of Değirmenlik (Kythrea)). The most described outcrop ([Ducloz, 1972; Baroz, 1979](#)) is nowadays within an inaccessible military area (upper Fortomenos valley, NE of Değirmenlik (Kythrea)).

In the first area studied by us, the melange is very locally exposed over a wide area to the southeast of Beylerbeyi (Bellapais) in the central range ([Fig. 8a, 10a](#)). Local exposures vary from west to east ([Fig. 9a-d](#)). Near Beylerbeyi (Bellapais), the contact between the Trypa Group, locally marble of the Hilarion Formation, is tectonically overlain by grey to pink pelagic chalks of the Lapithos Group ([Fig. 9a](#)). Common diagenetic chert concretions are typical of the Palaeocene–Early Eocene Ayios Nikolaos Formation. Farther east, the situation is comparable (although tectonically inverted), except that the two units are separated by sheared meta-serpentinite ([Fig. 10b](#)), which includes scattered blocks of marble ([Fig. 9b, 10c](#)).

Farther east, similar sheared meta-serpentinite, again with marble blocks, is unconformably overlain by pink pelagic carbonates ([Fig. 10d](#)). Interbedded mass-flow accumulations, with angular meta-carbonate clasts ([Fig. 10e](#)), are typical of the base of the uppermost Cretaceous Malounda Formation ([Robertson et al., 2012b](#)); i.e., the lowest of the three formations making up the Lapithos Group ([Fig. 9c](#)). During this study, the basal pelagic carbon-

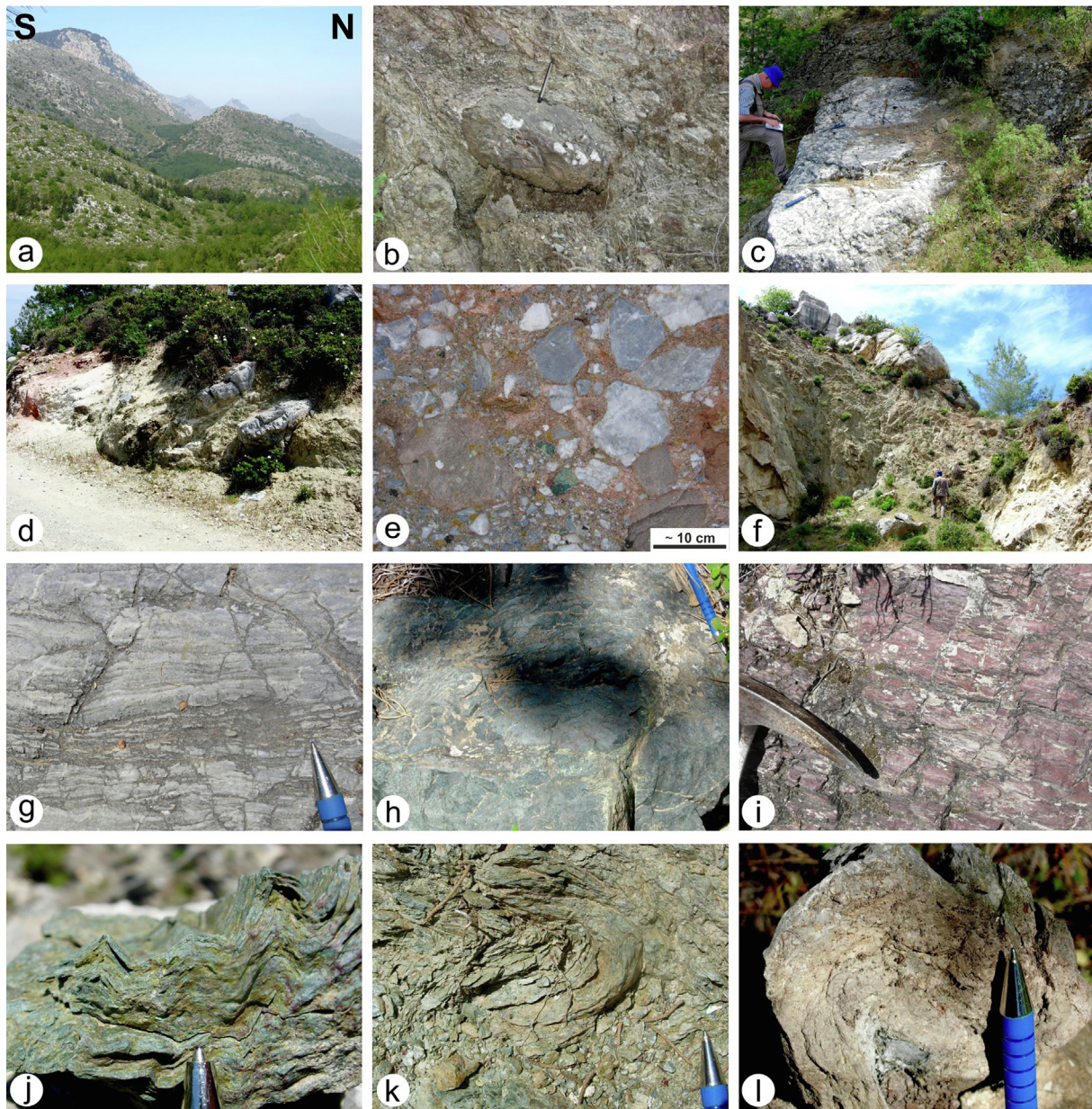


**Fig. 10.** Field photographs of the Upper Cretaceous ophiolite-related melange in the central Kyrenia Range. a, Extensive outcrop forming the low ground between more erosionally resistant carbonate rocks, mainly Jurassic platform carbonates (Hilarion Formation); see Fig. 8a; c, 2–4 km SE of Beylerbeyi; b, Rounded clast (phacoid) of serpentinitised harzburgite within sheared serpentinite; pen for scale, location near c; c, Typical sub-rounded marble block within sheared serpentinite (GPS: 36S 0517544/3908615); d, Serpentine melange with marble clasts, unconformably overlain by pink marl and breccia marking the base of the Maastrichtian Malounda Formation (Lapithos Group) (GPS: 36S 0535030/3906489); e, Undeformed, near-basal breccia of the Malounda Formation, including an angular clast of serpentinite derived from the underlying melange. The marble clasts were derived from the underlying Trypa Group carbonate rocks and/or the marble blocks in the melange; location near e; f, Small quarry exposing sheared and folded serpentinitised harzburgite with a marble block above (GPS: 36S 0535158/3906453); a–f, Exposures southeast of Beylerbeyi (Bellapais). g, Shearing and fragmentation within marble block (5x3 m); enclosed by sheared serpentinite; pen for scale (GPS: 36S 0546048/3904649); h, Block of metabasalt that has undergone blueschist metamorphism; pen for scale (GPS: 36S 0546136/3904601); i, Block of meta-chert that retains a primary reddish colour; hammer for scale, location near h; j, Small-scale isoclinal fold within sheared meta-serpentinite matrix of the melange; pen for scale, location near h; k, Isoclinally folded meta-serpentinite; melange outcrop near Alçiçek (Sisklipos), c. 4 km SE of Lapta (Lapithos) (GPS: 36S 0518423/3907609); g–k c. 2 km NE of Değirmenlik (Kythrea); l, Crenulated, sheared meta-serpentinite from the melange matrix; pen for scale (GPS: 36S 0546088/3904723). (For interpretation of the references to colour in this figure legend, the reader is referred to the web version of this article.)

ates above the melange (Malounda Formation) were dated for the first time as Late Maastrichtian, based on well-preserved planktic foraminifera (see Fig. 11h, 12C–F; Supplementary data (Table S1)). Further east again, Trypa Group marble is covered by laterally continuous (but poorly exposed) meta-serpentinite with marble blocks (Fig. 10f), with Lapithos Group pelagic carbonates above (Fig. 9d).

In the second outcrop, NE of Değirmenlik (Kythrea) (Fig. 8b), large blocks of foliated marble are exposed (Fig. 10g) together with smaller blocks of meta-basalt (locally pillowed) (Fig. 10h) and reddish meta-chert with recrystallised Radiolaria (Fig. 10i). Associated meta-serpentinite is sheared and locally deformed by early-stage isoclinal folding (recumbent to upright) (Fig. 10k,l) and later-stage brittle kink folding (Fig. 10j).

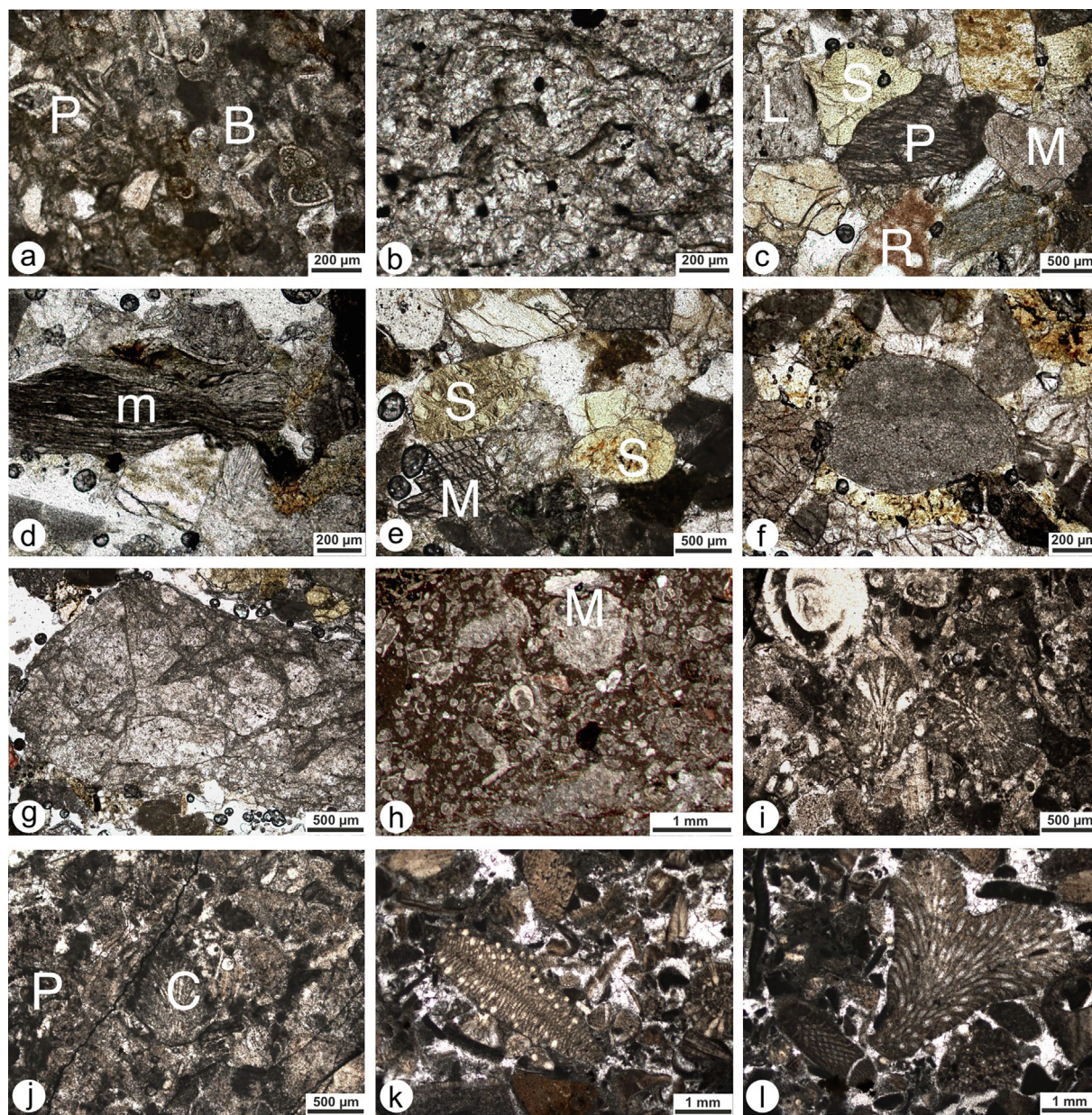


**Fig. 11.** Petrography of clastic and pelagic sedimentary rocks from sections studied. a, Clast of limestone from the basal conglomerate of the Upper Eocene-Oligocene Bellapais Formation, unconformably overlying the Middle Eocene Kalograia-Ardana Formation; showing abundant planktic foraminifera (P) and lesser amounts of benthic foraminifera (B), in a micritic matrix; Beylerbeyi, central range; plane-polarised light; KY/22/13; b, Block of fine-grained meta-sandstone from the ophiolite-related melange with abundant quartz and muscovite; plane-polarised light; Alçiçek (Sisklipos) outcrop of Baroz (1979), central range (see Fig. 8c); KY/22/08 (GPS: 36S 0518423/3907609); c, Medium-grained sandstone from above the ophiolite melange (Kiparisso Vouno Formation) including grains of phyllite (P), serpentinite (S), marble (M), radiolarite (R) and altered lava (L); plane-polarised light; KY/22/08, near a; d, Sample as above, showing grain of mylonite (m); e, Sample as above, including rounded grains of serpentinite (S) and angular grains of marble (M); f, Sample as above, including rounded grain of meta-micritic limestone; g, Sample as above, showing a tectonically fragmented grain of marble; h, Maastrichtian-aged pelagic carbonate unconformably overlying the ophiolite-related melange (see Fig. 8c). Planktic foraminifera (P) and grains of marble (M) in a micritic matrix; SE of Beylerbeyi (Bellapais), central range, plane-polarised light; KY/22/18; i, Clast of limestone from the Middle Eocene Kalograia-Ardana Formation, beneath the basal conglomerate of the Upper Eocene-Oligocene Bellapais Formation, near Beylerbeyi (Bellapais), central range (see Fig. 20c), showing packed benthic foraminifera in a micritic matrix; Late Maastrichtian age; plane-polarised light; KY/22/12 (GPS: 36S 0517448/3908964); j, Sample as above, including planktic foraminifera (P) and calcareous algae (C); k, Sample as above, showing *Nummulites* sp. (Palaeogene) in a bioclastic matrix (with calcite spar cement); l, Sample as above, showing well-preserved calcareous algae.

In the third outcrop studied, located in the west of the central range (near Sisklipos), the metamorphic rocks are intersliced with Trypa Group platform carbonates (Baroz, 1979) (Fig. 8c). Although the exposure is very poor within forest, sheared serpentinite locally contains small blocks of meta-siltstone, rich in quartz and fine-grained muscovite (Fig. 11b). The metamorphic unit is locally covered by a thin (<20 m-thick) interval (also poorly exposed) of medium-grained unmetamorphosed sandstones, which are corre-

lated with the Maastrichtian Kiparisso Vouno (Alevkaya) Formation, which has its type section nearby (Baroz, 1979; Chen et al., 2022b; Chen and Robertson, 2021; Glazer et al., 2021; Robertson et al., 2012a; Chen et al., 2021; Chen et al., 2022a; Robertson and Dixon, 1984; Robertson and Woodcock, 1984). In thin section, the sandstone is polymictic with a mixture of angular, sub-angular, sub-rounded, to well-rounded grains (Fig. 11c). Metamorphic grains include radiolarian chert (unmetamorphosed)

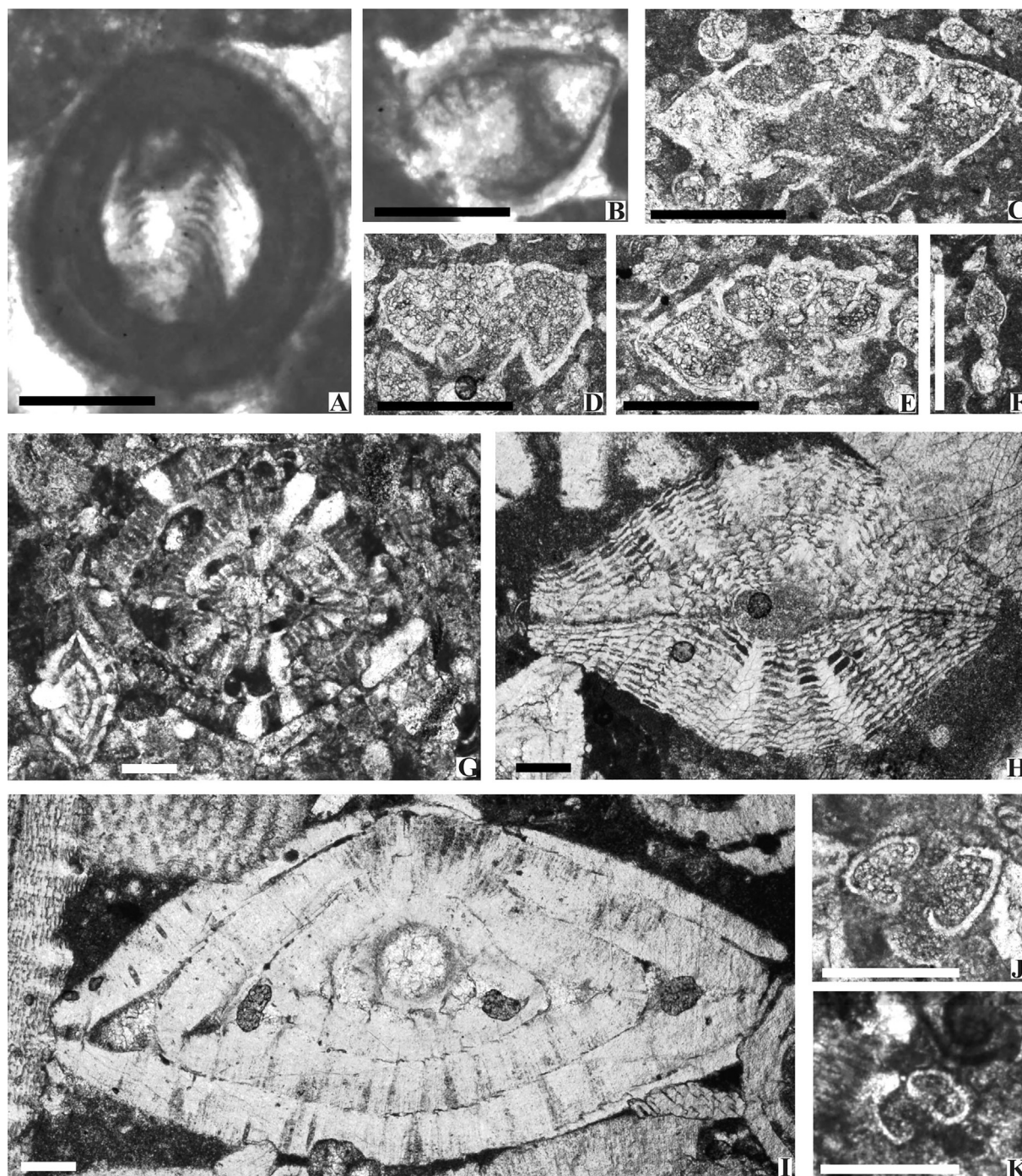


**Fig. 12.** Calcareous microfossils identified in thin section; see Supplementary Data, Table S1 for complete listing of taxa identified in samples. A, B. *Protopeneroplis striata*, KY22-1, KY22-2, reworked limestone clast, Middle-Upper Jurassic; C. *Globotruncanita stuarti*, D. *Globotruncana aegyptiaca*, E. *Globotruncana falsostuarti*, F. *Globigerinelloides subcarinata*, KY22-18, Maastrichtian; G. *Siderolites calcitrapoides* and *Sirtina orbitoidiformis* (bottom left), KY22-12, late Maastrichtian; H. *Discocyclus* sp., I. *Nummulites* sp., KY22-28, Palaeocene-Eocene; J. *Igorina* sp., K. *Pearsonites* cf. *P. broedermanni* KY22-13, Palaeocene-Eocene. Bar scales 0.25 mm.

(Fig. 11c), micaschist, polycrystalline quartz (paraquartzite), mylonite (Fig. 11d), meta-serpentinite (Fig. 11e), highly altered metalaava (Fig. 11c), rounded meta-micritic limestone (Fig. 11f) and angular brecciated marble (Fig. 11g) (see Robertson et al., 2012a for details).

Observations of several other very small exposures (e.g., near Besparmak (Pentadactylos) (Baroz, 1979) confirm that meta-serpentinite dominates the melange, together with minor occurrences of other ophiolite-related rocks (e.g., meta-gabbro).

More commonly within the central range the melange is absent and Trypa Group meta-carbonate platform rocks are unconformably overlain by basal breccias of the Malounda Formation, Lapithos Group (e.g., near the crest road, 2.5 km E of Kornos Mountain) (Robertson et al., 2012b). The basal breccias are dominated by clasts of marble that were derived from the Hilarion Formation and also dolomitic marble from the Sikhari Formation. Clasts of schist, serpentinite, meta-basites and meta-radiolarite are commonly observed, lithologies that are present in the melange (Ducloz,

1972; Baroz, 1979; Robertson et al., 2012a). This suggests that prior to erosion, the melange was originally thicker and more widespread above the Trypa Group Mesozoic carbonate platform.

#### 4.2.1. Petrography and geochemistry of meta-igneous blocks

Baroz (1979) recorded the presence of meta-basalt and metabasaltic tuff within the melange. Whole-rock chemical analysis of one sample of metatuff indicated a relatively high  $\text{TiO}_2$  (2.53 %) composition. Three other samples; i.e., volcanic breccia with amphibole, amphibolite and meta-gabbro contained < 0.25 %  $\text{TiO}_2$  (see [Supplementary Data](#), text).

During this study, eight samples from small exposures south-east of Beylerbeyi (Bellapais) (Fig. 8a) and NE of Değirmenlik (Kythrea) (Fig. 8b) were studied petrographically and geochemically. The following lithologies were identified in thin section (Fig. 13a–f): 1) *Glaucophane schist* (KY22-10 & 11), which shows nematoblastic textures with quartz, biotite, plagioclase, common green amphibole and glaucophane (Fig. 13 a,b). Glaucophane crystals display stubby, prismatic and acicular shapes. Plagioclase crystals, which are altered to albite and amphiboles, are rimmed by glaucophane. 2) *Garnet amphibolite* (KY22-14) which exhibits a

nematoblastic texture with amphibole, quartz, garnet, epidote and plagioclase. Preferential orientation of hornblende and plagioclase has created a well-developed foliation. Garnet porphyroblasts are accompanied by hornblende in the high-grade rocks (Fig. 13c). 3) *Microdiorite* (KY22-21), with microgranular to porphyritic textures, consists mainly of plagioclase and amphibole (Fig. 13d). The plagioclases are highly altered to epidote and the amphiboles to chlorite. 4) *Diabase* (KY22-25 & 26) displays a sub-ophitic texture, represented by plagioclase and clinopyroxene (Fig. 13e). Plagioclase and clinopyroxene crystals are partly altered to albite and amphibole, respectively, together with secondary epidote and chlorite. 5) *Basalt* (KY22-27) sample has an intersertal texture, mainly composed of plagioclase, clinopyroxene and olivine (Fig. 13f). Plagioclase is partly altered to albite, related to low-grade metamorphism or late-stage hydrothermal alteration. Clinopyroxene occurs either as subhedral to anhedral grains surrounded by plagioclase, or as infills of interstices between feldspars. Euhedral to subhedral olivine is transformed to iddingsite, together with secondary calcite, chlorite and opaque minerals.

The analyses of a total of eight samples of the basic volcanic and the meta-basic rocks are listed in [Supplementary Data \(Table S1\)](#).

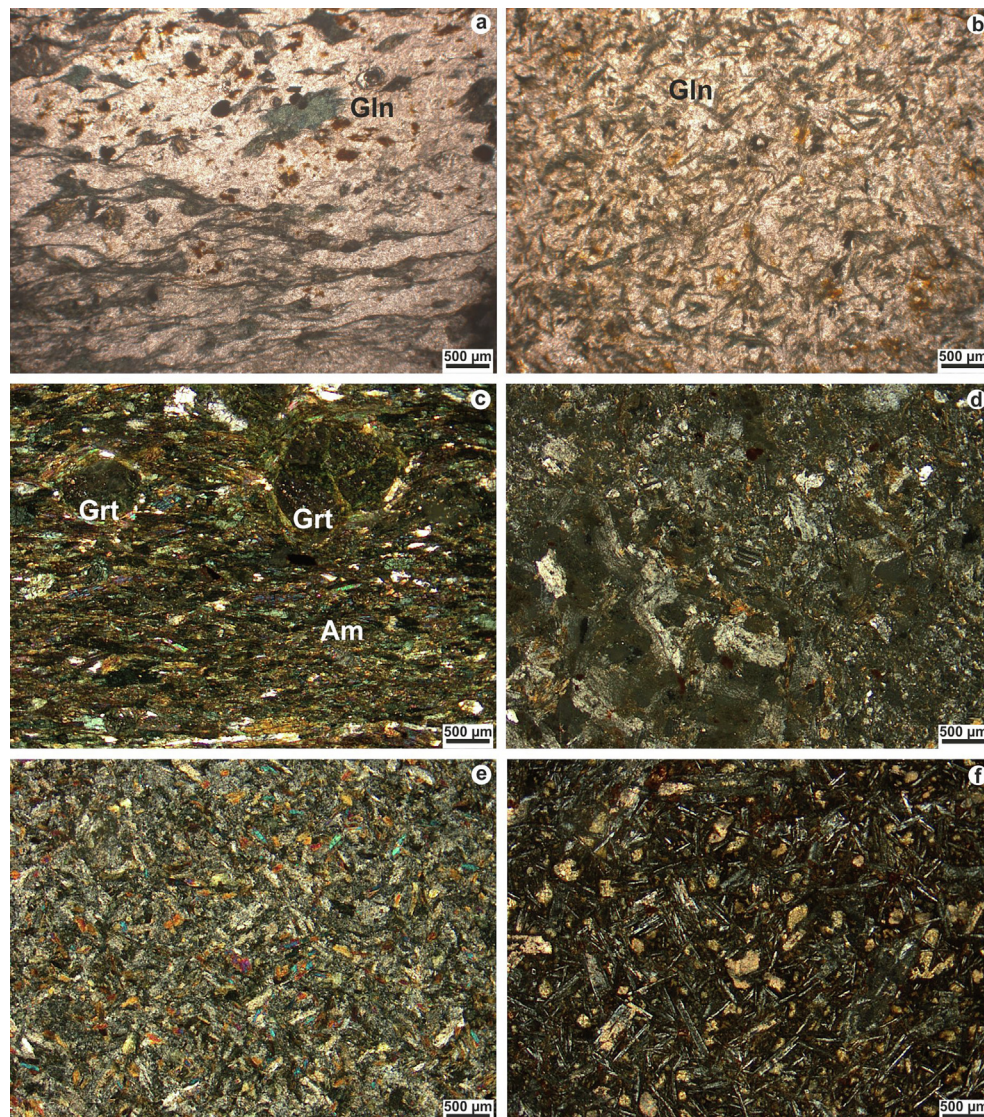


**Fig. 13.** Petrography of meta-igneous and mafic rocks from the latest Cretaceous ophiolitic melange. a, b, Photomicrographs of glaucophane schist with nematoblastic texture; c, garnet amphibolite with well-preserved garnet porphyroblasts accompanied by amphiboles; d, microdiorite; e, diabase; f, basalt. See text for discussion.

Because many elements are well known to be mobile during low-grade alteration (e.g., Hart et al., 1974; Humphris and Thompson, 1978), we focus on the chemically immobile elements including Ti, Nb, Th, Zr, Hf, Y and the REEs, which are widely used to identify rock groupings, petrogenetic trends and tectonic environments (e.g., Pearce and Cann, 1973; Floyd and Winchester, 1975, 1978; Pearce and Norry, 1979).

Overall, the basic igneous rocks fall into two geochemical groups. The first, composed of basic volcanics to meta-basic rocks, has low contents of Zr (3 to 27 ppm), Nb (0.4 to 2.74 ppm), Y (4.2 to 14.8 ppm), Th (0.06 to 0.28 ppm), Hf (0.14 to 0.75 ppm),  $TiO_2$  (0.17 to 0.54 wt%) and  $P_2O_5$  (0.01 to 0.04 wt%). In contrast, the second group is relatively 'enriched' (i.e., Zr: 175 to 187 ppm; Nb: 18.2 to 22.3 ppm; Y: 22 to 32.3 ppm; Th: 1.42 to 5.85 ppm; Hf: 3.64 to 4.53 ppm;  $TiO_2$ : 1.2 to 2.64 wt%;  $P_2O_5$ : 0.31 to 0.37 wt%) [Supplementary Data, Table S2].

The rock classification diagram of Pearce (1996), based on Zr/Ti versus Nb/Y, shows that both groups are exclusively basaltic in composition (Fig. 14a). The first group is represented by low Nb/Y ratios (0.05–0.1), whereas the second has higher Nb/Y ratios (0.35–1.01), indicating derivation from a more enriched (alkaline) magma source (Fig. 14a). The Y/Nb versus Y/Ta ratio/ratio plot of

incompatible elements characterises mantle source region of the volcanic rocks (Fig. 14b). The first group exhibits relatively high Y/Nb (10.5–21.7) and also Y/Ta (42–148) ratios similar to normal mid-ocean ridge basalts (N-MORB). The second group is transitional between enriched mid-ocean ridge basalts (E-MORB) and ocean island basalt (OIB) with lower Y/Nb (0.99–2.85) and Y/Ta (24–39) ratios (Fig. 14b). Chondrite-normalised rare earth element (REE) patterns for both groups are presented in Fig. 14c. REE patterns of N-MORB, E-MORB and OIB are included for comparison (Sun and McDonough, 1989). The REE concentrations of the first group varies from 0.84x to 11.42x chondritic values, whereas the second group varies from 4.31x to 108.86x chondritic values. The first group displays spoon-shaped REE patterns typical of boninites (Fig. 14c), with  $La_N/Sm_N$  and  $Sm_N/Yb_N$  ratios ranging from 0.59 to 1.76 and from 0.17 to 0.93, respectively. The N-MORB normalised multi-element spider diagram indicates that they are generally depleted in HFS (Nb, Zr, Ti, Hf, Y) but enriched in some of LIL elements (Cs, Rb, Ba, K) (Fig. 14d). The REE and multi-element patterns indicate that the first group is compositionally very similar to boninitic magmas, as found in the fore-arc regions of oceanic island arcs (Crawford et al., 1989; Falloon and Crawford, 1991; Shervais et al., 2021; Reagan et al., 2023). The second group exhi-

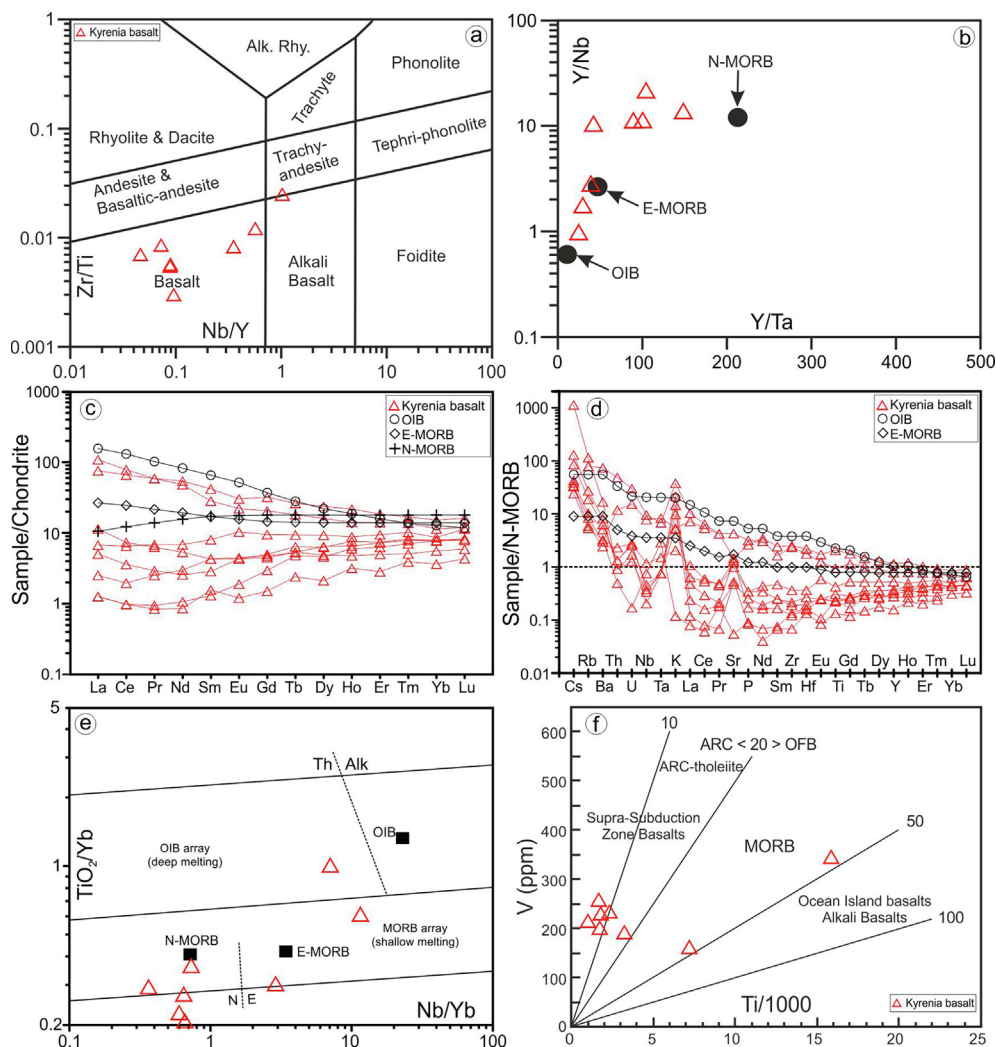


**Fig. 14.** Geochemistry of meta-igneous rocks from the latest Cretaceous ophiolitic melange (see Supplementary Data, Table S2 for analytical data). a, Rock classification diagram (after Pearce, 1996); b, Y/Ta versus Y/Nb plot for; c, d, sample versus chondrite and sample versus N-MORB diagrams; e, mantle source diagram utilizing the  $TiO_2/Yb$  vs. Nb/Yb (after Pearce, 2008); f, Ti versus V diagram for tectonic setting of the volcanic rocks (from Shervais, 1982). Source characteristics of N-MORB, E-MORB, OIB and normalising values are from Sun and McDonough (1989).



bits highly fractionated REE patterns ( $La_N/Yb_N = 2.04\text{--}9.54$ ) ranging from E-MORB to OIB (ocean-island basalt) in the N-MORB normalised multi-element diagram (Fig. 14c,d). The second group also displays coherent trends from light rare earth elements (LREEs) to heavy rare earth elements (HREEs), although with different degrees of fractionation from LREE to HREE (Fig. 14c). This can be explained by different degrees of partial melting of a compositionally similar mantle source at different depths (Fitton et al., 1991; Aldanmaz et al., 2000; Bağcı et al., 2020).

The tholeiitic rocks of the first, N-MORB-like group plot in the shallow melting array on the  $TiO_2/Yb$  versus  $Nb/Yb$  discrimination diagram of Pearce (2008) (Fig. 14e). In contrast, on the  $TiO_2/Yb$  versus  $Nb/Yb$  discrimination diagram (Fig. 14e), the more alkaline second group plots in the transitional field between the enriched shallow melting array (E-MORB) and the enriched deep melting array (OIB). These geochemical features are consistent with the chondrite-normalized REE and the N-MORB normalized multi-element patterns of both basic rock groups (Fig. 14c–e). On the V vs. Ti diagram the first group with low-Ti contents (0.17–0.54 %) is similar to island arc (IAT) tholeiites and/or to boninites (Shervais, 1982), whereas the second group with higher Ti contents (0.29–2.64 %) resembles E-MORB to OIB (Fig. 14f). The first group of metavolcanic rocks was derived from a depleted mantle source. The geochemical features suggest that they formed in an intra-oceanic subduction-related setting. The second group of metabasic and basic rocks was apparently derived from an enriched mantle source, transitional between E-MORB and OIB. The metabasic rock (garnet amphibolite/KY22-14) of the second group appears to have resulted from the metamorphism of an alkali basaltic rock.

#### 4.2.2. Tectonic significance of the melange

Taking the outcrops of the ophiolite-related and the metasedimentary rocks of the melange together: 1. They mainly occur sandwiched between the Trypa Group and the Lapithos Group, rather than more widely distributed between these units; 2. They represent a melange, in agreement with Glazer et al. (2021). However, not all of the lithologies (e.g., marble; schist) are potentially ophiolitic and therefore the term *ophiolite-related melange* is preferred here; 3. Sheared meta-serpentinite forms the matrix of the melange in the outcrops studied. However, schist (phyllite) could form the matrix locally because Ducloz (1972) mapped mainly schist; 4. The meta-serpentinite, meta-gabbro, meta-diorite and chemically depleted meta-basalts are interpreted as remnants of a supra-subduction zone ophiolite. In contrast, the E-MORB/OIB and meta-radiolarian cherts, taken together, were derived from an intra-plate setting; e.g., deep-water rift; 5. The evidence of HP-LT metamorphism, as represented by the presence of glaucophane schist, supports the interpretation of subduction based on the occurrence of crossite in meta-basite and in meta-chert (Beylerbeyi area) (Glazer et al., 2021); 6. One of the garnet amphibolites of the present study lacks a HP-LT imprint, either because it underwent only lower grade metamorphism, or because of retrograde metamorphism to greenschist facies; 7. The marble, schistose clastic sedimentary rocks and meta-siltstones have potential protoliths in the Mesozoic succession (Trypa Group), beneath the ophiolite-related melange; 8. The melange was rapidly eroded, probably sub-aqueously, as indicated by the abundance of clasts of lithologies similar to those in the melange within the overlying Malounda Formation (Lapithos Group). Specifically, the ophiolite-related melange was exhumed and transgressed by pelagic carbonates with clasts of Trypa Group-type meta-carbonate and meta-siliciclastic rocks prior to the Late Maastrichtian. Where melange is now absent, possibly as a result of erosion, Trypa Group carbonates were directly transgressed by the pelagic carbonates and breccias of the Malounda Formation. The exhumation and

transgression took place in relatively deep-water with no evidence of subaerial erosion or non-marine conditions during the Maastrichtian; 9. Maastrichtian-aged sandstones within the lower part of the Lapithos Group (Kiparissos Vouno Formation), where present, contain a similar range of lithologies (including mylonite) to the blocks in the melange; however, in contrast to the melange many of the grains are unmetamorphosed (e.g., radiolarite, basalt) suggesting a separate provenance, possibly from the Taurides, where similar lithologies are widely exposed (see Robertson et al., 2012a).

In the first tectonic model (Fig. 2b), the melange as a whole is Mesozoic in age, and represents an accretionary prism that was emplaced onto the Mesozoic carbonate platform (Trypa Group) related to regional northward subduction. The meta-boninite blocks show close similarities with boninitic volcanics, as described from the Troodos ophiolite (Pearce and Robinson, 2010; Woelki et al., 2018), from other eastern Mediterranean Upper Cretaceous ophiolites (Bağcı et al., 2008; Bağcı and Parlak, 2009; Saccani and Photiades, 2004, 2005; Beccaluva et al., 2005), from forearc areas of the SW Pacific region and from similar settings elsewhere (e.g., Reagan et al., 2023; Ishizuka et al., 2014, 2020). The meta-E-MORB and meta-OIB are chemically similar to volcanic rocks related to Triassic rifting of Neotethys, for example in the Mamonia Complex of SW Cyprus (Lapierre, 1975; Lapierre et al., 2007). Similar lithologies are present in the Güzelsu Corridor outcrop of the Antalya Complex to the north of Cyprus (Robertson and Waldron, 1990; Varol et al., 2007; Robertson and Parlak, 2020; Robertson et al., 2024), and also more extensively in the SW Antalya Complex (Maury et al., 2008; Bağcı et al., 2020). Compositionally similar volcanics also occur in the Koçali Complex (Adiyaman area) in SE Anatolia and elsewhere (Robertson et al., 2016b). The meta-amphibolites in the melange can be compared with the Upper Cretaceous metamorphic soles beneath ophiolites in the Taurus Mountains, including the Mersin, Beyşehir-Hoyran, Tekir-ova and Lycian ophiolites (Parlak et al., 1995, 2019; Çelik and Delaloye, 2003, 2006).

In the second tectonic model (Fig. 2e), the ophiolitic melange could represent an Upper Cretaceous accretionary complex that was emplaced, together with the Troodos ophiolite, onto the North African/Arabian continental margin, associated with westward rollback of the SSZ oceanic slab from S Neotethys located far to the NE/E. The melange blocks are also similar to the composition of the metamorphic sole, the deep-sea sediments (e.g., radiolarian chert) and some of the rift-related meta-igneous rocks that were emplaced from the S Neotethys onto the Arabian continental margin during the latest Cretaceous (e.g., Al-Riyami et al., 2002). However, there is no evidence of such emplacement towards the North African margin from the Eratosthenes Seamount to the south of Cyprus, where the Cretaceous-Cenozoic succession drilled by ODP lacks evidence of significant tectonic disturbance (e.g., Robertson, 1998).

In the third tectonic model (Fig. 2i), the metamorphic rocks within the melange are late Precambrian (Ediacaran) in age, representing fragments of a Cadomian SSZ-type ophiolite and related rock types (Glazer et al., 2021), in general agreement with Ducloz's (1972) original suggestion of a continental basement origin. This interpretation is consistent with the hypothesis that any continental crust beneath the easternmost Mediterranean deep basin is Cadomian-aged (Avigad et al., 2016). Meta-basic fragments of E-MORB composition are present within HP-LT melange of the Alanya Massif (Robertson and Parlak, 2020), where associated felsic intrusions are radiometrically dated as  $550.2 \pm 8.2$  Ma by the U/Pb method, using zircons (Çetinkaplan, 2018). Cadomian-aged subduction-related rocks, interpreted as a continental arc, or back-arc basin, are documented in several other areas of Turkey and also along the northern margin of the Arabian plate (e.g., Gürsu et al., 2015).

On the other hand, it is unclear how such deep crustal rocks could have been emplaced within the melange, together with metavasals and meta-sediments (e.g., radiolarites). Meta-ophiolites, as exposed in several parts of Egypt, appear to be considerably older (>720 Ma) than the above-mentioned felsic arc-related units (e.g., Stern and Ali, 2020). Glazer et al. (2021) include a concordia diagram for the three youngest concordant zircons from the metabasic rock (their Fig. 6a), which suggested a maximum age of magmatism of 550 Ma. However, it cannot be excluded that these grains represent inherited (redeposited) Precambrian zircons of widely varying ages, similar to the older grains in the sample. The photomicrograph of their metabasite (their Fig. 6c) might represent a metamorphosed mixed basic volcanoclastic-terrigenous sedimentary rock, rather than a homogenous basaltic rock (extrusion or intrusion). Consistent with this possibility, Baroz (1979) noted the presence of tuffaceous rocks associated with the metaigneous rocks in the same area (see Supplementary Data, text).

A late Neoproterozoic (Cadomian) age for the ophiolite-related melange cannot be ruled out based on the existing evidence. However, in the regional context, the range of lithologies (e.g., radiolarian chert), and the chemical compositions of the meta-basaltic blocks present point towards an origin of the melange as an Upper Cretaceous ophiolite-related subduction complex. An additional option is that both Precambrian and Mesozoic fragments are present within the melange but if so, these cannot currently be differentiated.

#### 4.3. Latest Cretaceous–Paleogene tectonic setting

Much debated is whether the Triassic–Cretaceous shallow-water carbonates (Trypa Group) of the Kyrenia Range, as exposed today, represent detached blocks (olistoliths) of variable size and shape, a coherent stratigraphical succession, or a combination of both. Ducloz (1972) interpreted the Trypa Group as an allochthonous unit that was thrust over the Lapithos Group during the Eocene (see Supplementary Data, text). In contrast, Baroz (1979) mapped the Trypa Group of the central and western ranges as a thrust-dissected stratigraphic unit, c. 40 km long. In the eastern range, variable sized detached blocks of Permian limestone (Kantara Formation) are well mapped within an Eocene sedimentary matrix, as represented by the Kalograia–Ardana Formation (Ducloz, 1972; Baroz, 1979; Robertson et al., 2012a).

McPhee and van Hinsbergen (2019) interpret the Mesozoic rocks of the central range as a dominantly coherent stratigraphical unit but, in contrast, they interpret small outcrops of Trypa and Lapithos group rocks along the northern margin of the central range as olistoliths within a matrix of Lapithos Group marine carbonates. On the other hand, Baroz (1979) presented 10 measured and dated sections of the Malounda and/or Ayios Nikolaos formations throughout the Kyrenia Range, which show thrust slices rather than exotic blocks, other than for the Eocene Kalograia–Ardana Formation. Also, studies of the associated volcanic rocks of the Malounda and Ayios Nikolaos formations have revealed a thrust-dissected succession rather than exotic blocks (Robertson et al., 2012b; Chen and Robertson, 2021). Relatively coarse-grained material within the pelagic carbonates of the Malounda and Ayios Nikolaos formations is restricted to localised metre-thick debris-flow intercalations derived from the Trypa Group, mainly near the base of the Malounda Formation.

To test the presence or absence of exotic blocks within the Paleogene succession, a critical outcrop was investigated along the northern margin of the central range, which includes olistoliths according to MCPhee and van Hinsbergen (2019). In agreement with Baroz (1979), the Trypa Group rocks in this area are dissected by south-vergent thrust faults (Fig. 15a,b, 16a) and cut by prominent c. NW–SE high-angle faults (Fig. 15a). The tectono-

stratigraphy of this area is illustrated as three discontinuous thrust sheets in Fig. 15b. The lowest of these thrust sheets exposes chert-bearing chalks typical of the Ayios Nikolaos Formation (the Malounda Formation is chert-free), passing upwards into debris-flow deposits that are correlated with the Middle Eocene Kalograia–Ardana Formation. A previously unmapped exposure of the Kalograia–Ardana Formation was discovered in a small, abandoned quarry near the track from the crest road to Lapta (GPS: 36S 0517544/3908615). The second thrust sheet comprises Hilarion Formation platform carbonates (Trypa Group) passing upwards into carbonate breccias (Fig. 15b, 16e); these breccias have a matrix of undeformed pink pelagic carbonate similar to the lithology at the base of the Malounda Formation elsewhere in the central range (e.g., 2.5 km E of Kivançtepe (Kornos Mountain)) (Robertson et al., 2012b). The third thrust sheet is made up of pink chert-bearing chalk of the Ayios Nikolaos Formation, passing upwards into debris-flow deposits of the Kalograia–Ardana Formation, with basal conglomerates of the Upper Eocene–Oligocene Belapais Formation above (Fig. 15a,c). The debris-flow deposits of the Kalograia–Ardana Formation locally contain clasts of tectonic breccia, typical of the metamorphosed Trypa Group meta-carbonates rocks beneath the Lapithos Group unconformity (Fig. 16f). The above three thrust sheets are cut and offset by c. NW–SE trending high-angle faults that show evidence of lateral (strike-slip) offsets. The exposures in this area are strongly affected by differential Pleistocene erosion; the NW–SE fault zones have been preferentially eroded creating valleys, with upstanding ‘highs’ of relatively intact Trypa Group rocks between them.

According to MCPhee and van Hinsbergen (2019), a structural origin for the ‘blocks’ would require the existence of numerous transecting faults (i.e., thrust-related transfer faults), which they did not identify. However, previous mapping does indeed indicate a plethora of such generally N–S transecting faults (Ducloz, 1972; Baroz, 1979; Harrison et al., 2004; Robertson and Kinnaird, 2016). Baroz (1979) maps the major c. N–S faults in this area as also cutting the Kythrea Group above. Along the north margin of the range, Ducloz (1972) maps some of the c. N–S faults as extending into the Kythrea Group. c. N–S faults are widespread elsewhere, particularly along the southern front of the range (McCay and Robertson, 2013; Robertson and Kinnaird, 2016), where they are related to the Late Miocene deformation, and they are also found within the Mesaoria Basin to the south (north of the Ovgos (Dar Dere) Fault) (Harrison et al., 2004). There is therefore no evidence that the c. N–S faults as a whole are sealed by an ‘upper Lapithos’ stratigraphy, as suggested by MCPhee and van Hinsbergen (2019).

A further problem is that MCPhee and van Hinsbergen (2019) do not present lithological or age data to indicate which part of the Lapithos Group their olistoliths are located within (their summary logs show them as mainly in the lower part). However, as noted above, the succession is well documented to be divisible into the Maastrichtian–Palaeocene Malounda Formation, the Palaeocene–Lower Eocene Ayios Nikolaos Formation and the Middle Eocene Kalograia–Ardana Formation (Fig. 4) (Baroz, 1979; Robertson and Woodcock, 1984; Robertson et al., 2102, 2013). Even without microfossil dating, the two lower formations are distinguishable in the field, because red nodular chert of diagenetic replacement origin is mainly restricted to the stratigraphically higher Ayios Nikolaos Formation (Robertson et al., 2014).

The tectonic versus gravitational (olistostromal) origin of the block-like exposures was tested elsewhere along the northern margin of the central range. Farther east, the previously mapped Trypa Group outcrop, on which Hilarion castle (GPS: 36S 0525548/3907764) is perched, was confirmed to be a fault-bounded thrust sheet rather than an olistolith. The main reasons are that the dip and dip direction of the carbonate rocks are consis-

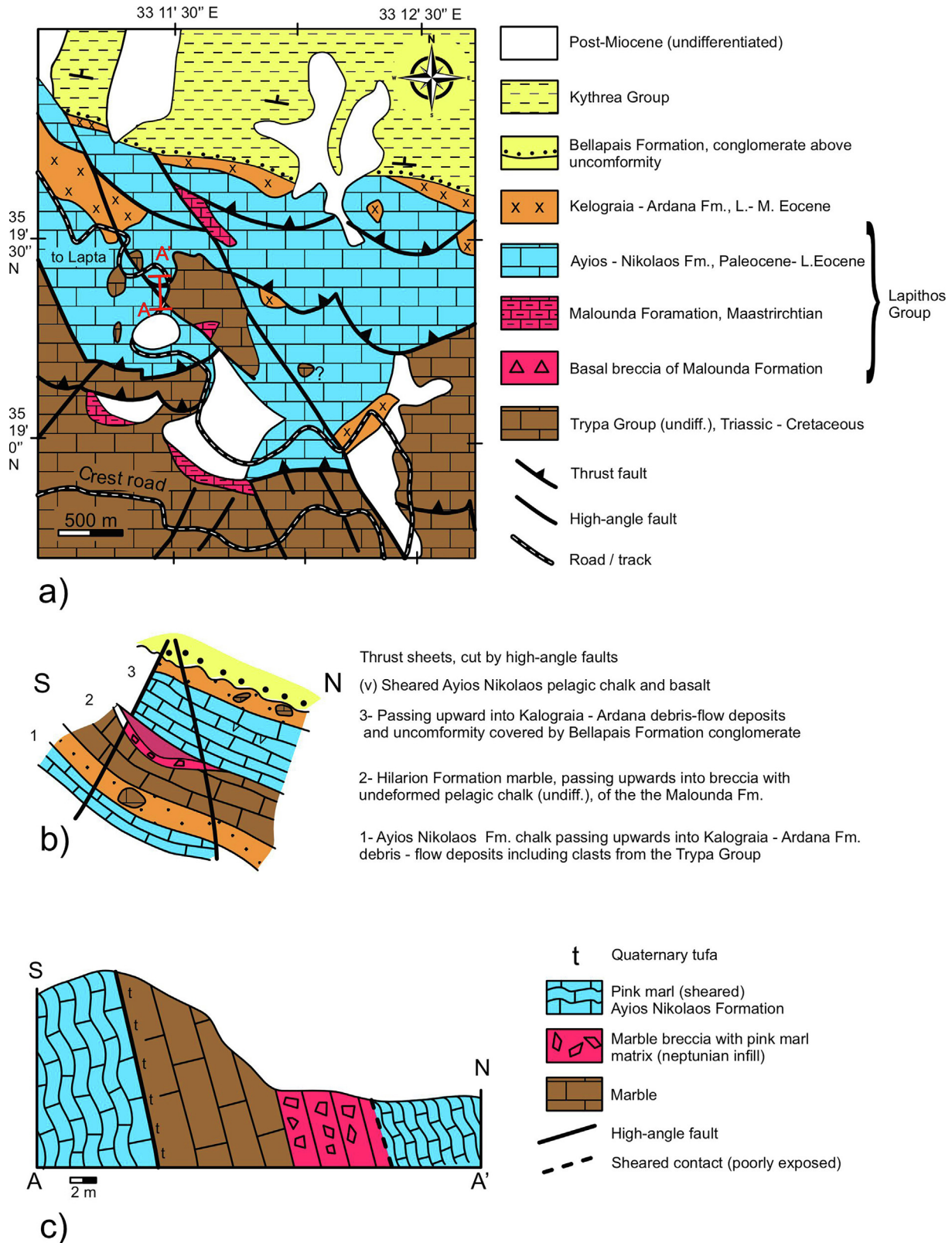


**Fig. 15.** Geological map and cross sections of a critical area along the northern flank of the central range; a, geological map of SE of Lapta (Lapithos); b, rock-relations diagram of the above area; c, cross-section of the same area.

tent with the adjacent Trypa Group, and there is no evidence of a sedimentary matrix to a possible block.

Consistent with previously studies of the central and western ranges (Baroz, 1979; Robertson et al., 2014), the present study of

the northern margin of the central range did not reveal olistoliths within the Malounda and Ayios Nikolaos formations (Fig. 15a). Olistoliths are restricted to within debris-flow deposits of the Middle Eocene Kalograia-Adana Formation, as exposed in the eastern

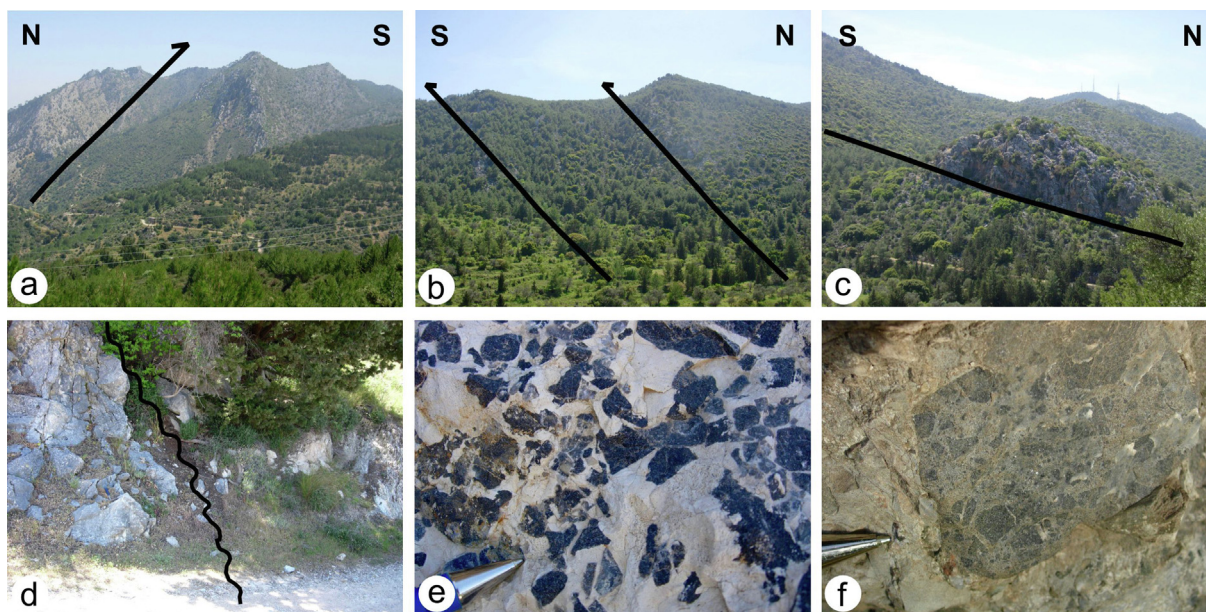


**Fig. 16.** Photographs of thrust and fault-controlled Trypa-Lapithos Group outcrop; N flank of the central range. a, View E to imbricated Trypa Group-Lapithos Group succession; NE of Lapta; b, View W of imbricated Trypa Group (ridges)-Lapithos Group succession; NW of Lapta; c, Example of one of many c. N-S high-angle faults that dissect the thrust stack; dirt road S of Lapta; d, Unconformity between Hilarion Formation (mainly Jurassic) to left, and Lapithos Group (right), pinkish (GPS: 36S 0517448/3908964); e, Basal breccia of the Lapithos Group, near the base of the thrust sheet in d (GPS: 36S 0517544/3908615); f, Clast of tectonically brecciated marble in basal conglomerates/breccias of the Bellapais Formation (Kythrea Group), near Lapta (GPS: 36S 0516279/3909903).

range, the Karpaz (Karpas) Peninsula, and also locally in the western ranges (e.g., E of Kayalar (Orga)) (see [Supplementary Data, Fig. 1 S1 a,b](#)). The presence of the small exposure of the Kalograia-Ardana Formation, with one or more olistoliths derived from the Trypa Group, as identified along the northern margin of the central range ([Fig. 15a, b](#)), suggests that the Kalograia-Adana Formation was originally more widespread compared to its present outcrop.

The latest Cretaceous–Early Eocene tectonic development of the Kyrenia Range is explained differently in tectonic models 1, 2 and 3.

In model 1, the Maastrichtian–Lower Eocene succession, which is dominated by pelagic carbonates and basic volcanics, accumulated in a volcanically active extensional (or transtensional) basin. Dominantly within plate-type basaltic volcanics erupted during the Maastrichtian in a deep-water carbonate-depositing setting (Malounda Formation), and later again during the Palaeocene–Early Eocene (Ayios Nikolaos Formation) ([Pearce, 1975; Robertson and Woodcock, 1986](#)). An incipient back-arc setting along the southern margin of the Tauride crustal blocks was proposed by [Chen and Robertson \(2021\)](#).

In model 2, passive margin deposition resumed after emplacement of the Troodos ophiolite onto the distal N African continental margin. The exhumation of the Trypa Group took place along a north-down extensional detachment, such that the Lapithos Group represents a supra-detachment basin ([McPhee and van Hinsbergen, 2019](#)). The margin was unstable and blocks of shallow-water carbonate rocks repeatedly slid downslope from the Trypa Group substratum, giving rise to large (up to 100s m-sized) exotic blocks within a matrix of contemporaneous deep-water carbonates (Lapithos Group) ([Fig. 15a,b](#)). On the other hand, the new evidence presented above from the central range does not support gravity emplacement of detached blocks (‘olistoliths’) during the Maastrichtian–Eocene accumulation of the Lapithos Group. Also, it is unclear why a supra-detachment basin was so magmat-

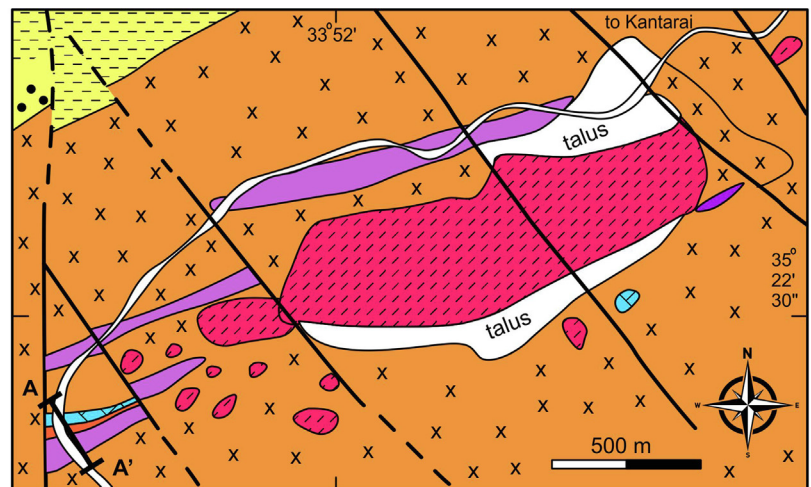
ically active during much of Maastrichtian–Paleogene time ([Chen and Robertson, 2021](#)).

In model 3, the allochthonous origin of the Kyrenia Range is supported by the relative abundance of Carboniferous detrital zircons ([Glazer et al., 2021](#)), as observed in the Maastrichtian sandstones of the Kiparisso Vouno Formation ([Chen et al., 2019, 2022](#)). However, this model does not specify any particular contemporaneous setting.

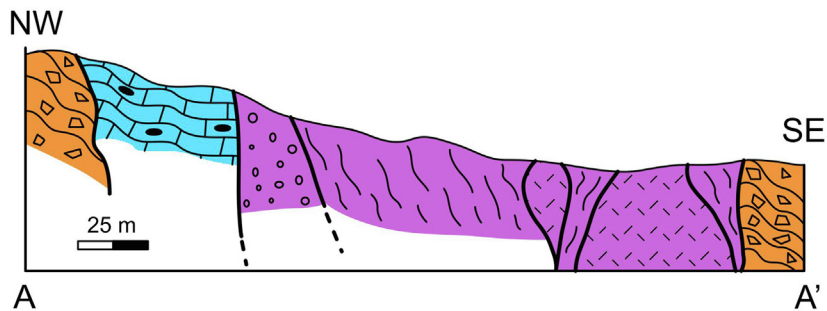
#### 4.4. Middle Eocene mass-transport unit: Active or passive margin?

An important Middle Eocene mass-transport unit (olistostrome) dominates the Kalograia-Ardana Formation ([Baroz, 1979; Robertson and Woodcock, 1986; Robertson et al., 2014](#)), as noted above. This mass-transport unit is mainly exposed in the eastern range and the Karpaz (Karpas) Peninsula, stratigraphically above the Ayios Nikolaos Formation. There are also smaller outcrops in the central range (e.g., [Fig. 16a,b](#)) and in the western range that have hitherto received little attention ([Supplementary Data, Fig. S1a,b](#)), again overlying the Ayios Nikolaos Formation. In the western range, along the coast (E of Kayalar), the Kalograia-Ardana Formation is dominated by debris-flow deposits containing a small number of shallow-water limestone blocks (up to 10s m across) ([Fig. 19k](#)). The formation is unconformably overlain by conglomerates and sandstones of the Bellapais Formation ([Fig. 19l, 20a](#)). In the central range, the uppermost levels of the Kalograia-Ardana Formation include detached blocks of pillow lava (highly altered), radiolarian chert and serpentinised harzburgite ([Fig. 19a](#)).

The matrix of the Kalograia-Ardana Formation is mainly pelagic carbonate and marl. [Hakyemez et al. \(2002\)](#) listed an assemblage of planktic foraminifera within the chalk-marl matrix, which they interpreted as Middle Eocene (Bartonian; c. 41.2–37.7 Ma). Calcarenes yielded Lutetian–Priabonian ages (Middle–Late Eocene), mainly based on benthic foraminifera. The assemblages of planktic and benthic foraminifera, and also of calcareous nannoplankton,



a)

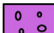






b)

**MAP LEGEND**

	Post - Miocene including talus
	Kythrea Group, Eocene - Miocene
	Bellapais Formation, Eocene
	Ophiolitic blocks in Kalograia-Ardana Fm.
	Kalograia - Ardana Fm.
	Ay. Nikolaos Fm., Paleocene - Eocene
	Kantara Fm., Permian

**SECTION LEGEND**

	Serpentinite debris - flow unit (sheared)
	Harzburgitic serpentinite (sheared)
	Basalt (sheared)
	Polimicritic debris - flow, Kalograia - Ardana Fm.
	Chalk & Marl, Ay. Nikolaos Fm.

**Fig. 17.** a, geological map, and b, cross-section of one of the best exposures of the Eocene mass-transport unit (Kalograia-Ardana Formation) in the eastern Kyrenia Range. Note the strong tectonic dislocation and the intercalations of sheared serpentinite. The outcrop is cut by c. NE-SW high-angle faults that are typical of the Kyrenia Range.

indicate an overall Middle Eocene (Lutetian-Bartonian) age for the background marls and chinks of the Kalograia-Ardana Formation (Robertson et al., 2012a). In the western range, the Kalograia-Ardana Formation includes detached blocks of neritic limestone (up to 10s m across); limestone clasts in associated mass-flow conglomerates contain Middle-Upper Jurassic benthic foraminifera (Fig. 12A,B; Supplementary Data, Table S1) suggesting derivation from the Hilarion Formation (Trypa Group) or a similar unit elsewhere.

The Kalograia-Ardana Formation in the eastern range begins with deep-water marls, chinks and turbidites (rich in serpentinite debris). The deposits become increasingly coarse-grained and thick bedded, and then pass upwards into large-scale mass-flow depos-

its (Robertson et al., 2012a). The accumulations in the eastern range and the Karpaz (Karpas) Peninsula include prominent detached blocks (olistoliths) of Permian shallow-water limestones (Kantara Formation) (Baroz, 1979; Robertson and Woodcock, 1986). A Late Permian age is documented based on benthic foraminifera including *Neoschwagerina* sp., *Verbeckina* sp., *Glomospira* sp., *Dagmarita* sp., *Globivalvulina* sp. and *Geinitzina* sp. (Hakyemez et al., 2002). In contrast to earlier suggestions (Baroz, 1979; see Robertson et al., 2013) Carboniferous is not confirmed. In the Antalya Complex to the north and northwest, Late Permian is transgressive on Early Palaeozoic, without intervening Carboniferous. In contrast, Carboniferous is well developed within nappes emplaced from the north (Bolkar and Hadim (Aladağ)) (Özgül, 1984a, 1997;

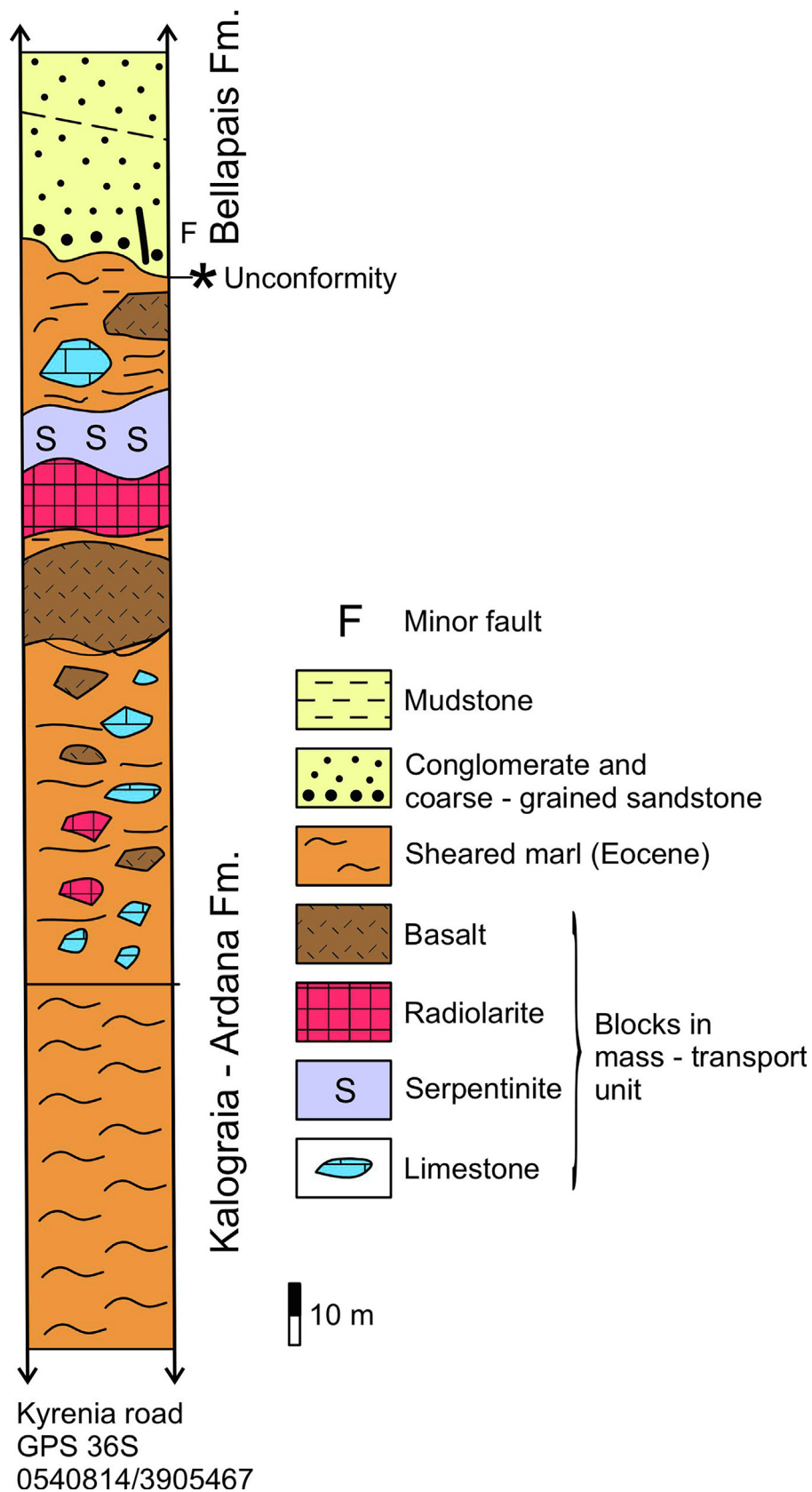
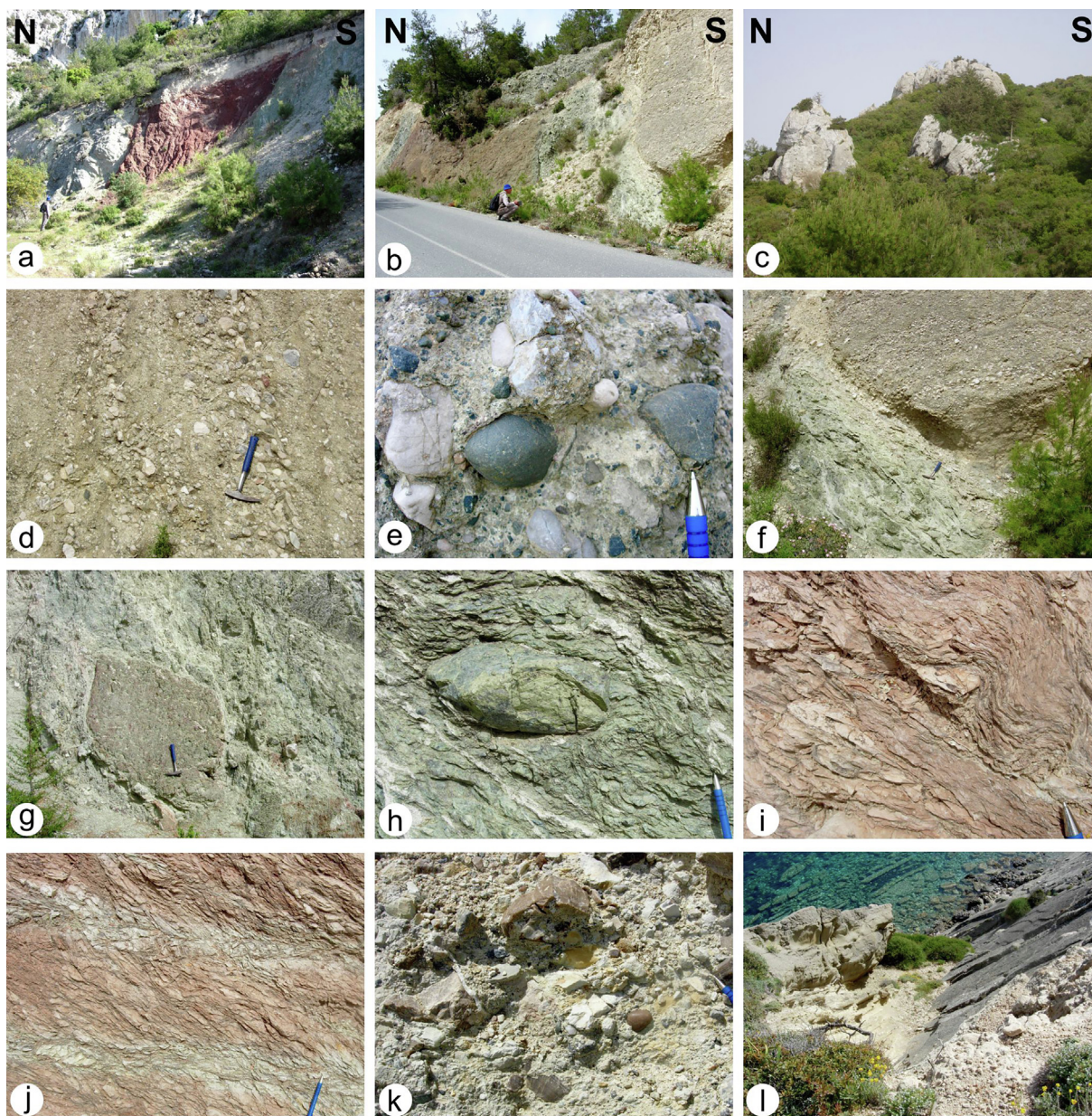


Fig. 18. Summary log of the mass-transport unit (Kalograia-Ardana Formation) in the central Kyrenia Range. Note the transition from mainly marl to matrix-supported debris-flow conglomerates and finally to large bodies (olistoliths) emplaced by gravity sliding; Girne (Kyrenia) road near Beşparmak (Pentadactylos).



**Fig. 19.** Field photographs of the L-M. Eocene Kalograia-Ardana Formation in the western, central and eastern Kyrenia Range. a, Debris-flow deposits including deformed block (olistolith) of red radiolarite; Kyrenia-Nicosia road cutting, near Besparmak (Pentadactylos), central range (GPS: 36S 0540814/3905467); b, Intersliced basalt, serpentinite (ophiolitic) and debris-flow deposits; road to Kantara, near ridge crest (GPS: 36S 0578309/3915495) (see Fig. 17a,b); c, Blocks of Permian limestone (Kantara Formation) in a matrix of Eocene debris-flow deposits, tree covered; near Kantara castle, eastern range (see Fig. 17a,b); d, Vertically dipping mass-flow deposits, dominated by pelagic limestone clasts derived from the Lapithos Group; Kantara main road, near ridge crest (near e); e, Debris-flow deposit interbedded with d above, locally including well-rounded chert clasts (near d) (see Fig. 17b); f, Detail of b, showing thrust contact between highly sheared serpentinite (lower) and bedded debris-flow deposit (upper right); g, Weakly bedded debris-flow deposit; dominated by sheared serpentinite; crosscut by a later shear fabric; near e; h, Sheared serpentinitised harzburgite cut by later stage shear fabric (calcite filled); near e; i, Sheared and folded pink marl (Lapithos Group); near e; j, Highly sheared pink marl (Lapithos Group), crosscut by a later shear fabric (near e); k, Massive debris-flow deposit full of mainly angular clasts of chert and chalk in a pebbly calcareous matrix; near a (GPS: 36S 0500498/3913915); l, Interbedded debris-flow conglomerate (lower right), sandstone with 'floating' rounded chalk clasts (dark; upper right) and bedded sandstones (mass-flow deposits and high-density turbidity current deposits (left); W of Kayalar (Orga), western range (GPS: near 36S 0500464/3913915). (For interpretation of the references to colour in this figure legend, the reader is referred to the web version of this article.)

Mackintosh and Robertson, 2014; Robertson et al., 2020). Baroz (1979) and Hakyemez et al. (2002) also report faunal elements of Late Permian, Late Triassic, Norian-Rhaetian, Carnian-Early Jurassic?, Late Jurassic-Early Cretaceous and Late Cretaceous (Maastriichtian) age, mainly based on the identification of benthic foraminifera.

In the eastern range (Fig. 17) and locally in the central range (Fig. 18), the Kalograia-Ardana Formation includes blocks (up to 10s of km in size) and small thrust sheets (up to several km long)

of ophiolitic rocks, including serpentinitised harzburgite, gabbro and basalt (Ducloz, 1972; Baroz, 1979; Robertson and Woodcock, 1986). There is no ophiolite as such (cf. Aldanmaz et al., 2020) but instead only variable-sized ophiolitic blocks and small slices that were transported to their present position within the gravitational Kalograia-Ardana Formation. Geochemical evidence from peridotites of the Upper Cretaceous Neotethyan ophiolites in Southern Turkey and from the ophiolitic blocks and small slices in northern Cyprus is interpreted to indicate that they experienced

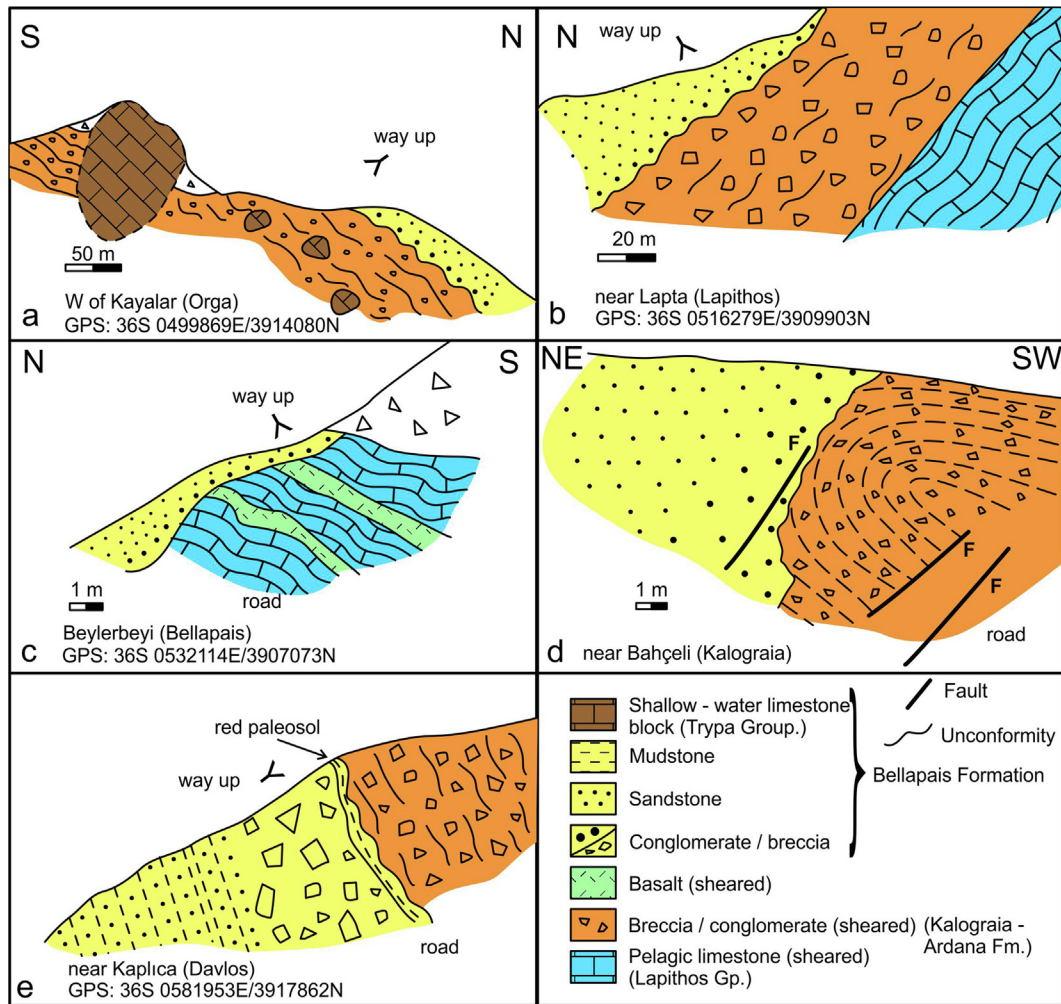


**Fig. 20.** Field sketches of key field relations between the Middle Eocene Kalograia-Ardana Formation and the unconformably overlying Upper Eocene-Oligocene Bellapais Formation (Kythrea Group). a, Deformed debris-flow deposits with a olistolith of Mesozoic carbonate rocks (Trypa Group), overlain by stratified basal conglomerates of the Bellapais Formation; western Kyrenia Range; b, Similar field relations in the central range; c, Angular discordance between the Kalograia-Ardana Formation and the unconformably overlying Bellapais Formation in the central range; d, Folded Kalograia-Ardana Formation overlain by stratified Bellapais Formation in the central range, near Bahçeli (Kalograia) (GPS: 36S 0557384/3910600); e, Deformed stratified breccia-conglomerate of the Kalograia-Ardana Formation overlain by unusually coarse basal breccia-conglomerate (undeformed) of the Bellapais Formation.

two-stage melt depletion, first at a mid-oceanic spreading centre, and secondly related to fore-arc spreading during subduction initiation (Aldanmaz et al., 2020). Melt compositions evolved to arc tholeiites and then to boninites, as in many of the Upper Cretaceous eastern Mediterranean ophiolites (Bağcı et al., 2008; Bağcı and Parlak, 2009; Aldanmaz et al., 2020).

Basaltic clasts of boninitic composition, which are commonly well rounded, occur within the Kalograia-Ardana Formation especially in the eastern range, where they were interpreted as the remnants of an eroded fore-arc ophiolite (Robertson et al., 2012a; McCay, 2011). The boninite clasts were probably derived from the same ophiolite as the nearby blocks and small thrust sheets of ophiolitic rocks in the eastern range. The erosion and sedimentary transport of the boninitic extrusive clasts are likely to have taken place in a high-energy fluvial and/or coastal-marine setting, prior to incorporation into the mass-transport facies of the Kalograia-Ardana Formation.

During this study, the upper part of the Kalograia-Ardana Formation was restudied in road sections in the eastern range, where the ophiolitic rocks and the Permian limestones (Kantara Formation) are well exposed (Fig. 17a,b, Fig. 18). The Permian limestone

blocks in this area range from approximately equidimensional to elongate (Fig. 19c). In contrast, the ophiolitic rocks form narrow elongate outcrops dominated by variably sheared serpentinite (Fig. 19b), consistent with an origin as small thrust sheets that were emplaced within the gravitational Kalograia-Ardana Formation (Fig. 18).

The Kalograia-Ardana Formation contains variable abundances of clasts that were potentially derived from the Lapithos Group (e.g., chalk, marl, basalt), from the Trypa Group (e.g., marble, dolomite), from the Kantara Formation (Permian limestone), and from unmetamorphosed ophiolite-related rocks including basalt, diabase, gabbro, radiolarian chert and serpentinite (Fig. 19d). The clasts range from highly angular to very well-rounded (including chert), even within individual bedded units (Fig. 19e).

The sedimentary debris-flow accumulations are intercalated with sheared serpentinite (Fig. 19b,f). In places, the serpentinite is conglomeratic and includes non-ophiolitic clasts (e.g., limestone) showing that sea-floor reworking has taken place. More or less sheared serpentinites are tectonically interleaved in places to form phacoidal blocks (Fig. 19g,h). In places, the serpentinite is intensely sheared, with the two-stage development of a penetrative shear



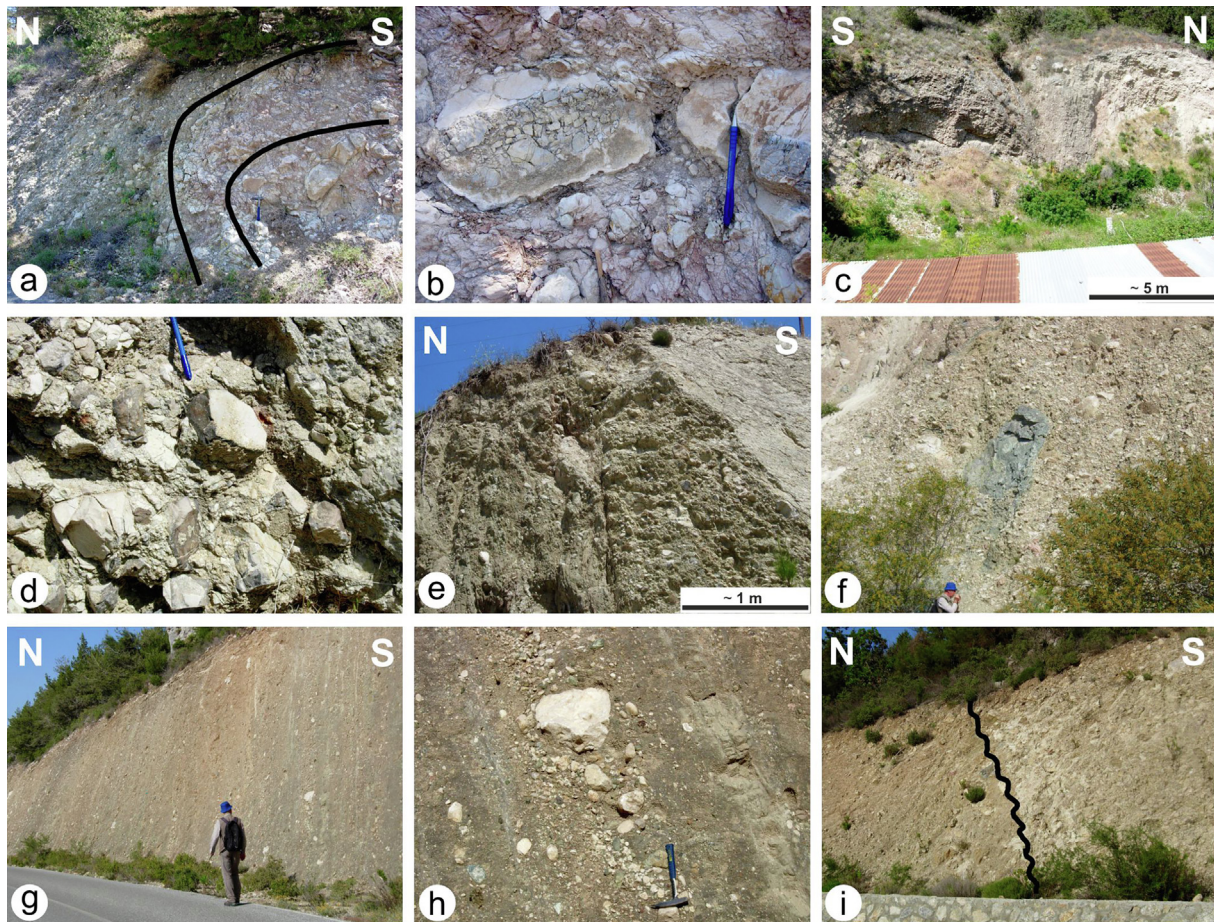


**Fig. 21.** Field photographs of the unconformity between the Upper Cretaceous-Eocene Lapithos Group and the Upper Eocene-Upper Miocene Kythrea Group, focussing on the more highly deformed nature beneath the unconformity compared to above it. a, Folded (N-verging) matrix-supported conglomerates including pink chalk, chert and nummulitic limestone; Eocene Kalograia-Ardana, overlain unconformably by unfolded clast-supported conglomerates of the Bellapais Formation, near Bahçeli (Kalograia) (GPS: 36S 0557384/3910600); b, Sheared debris-flow deposits (Middle Eocene Kalograia-Ardana Formation) below the above contact; diagenetic replacement chert is highly brecciated, whereas adjacent pink marl is highly sheared. The angular nature of the clasts indicates that they were tectonically fragmented before being incorporated into the mass-flow, location as a; c, Open folded but otherwise little deformed conglomerates of the Bellapais Formation, location near a; d, Chert-rich debris-flow deposits (Middle Eocene Kalograia-Ardana Formation); chert-bearing clasts are mostly angular; Geçitkale (Lefkoniko)-Girne (Kyrenia) road, SE side of gorge (GPS: 36S 0564951/3912525); e, Steeply dipping (overturned) near-basal conglomerates of the Bellapais Formation; bedding becomes more distinct up section (to left); cut by steep faults with minor shear displacement; near d; f, Unsorted massive breccia-conglomerate near the base of the Bellapais Formation; includes large block of serpentinitised harzburgite; road cutting S of Kaplica (Davlos) (GPS: 36S 0581953/3917862); g, Weakly bedded, sub-vertical conglomerate, c. 10 m higher in the local sequence than g, above; note lack of deformation; h, Detail of the conglomerate in g; interbedded debris-flow deposits and pebbly sandstone without way-up indication (i.e., no preferential grading); i, Overturned unconformity between mass-flow deposits of the Kalograia-Ardana Formation and the basal breccia-conglomerate of the Bellapais Formation. The contact is also locally sheared related to Late Miocene deformation (GPS: 36S 0577773/3916022). (For interpretation of the references to colour in this figure legend, the reader is referred to the web version of this article.)

fabric (Fig. 19h). Associated, pelagic marls are also strongly sheared and folded, again showing two-stage deformation (Fig. 19i,j).

The Middle Eocene development is interpreted differently in the three tectonic models.

In tectonic model 1, the south-Tauride hypothesis (Fig. 2c), the mass-transport unit is interpreted as representing an Eocene convergent margin setting, either a subduction complex, a deformed foreland basin, or a combination of both (Robertson et al., 2012a; Robertson and Dixon, 1984; Robertson and Woodcock, 1984). The Eocene mass-transport unit was derived from the Kyrenia Range and, or from the Taurides to the north (Robertson et al., 2012a). Much of the clastic material, especially the chalk and chert and the meta-carbonate rocks, could have been derived locally from the Lapithos and Trypa groups. However, the clasts include some lithologies that are absent from the intact succession within the Kyrenia Range (Trypa Group). These include quartz-muscovite-rich quartzarenites rich in plant debris, which are typical of Mid-Late Triassic turbidites of the Taurides generally (e.g., Gutnic

et al., 1979) and also the Mamonia Complex in SW Cyprus (e.g., Robertson and Woodcock, 1979; Torley and Robertson, 2018). The unmetamorphosed ophiolite-related rocks including the serpentinitised harzburgite, basalt (including boninite) and radiolarian chert were also derived from outside the Kyrenia Range as now exposed. These ophiolitic rocks could not have been reworked from the ophiolite-related melange beneath the Lapithos Group as, in contrast, this is metamorphosed (see above).

The ophiolite rocks in the Kalograia-Ardana Formation (e.g., boninite) have counterparts in the Tauride Mountains to the north including in the Mersin area (Parlak et al., 1996; Parlak and Robertson, 2004; Ishimaru et al., 2018; Saka et al., 2019; Aldanmaz et al., 2020), Hatay (Bağcı et al., 2008; Karaođlan et al., 2013; Aldanmaz et al., 2020; Chen et al., 2020; Şimşek et al., 2023) and Baer-Bassit (N Syria) (Al-Riyami et al., 2002). The evidence of two-phase south-verging deformation, as documented in the ophiolitic rocks of the Kalograia-Ardana Formation, is consistent with regional convergence and/or collision, as is known to

have affected the Taurides (e.g., Özgül, 1984a) but not the Troodos ophiolite (which also includes boninites) to the south (e.g., Pearce and Robinson, 2010).

In tectonic model 2, the Kalograia-Ardana Formation is interpreted as the result of large-scale down-margin sliding/slumping from a proximal to a more distal setting (from S to N) along the North Africa margin, essentially a magnification of the setting inferred for Maastrichtian-Early Eocene time (Fig. 2f). Exotic material slid down a tectonically unstable slope that was still located along the N African continental margin (Fig. 2f). However, in this case the derived material should have been mainly from the upper parts of the succession (i.e., Lapithos Group chalk and basalt) rather than from all levels of the Kyrenia Range stratigraphy including Permian limestone, as observed. Also, it is questionable in this interpretation how some of the clasts (e.g., chert) could have become very well rounded in such a marine setting before being included in the mass-transport unit (Fig. 19e). In model 2, the ophiolitic rocks represent remnants of the Troodos ophiolite that was overthrust during the latest Cretaceous (Fig. 2f). In line with this interpretation, Aldanmaz et al. (2020) suggest that the ophiolitic rocks represent a remnant of the Troodos ophiolite that was exhumed together with the Trypa Group. However, as noted above, the ophiolite-related rocks in the Kalograia-Ardana Formation are unmetamorphosed in contrast to the ophiolite-related rocks in the underlying melange (see above). Direct derivation from the Troodos ophiolite to the south is also unlikely as this was covered by marine sediments effectively until the Pleistocene (e.g., Robertson et al., 1991b).

In tectonic model 3, the Eocene was the time when the entire Kyrenia Range was emplaced from outside the present E Mediterranean region (Glazer et al., 2021) (Fig. 2j). As a result, the provenance changed drastically and the supply of Upper Palaeozoic zircons was greatly curtailed in younger formations (Shaanan et al., 2021; Chen et al., 2019, 2022). In the above tectonic model, the Kalograia-Ardana Formation could represent mass-wasting from the regional-scale allochthon as it approached its present position. However, the stratigraphy of the Kyrenia Range does not match that of any known areas, other than adjacent areas near the northern margin of the E Mediterranean basin and its extension into SE Turkey. For example, potential source areas within Palaeotethys or the adjacent Anatolides (north of the Taurides) lack Cenozoic deep-sea pelagic carbonates and related volcanic rocks as exposed within the Lapithos Group (e.g., Robertson et al., 2009; Pourceau et al., 2010).

#### 4.5. Late Eocene-Oligocene structural-stratigraphical break or continuing passive margin deposition?

In view of the major differences in interpretation (i.e., presence or absence of Eocene thrusting), well-exposed contacts between the Lapithos and Kythrea groups were studied, mainly along the north margin of the range because this area was much less affected by Late Miocene deformation than the southern margin of the range. The Kythrea Group along the northern margin generally rests on any one of the three formations of the Lapithos Group but the contact is commonly faulted related to Late Miocene deformation (see below).

Along the coast in the far northwest (E of Kayalar; western range), the deformed Kalograia-Ardana Formation mass-transport unit is overlain, with a minor angular discordance, by texturally and compositionally contrasting bedded conglomerates (clast-supported) of the Bellapais Formation (Fig. 19k,l). At Lapta, similarly deformed Kalograia-Ardana Formation debris-flow deposits are disconformably overlain by contrasting undeformed, stratified, clast-supported Bellapais Formation conglomerates (Fig. 20b). Near Beylerbeyi, strongly deformed Kalograia-Ardana Formation

sheared debris-flow deposits (Fig. 11i-l; Supplementary Data, Fig. 1j,k) are unconformably overlain by nearly undeformed Bellapais Formation basal conglomerates (Fig. 11a; 20c). Limestone clasts contain both Upper Maastrichtian and Palaeocene-Eocene benthic foraminifera (Fig. 12 J,K), showing that detritus was derived from different levels of the post-Trypa Group stratigraphy.

At a key locality further east, near Bahçeli, deformed debris-flow deposits of the Kalograia-Ardana Formation were folded (with northerly vergence), sheared and then unconformably overlain by contrasting, virtually undeformed and compositionally different stratified conglomerates making up the basal Bellapais Formation of the Kythrea Group (Fig. 20d, 21a,c). The Kalograia-Ardana Formation at this location is cleaved and diagenetic replacement chert (highly competent) is strongly brecciated (Fig. 21b). Deformed Kalograia-Ardana Formation mass-flow deposits contain highly angular clasts of diagenetically formed chert, derived from the subjacent Ayios Nikolaos Formation (Fig. 21d). Limestone clasts in the overlying basal conglomerates of the Bellapais Formation include Palaeocene-Eocene large foraminifera (Fig. 12H-I; Supplementary Data, Fig. S1), pointing to local derivation from the Kalograia-Ardana Formation. The overlying basal breccia-conglomerate of the Bellapais Formation differs in texture and composition from that of the underlying Lapithos Group; also, deformation is mainly absent, other than for occasional high-angle faults (see Supplementary Data, Fig. S2b).

Further east, S of Kaplıca, deformed debris-flow deposits are overlain by the Bellapais Formation, which, unusually, begins with a thin reddish palaeosol (Fig. 20e), and then passes upwards into debris-flow deposits that include exceptionally large clasts (e.g., m-scale serpentinite clasts) (Fig. 21f). Unusually thick, stratified alluvial fan conglomerates appear above this (Fig. 21g,h). Further east again, the Kalograia-Ardana Formation contact is overturned and sheared, related to Late Miocene deformation (Fig. 21i).

Similar field relations also exist along the southern margin of the range, although Late Miocene deformation is much greater there. At Geçitköy (Panagra) gorge in the western range, a clearly defined contrast exists between the highly deformed Lapithos Group below (Ayios Nikolaos Formation) and the basal Bellapais Formation conglomerates above, although the contact is locally sheared owing to Late Miocene deformation (Supplementary Data, Fig. S1d,e). Interestingly, a packstone clast from the basal conglomerate, rich in Upper Maastrichtian benthic foraminifera and calcareous algae, is unlikely to have been locally derived because the Maastrichtian Malounda Formation is of relatively deep-water origin. Near Değirmenlik, on the southern flank of the central range, a striking contrast again exists between highly deformed Lapithos Formation chalk and thick, stratified Bellapais Formation conglomerates above (again with a sheared contact between the two units related to Late Miocene deformation).

Along the eastern range south flank, Kalograia-Ardana Formation debris-flow deposits are in sheared contact with Bellapais Formation conglomerates, marked by an angular discordance and, or an abrupt change in clast texture and composition (Supplementary Data, Fig. S2c,d). Elsewhere in the eastern range and the Karpaz (Karpas) Peninsula the contact between the two formations is rarely well exposed due to lower topography, Plio-Quaternary cover and/or landslipping (Fig. 17a).

In tectonic model 1 (Fig. 2a-d), there is a profound structural and stratigraphical break between the Middle Eocene Kalograia-Ardana Formation (Lapithos Group) and the overlying Bellapais Formation (Kythrea Group). Geological mapping (1:25,000) of the central range has identified a structural and stratigraphical break between the Lapithos and Kythrea groups (see Supplementary Data, text), as mapped by Ducloux (1963–1964) (sheet 1 in the west) and by Knup and Kluyver (1969) (sheets 2 & 3, farther east), as published by the Geological Survey Department, Republic of

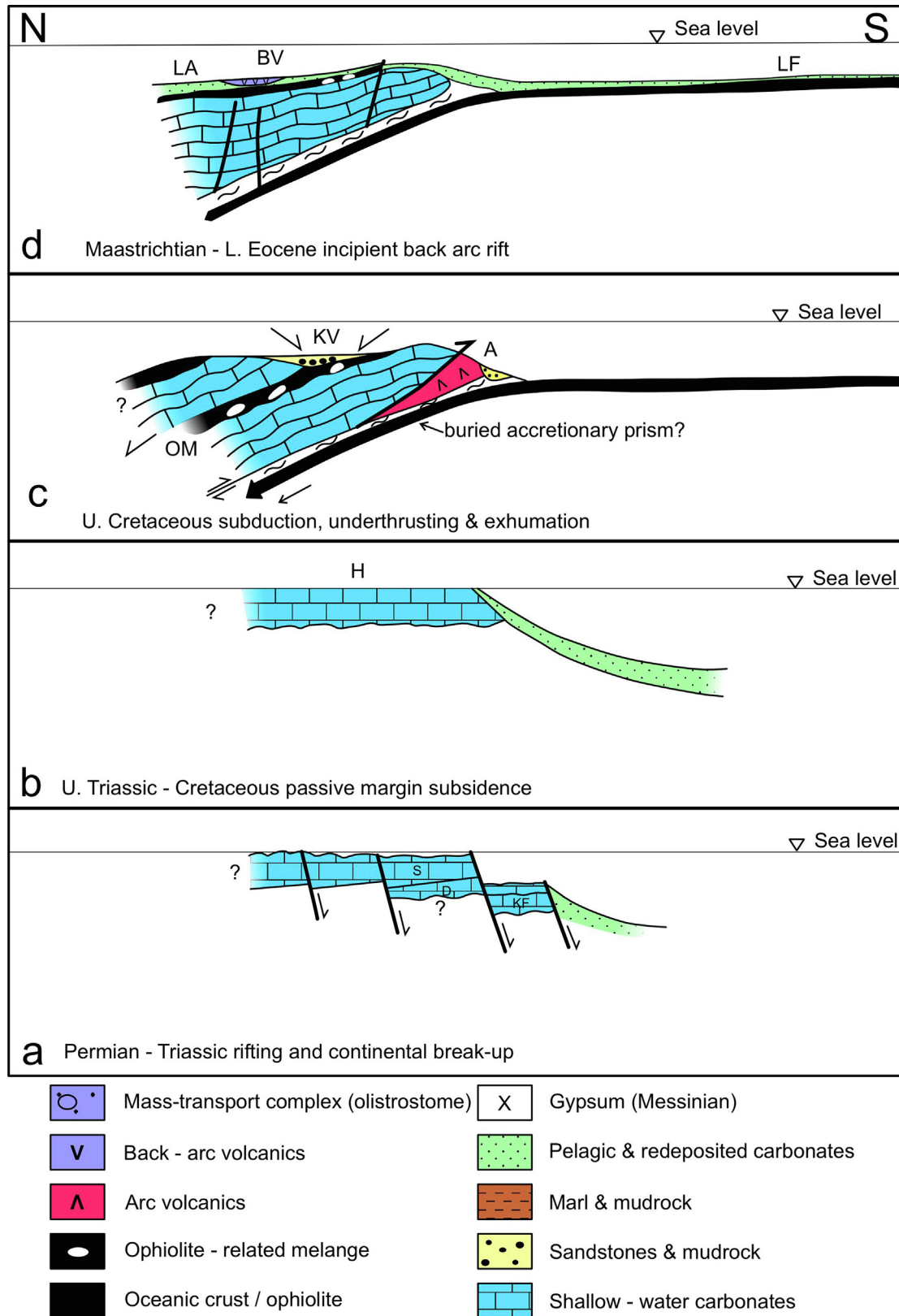


**Fig. 22.** Cartoons showing eight main stages in the development of the Kyrenia Range along the northern continental margin of the southern Neotethys. a, Late Permian-Middle Triassic rifting. The Upper Permian shallow-water Kantara Formation limestones are tentatively restored along the distal rifted margin; b, Late Triassic-Cretaceous. Passive margin subsidence and growth of a carbonate platform; c, Upper Cretaceous underthrusting/subduction, accretion of continental margin arc volcanics and exhumation (see text for multiple stages); d, Maastrichtian-Early Eocene. Incipient back-arc volcanism in an extensional (or transtensional) setting; e, Middle-Late Eocene thrusting and infill of a foredeep basin. The presence of mass-transport facies above as well as below the allochthon suggests some derivation from a no-longer exposed higher thrust sheet (see text); f, Oligocene-Early Miocene. Turbidite accumulation in a foredeep basin to the south; formation of the deep-water Cilicia Basin to the north; g, Late Miocene (later Messinian). Culmination of southward thrusting including re-activation and steepening of previous structures; h, Pleistocene uplift and localised left-lateral strike slip. Likely drivers are underthrusting of the Kyrenia Range and slab-break-off.

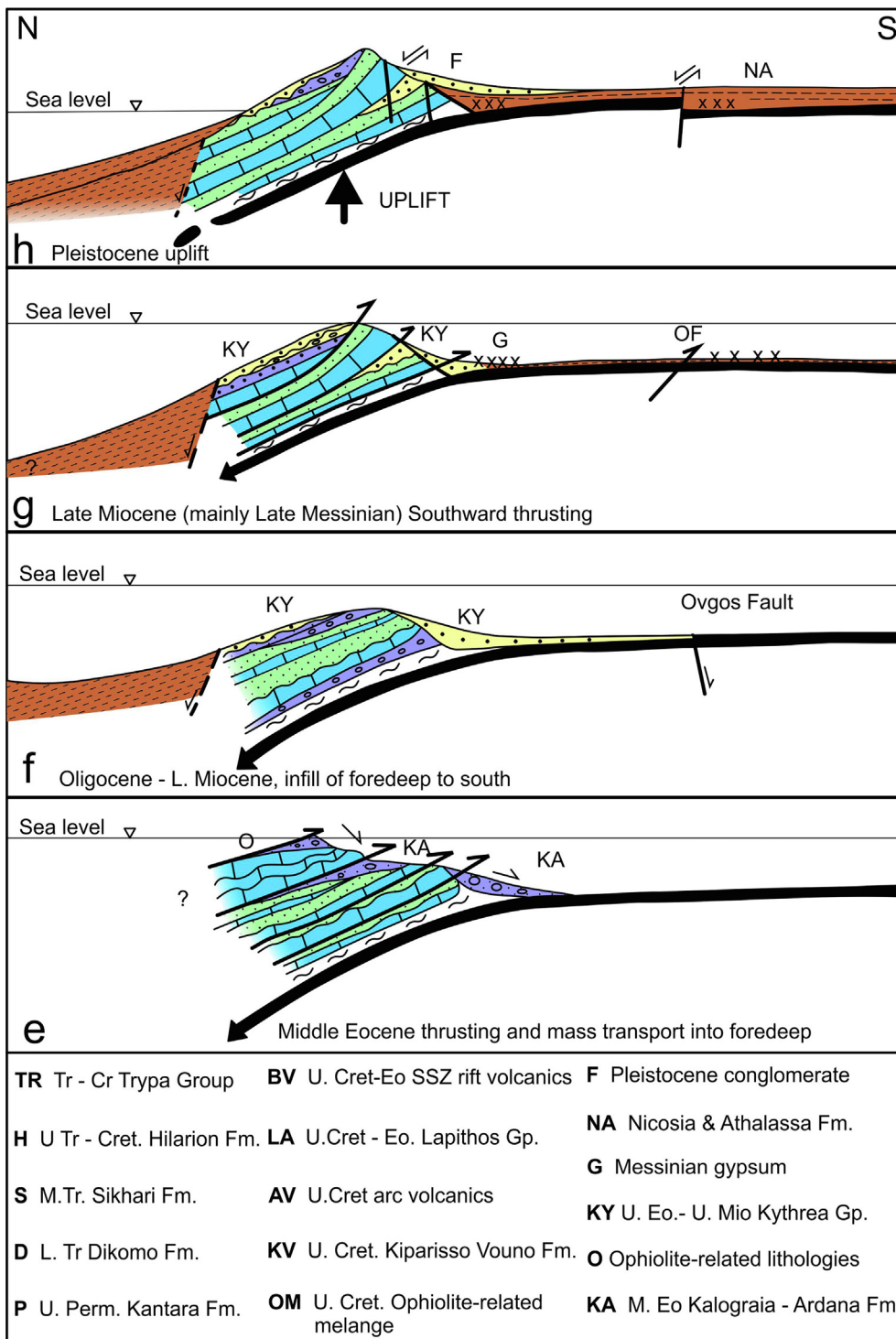


Fig. 22 (continued)

Cyprus. An equivalent structural and stratigraphical break is mapped by Baroz (1979) (1:25,000) throughout the western, central and eastern ranges. Such features can be clearly seen on the maps of the above authors, for example, marked by abrupt changes in dip and strike near the contact between the two groups in some places (e.g., near Beylerbeyi) (Ducloz, 1972). Baroz (1979) inferred an important phase of Eocene thrusting throughout the western, central and eastern ranges. Interestingly, Baroz (1979) reported mainly N-directed Eocene thrusting based mainly on outcrop-

scale fold and thrust geometry. Robertson and Woodcock (1984) inferred mainly S-directed Eocene thrusting and associated folding, which resulted in repetition of the Trypa and Lapithos groups to form a stack of thrust sheets, as best developed in the central range. Robertson and Kinnaird (2016) documented contrasting, greatly reduced deformation styles above a regional Eocene unconformity, mainly based on the interpretation of thrusts, folds and high-angle faults. Also, McCay and Robertson (2013) inferred a major structural and stratigraphical break, during which the

recently deformed Kalograia-Ardana Formation was eroded terrestrially, shedding the basal conglomerates of the Bellapais Formation, initially in a non-marine alluvial fan setting. Such a non-marine setting is confirmed by the local presence of palaeosols.

In tectonic model 1, there is a major stratigraphic and structural break between the Lower Eocene Kalograia-Ardana Formation and the overlying Mid-Upper Eocene base of the Kythrea Group. There was an upward facies change within the Kythrea Group from terrestrial, to shallow marine, to deep marine. The changes in depositional environment generally correspond to the time of marked diminution of Carboniferous detrital zircons (Shaanan et al., 2021; Chen et al., 2019, 2022). This reduction in detrital zircon input could be explained by isolation of clastic sediment supply from the Turkish mainland to the north as the modern Cilicia Basin (Fig. 1) formed (Robertson and Woodcock, 1986; McCay and Robertson, 2012). The sedimentary supply switched to westwards from a source area to the east that included relatively much less abundant Carboniferous zircons (Shaanan et al., 2021), which is consistent with palaeocurrent data from the Kythrea Group (Weiler, 1970; McCay and Robertson, 2013).

In tectonic model 2 (Fig. 2e–g), no structural break exists between the Lapithos and Kythrea groups and sedimentation continued from the Eocene to the Oligocene without any major break (McPhee and van Hinsbergen, 2020). Any Eocene structural break is illusory in this interpretation and largely resulted from competency differences between lithologies above and below the unconformity as inferred by other authors. Specifically, marls and cherts of the Lapithos Formation were more easily deformed than the conglomerates, sandstones and mudrocks of the overlying basal Kythrea facies in this interpretation. The two formations above and below are subparallel without significant angular discordance and both are conglomeratic with potentially similar provenance, according to MCPhee and van Hinsbergen's (2020) interpretation.

Several other lines of evidence suggest a different interpretation: 1. Chert was formed diagenetically within the Lapithos Group to create hard (brittle) material that was then brecciated and reworked above the Bellapais Formation unconformity (Supplementary Data, Fig. S1f). The weakly consolidated mudrocks of the Bellapais Formation, and locally also palaeosols, represent among the least competent lithologies in the entire succession but have remained virtually undeformed; 2. Folding and differential tilting are observed on local outcrop, to mappable scales between the Kalograia-Ardana Formation below (which ends abruptly) and the Bellapais Formation above (Ducloz, 1972; Baroz, 1979; Fig. 20d); 3. Depositional processes are systematically different between the two formations; the Kalograia-Ardana Formation accumulated by subaqueous mass flow. In contrast, the Bellapais Formation initially accumulated as terrestrial alluvial fan deposits (including local fan deltas) (Supplementary Data, Fig. S1i), passing upwards into marine deltaic deposits and then deep-sea deposits (McCay and Robertson, 2012); 4. Clast compositions are consistently different, with the uppermost levels of the Kalograia-Ardana Formation commonly being mainly derived from the adjacent Ayios Nikolaos Formation chalk and chert. In contrast, the Bellapais Formation conglomerates generally include relatively greater numbers of clasts made up of Trypa Group-type marbles, and also ophiolite-related rocks including dolerite (diabase), basalt (e.g., commonly boninitic) and radiolarian chert (McCay and Robertson, 2012); 5. Assuming that no compressional thrusting and folding took place during the Eocene as in model 2, the mapped imbrication of Trypa and Lapithos group lithologies (Ducloz, 1972; Baroz, 1979) (e.g., Fig. 8a–c and 16a,b) would be surprising. In this case, intercalations of Neogene sediments would be expected between Trypa and Lapithos group thrust sheets. Incorporation of such Neogene clastic sediments into the thrust belt is indeed documented but only near the structural base of the west-

ern range (i.e., Selvili Tepe) (Robertson and Kinnaird, 2016). This local intercalation can be explained by tectonic accretion to the base of the Kyrenia Range allochthon during Late Miocene southward thrusting.

In tectonic model 2 (passive margin of North Africa hypothesis) (Fig. 2f), uplift and erosion are proposed (without compressional deformation), related to some form of far-field crustal deformation (McPhee and van Hinsbergen, 2019). In this case, the clastic supply should again have been mainly from the underlying Lapithos Group in response to surface uplift. In reality, all levels of the stratigraphy including abundant clasts from the Trypa Group are present in the Bellapais Formation basal conglomerates. Ducloz (1972) noted that clast composition in the base of the Kythrea Group tends to reflect the local subcrop in some areas (see Supplementary Data, text). However, McCay and Robertson (2013) noted the common presence of clasts (e.g., boninite; radiolarian chert) that could have been derived from the Eocene Kalograia-Ardana Formation even where this is not locally exposed.

McPhee and van Hinsbergen's (2019) supported their interpretation with observations along the c. N-S line of their balanced cross section. This section cuts the northern flank of the central range in the vicinity of Hilarion castle. In this area, both the Lapithos Group and basal Kythrea Group are poorly exposed beneath Pleistocene colluvium, with evidence of landslipping. Also, the basal conglomerates of the Bellapais Formation are unusually thin in this area (without measurable paleocurrent data).

Whereas much of the clastic material in the Bellapais conglomerates was apparently derived locally from the subjacent Trypa and Lapithos groups, other lithologies especially radiolarite, serpentinite and boninite clasts do not have such a ready source in the underlying strata. It is likely that the Kalograia-Ardana Formation, including the ophiolite-related rocks, was originally thicker and more extensive throughout the Kyrenia Range but was largely eroded (subaerially) throughout the central and western ranges before the Late Eocene-Late Miocene accumulation of the Kythrea Group. This inferred former cover could explain MCPhee and van Hinsbergen's (2019) point that there is no evidence of an overburden that could have caused deformation within the underlying Lapithos Group. Initially generally southward-trending palaeocurrents (from clast imbrication) suggest that the source topography was originally highest to the north of the present outcrop during Late Eocene-Early Oligocene, which is unexpected if ocean lay in this direction.

In tectonic model 3 (Fig. 2i–j), the Eocene contact between the two stratigraphical groups could represent the time when the Kyrenia Range allochthon reached its present relative position (Glazer et al., 2021; Shaanan et al., 2020). As noted above, Upper Palaeozoic detrital zircons feature in the Kyrenia Range sandstones (i.e., Triassic, Late Cretaceous and Early Eocene) until the Oligocene (Kythrea Group) when they largely disappear (Shaanan et al., 2021; Chen et al., 2019, 2022). The inferred reason was that the Kyrenia Range had by then been tectonically translated away from its original position wherever this was (e.g., associated with a Palaeotethyan suture zone).

In summary, the combined new and literature data corroborate the existence of a major structural, stratigraphical and compositional break between the Middle Eocene Kalograia-Ardana Formation and the Upper Eocene-Oligocene Bellapais Formation, in agreement with tectonic model 1 (Fig. 2c), and potentially also with tectonic model 3 (Fig. 2j). The Eocene deformation gave rise to gently inclined thrust sheets, such that the unconformity was typically low-angle and not always obvious in individual outcrops. The probable driving force of the Kalograia-Ardana Formation mass-transport complex was downflexure in advance of a thrust load that moved southwards to form a foreland basin, as supported by comparisons with other similar convergent units and modelling studies (e.g., Heller et al., 1988; DeCelles, 2011).

#### 4.6. Late Miocene thrusting: presence or absence of coeval surface uplift?

In all of the three tectonic models (Fig. 2), the Late Miocene is accepted as an important time of southward-directed thrusting and folding in the Kyrenia Range, in keeping with previous studies (Henson et al., 1949; Ducloz, 1972; Baroz, 1979; Robertson and Woodcock, 1984; Harrison et al., 2004; McCay and Robertson, 2012; Robertson and Kinnaird, 2016). However, the timing of deformation and surface uplift within the Kyrenia Range is interpreted differently by several authors.

In several well-documented sections to the south of the western range (e.g., Lapatza Hill) (Necdet and Anil, 2006; Varol and Atalar, 2017; unpublished data), the eastern range (e.g., Çınarlı (Platani)-Altınova (Ayios Lakovos) (McCay and Robertson, 2012; McCay et al., 2013), and the Karpaz (Karpas) Peninsula (near Ziamet (Leonariso) (Robertson et al., 2019) sandstones and mudrocks of the Kythrea Group pass upwards into fine-grained sediments including marls, mudrocks and sapropels and then abruptly but conformably into Messinian evaporites. The Kyrenia Range is interpreted as a low-relief island during the Early Messinian with sapropels accumulating in small semi-isolated marine basins to the south (Robertson et al., 2019). Recent work suggests that the evaporites formed in small, restricted basins to the south of the Ovgos (Dar Dere) Fault (Fig. 3), which became more active during the later period of gypsum deposition, associated with southward reworking as gravity flows (Artiaga et al., 2021).

In tectonic model 1 (Fig. 2d), northward underthrusting/subduction of the Troodos ophiolitic crust took place during Late Eocene-Late Miocene, during which the Kythrea Group accumulated in a mainly deep-marine setting (McCay and Robertson, 2012). Baroz (1979) inferred that Late Miocene thrusting took place between the end of gypsum deposition but before the beginning of the Early Pliocene. In general agreement, other authors (Robertson and Woodcock, 1986; McCay et al., 2013; McCay and Robertson, 2012; Palamakumbura and Robertson, 2018) inferred that southward thrusting, as well documented along the southern margin of the range, mainly took place during and soon after the Messinian accumulation of evaporites (mainly gypsum) within the Mesaoria Basin. Afterwards, marine deposition resumed during the Early Pliocene-Early Pleistocene with the accumulation, initially of marls (Myrtoú (Çamlıbel) and the Nicosia Formation, and later of shallow-marine carbonates (Athalassa (Gürpınar)) Formation, with little evidence of preceding (Late Miocene) or contemporaneous (Early Pliocene-Early Pleistocene) surface uplift. This is consistent with seismic reflection profiles off northwest Cyprus that show that deformation in the subaqueous westward extension of the Kyrenia Range (related to south-verging thrusting) was sealed by an inferred upper Messinian unconformity (without local well control); this reflector was itself folded and faulted during the inferred Plio-Quaternary (Calon et al., 2005a). Similar relationships are seen on seismic profiles across the submerged eastward extension of the Kyrenia Range and in the outer part of the Latakia Basin (Fig. 1) (Calon et al., 2005b).

In tectonic model 2 (Fig. 2g), the Kyrenia Range was transferred from the North African continental margin to near its present position in response to northward subduction that took place between the Kyrenia Range in the south and the Tauride continental crust to the north (McPhee and van Hinsbergen, 2019). During this time the Kyrenia Range was transferred from the N African continental margin to the S Eurasian (S Tauride) continental margin as remnant S Tethyan oceanic crust was consumed. Northward subduction culminated in initial continental collision with the Tauride continent during the Tortonian-Messinian resulting in uplift, followed by further surface uplift during Plio-Pleistocene. MCPhee and van Hinsbergen (2019) infer up to 1000 m of erosion during or after

the major phase of thrusting, mainly based on the interpretation of their balanced and restored N-S section across the central range. In support of this interpretation, they cite an isolated outcrop of sub-horizontal gypsum, of assumed Messinian age, to the south of the range that they believe to have accumulated on tectonically steepened and eroded strata of the Kythrea Group; if correct this implies thrusting and surface uplift as early as the Tortonian. However, the authors note that the contact is not exposed (see their Fig. 4C). On the other hand, stratigraphical, sedimentological and structural evidence does not indicate significant deformation and stratal steepening until the Messinian.

Common to all three tectonic models is the view that intense surface uplift of the Kyrenia Range took place during the Pleistocene. This was characterised by marine regression to lagoonal facies, followed by coarse-grained terraced terrestrial facies (see Palamakumbura and Robertson, 2016). Structural studies show that the Pleistocene uplift was accompanied by continuing compressional and/or transpressional deformation in some areas of the Kyrenia Range (McCay and Robertson, 2012), and also within the Mesaoria Plain to the south, especially associated with the E-W Ovgos (Dar Dere) fault lineament (Harrison et al., 2004; McCay and Robertson, 2013). In the above interpretation, the Pleistocene uplift of the Kyrenia Range, as for the Troodos Massif to the south, can be explained by collision of the Eratosthenes Seamount, representing the leading edge of the North African passive continental margin (e.g., Palamakumbura et al., 2016).

In summary, Late Miocene thrusting and stratal rotation within the Mesaoria Basin (Kythrea Group) mainly took place during the later Messinian-earliest Pliocene. Major surface uplift of the Kyrenia Range did not take place until the Pleistocene, probably driven by collision with the leading edge of the North African continent (Eratosthenes Seamount).

## 5. Discussion: Evaluation of the alternative tectonic models

McPhee and van Hinsbergen (2019) questioned several aspects of the previously published version of model 1 (Robertson et al., 2012a, 2014). In model 1, the Upper Cretaceous-Pleistocene convergence zone (subduction/collision) is placed between the Kyrenia Range and the Troodos Massif, whereas in model 2 this is placed between the Kyrenia Range and mainland Turkey. MCPhee and van Hinsbergen (2019) estimate that 300–400 km of post 35–40 Ma Africa-Europe convergence at the longitude of Cyprus was accommodated by active subduction to the south of the Taurides.

Consistent with the above interpretation, MCPhee and van Hinsbergen (2019) did not find any evidence of pre-Tortonian deformation in the Mesaoria Basin. The important transecting c. E-W Ovgos (Dar Dere) Fault within the Mesaoria Basin was interpreted by them as an extensional fault, in agreement with McCay and Robertson (2013), who previously interpreted this lineament as a north-down extensional (or transtensional) fault zone during Oligocene to Mid-Miocene times. Troodos ophiolitic basement is known to extend to near the Ovgos Fault, as indicated by the Lefkoniko borehole (e.g., Cleintuar et al., 1977). The compiled aeromagnetic anomaly map of Cyprus (Vine et al., 1973) extends approximately as far north as the Ovgos Fault. However, the nature of the basement between the Ovgos Fault and the Kyrenia Range, and that beneath the thrust front of the Kyrenia Range; i.e., the Kythrea (Değirmenlik) Fault are unknown and could have accommodated Neogene convergence. A Cenozoic subduction complex could be buried beneath (and to the north of) the Kyrenia Range; alternatively subduction-erosion could have taken place.

On the other hand, problematic for tectonic model 2 is that there is no obvious evidence of a subduction-accretion complex

related to northward subduction between the Kyrenia Range and the Turkish mainland (their S Neotethyan suture zone). As noted by McPhee and van Hinsbergen (2019), the nature of the basement beneath the thick deep-marine sediments of the intervening Cilicia Basin is unknown (Aksu et al., 2005) (Fig. 1). Northward subduction, continuing until the Messinian, should have produced a trench-accretionary complex or at least the trace of a subduction trench (detachment surface) in their interpretation; however, such features are not observable on the seismic reflection profiles of the Cilicia Basin (Calon et al., 2005a,b). Greenschist facies Mesozoic carbonate platform lithologies on either side of the Cilicia Basin (Kyrenia vs. Alanya Massif) (Fig. 1) have been correlated (Çetinkaplan et al., 2016; Robertson et al., 2012a), which is not easily reconcilable with a former oceanic separation. The Cilicia Basin to the north of the Kyrenia Range has alternatively been interpreted as a flexural foreland basin associated with southward thrusting of the Tauride allochthon (Aksu et al., 2005), although a supra-subduction zone extensional basin origin has also been proposed (Robertson et al., 2012 and references).

McPhee and van Hinsbergen (2019) do not envisage a tectono-stratigraphic link between the Kyrenia Range and the adjacent Taurides until the Late Miocene. However, this is far from supportable. The Kyrenia Range is well established to run northeastwards under the sea (Evans et al., 1978; Kempler and Garfunkel, 1994; Hall et al., 2005; Aksu et al., 2005) and then emerge as the Misis-Andırın Range; this has a very similar structural history including an Eocene mass-transport complex known as the Bulgurkaya Sedimentary Melange within the Misis-Andırın Range, which is similar to the Eocene Kalograia-Ardana Formation. This unit contains exotic blocks of Mesozoic shallow-water carbonate rocks and ophiolite-related rocks in a matrix deposited by gravity flows (Schietecatte, 1971; Kozlu, 1987; Kelling et al., 1987; Gökçen et al., 1988; Robertson et al., 2004). This melange lineament extends northeastwards from the coastal Misis Range through the Andırın Range, which has similarities in terms of its origin and timing of deformation (Yılmaz and Güner, 1995; Robertson et al., 2004; Akıncı and Ünlügenç, 2020, 2021). The melange lineament then continues eastwards through and beyond the Engizek Mountains (e.g., Çağlayanerit area), where the lower levels of the tectono-stratigraphy are dominated by the Bulgurkaya Sedimentary Melange of Eocene-Oligocene(?) age. The melange is interpreted to have formed related to Eocene northward convergence (subduction) coupled with southward nappe emplacement (Robertson et al., 2004; Akıncı et al., 2016). Eastwards, the lineament runs south of the Pütürge metamorphic massif and then south of the Bitlis metamorphic massif, where it is known as the Bitlis suture zone (e.g., Oberhänsli et al., 2010, 2013). Another relevant comparison is that the Trypa Group of the Kyrenia Range has been compared with the mainland Alanya Massif (Robertson et al., 2012a); also the Alanya Massif has been correlated with Bitlis Massif as a single c. E-W tectonic unit (Özgül, 1976; Çetinkaplan et al., 2016; Barrier et al., 2018; Robertson et al., 2020). Alternatively, it has been proposed that the Alanya, Pütürge and Bitlis massifs represent separate rifted continental blocks within Tethys (Robertson et al., 2012a; Şengör and Yılmaz, 1981; Robertson and Dixon, 1984; Robertson and Woodcock, 1984). The frontal thrust of the Misis-Andırın-Engizek-Bitlis suture is in the same relative position as the frontal thrust (i.e., the Değirmenlik (Kythrea) Fault) of the Kyrenia Range. In all of these areas allochthonous units occur above Upper Cretaceous ophiolites to the south; e.g., the Amanos ophiolite in SE Turkey (Duman et al., 2017).

In tectonic model 2, the Troodos ophiolite was emplaced onto the distal North African continental margin (Fig. 2e). The Mesozoic

geology of the distal North Africa margin remains poorly known (at least in the public domain). However, the stratigraphy would be expected to resemble that of the Eratosthenes Seamount south of Cyprus. ODP drilling revealed Early Cretaceous shallow-water carbonates related to the development of a large, isolated carbonate platform, as further revealed by seismic data (Feld et al., 2017; Gao et al., 2020; Burchette et al., 2023). The shallow-water carbonates are overlain by pelagic carbonates (mainly chalk), followed by Miocene reef-related carbonates without any significant tectono-stratigraphic break during the latest Cretaceous time of regional ophiolite emplacement (Robertson, 1998). Elsewhere, ophiolite (e.g., Oman) emplacement onto the Arabian continental margin generated a regional flexurally-controlled foredeep and regional-scale unconformity (Ali and Watts, 2009; Patton and O'Connor, 1988; Robertson, 1987). There is, therefore, no obvious supporting evidence of Late Cretaceous ophiolite emplacement onto or near the North African continental margin.

The Kyrenia Range is also unlikely to represent a far-travelled rootless allochthon as in tectonic model 3 because the correlative crustal units in S and SE Turkey occur at a low level in the overall tectono-stratigraphy, above the Arabian plate. These units (e.g., Kyrenia, Alanya, Pütürge, Bitlis) could have achieved such a rootless position by far-travelled out-of-sequence thrusting (thick-skinned) but there is no obvious evidence of this (e.g., Yılmaz, 1993, 2019).

Glazer et al.'s (2021) interpretation of the Kyrenia Range as a grossly allochthonous body of rocks (pre-Oligocene) rests heavily on the occurrence of Upper Palaeozoic (mainly Carboniferous) detrital zircons within Triassic, Upper Cretaceous and Eocene sandstones of the Kyrenia Range, for which they consider a tectonic link with Paleotethyan crust which is located to the north of the Taurides (Glazer et al., 2021). One option is that the Kyrenia Range overstepped the Taurides during the Eocene regional compressional event that accompanied final closure of the northern Neotethys (Inner Tauride ocean and/or İzmir-Ankara-Erzincan ocean) (e.g., Şengör and Yılmaz, 1981; Özgül, 1984a, 1997; Andrew and Robertson, 2002). The Alanya metamorphic massif was emplaced northwards during the Eocene (Monod, 1977; Demirtaşlı et al., 1979; Özgül, 1984a; Okay and Özgül, 1984; Özgül, 1984b; Robertson et al., 2024). However, soon after its northward emplacement (within the Eocene) the Alanya Massif was overthrust southwards by the leading edge of the Hadım (Aladağ) nappe (Özgül, 1984a; Robertson et al., 2020; Robertson and Parlak, 2020; Özgül, 1984b). Therefore, in principle a Kyrenia Range allochthon might have formed part of the Hadım nappe or have piggy backed over it. However, the tectonostratigraphy of the Kyrenia Range and the Hadım Nappe are fundamentally different, and there is no evidence of any formerly existing thrust sheet above (e.g., associated erosional detritus). Also, the Kyrenia Range stratigraphy, especially the Lapithos Group, is quite unlike the tectono-stratigraphy of the Anatolide crustal unit between the Taurides and the Palaeotethyan suture zone to the north (e.g., Okay and Tüysüz, 1999; Pourteau et al., 2010; Robertson et al., 2009; Göncüoğlu, 2011). Another option (potentially promising) is sediment transport from Upper Palaeozoic zircon-rich units that were emplaced southwards together with the Bolkar (Aladağ) nappe during latest Cretaceous (to the east of the Alanya Massif) (Robertson et al., 2022 and references).

New detrital zircon data are increasingly becoming available for Palaeozoic-Mesozoic Tauride sandstones (Chen et al., 2022a,b) and their Miocene sedimentary cover (Chen et al., 2021), and also for the Arabian continental margin in the Amanos Mountains (Chen et al., 2024). It remains to be evaluated whether the combined

information supports the interpretation of Chen et al. (2019, 2021, 2022, 2024) that the Upper Palaeozoic detrital zircons were reworked, episodically, generally southwards from the Palaeotethyan suture zone to the north of the Taurides, associated with Triassic, Late Cretaceous and Eocene regional tectonic events.

### 6. Summary of the tectonic development of the Kyrenia Range

The following main stages of tectonic development are inferred in the wider geological context, in the light of our favoured tectonic interpretation (model 1). For brevity most previously cited references are not repeated.

#### 6.1. Late Palaeozoic-Early Mesozoic rifting of S Neotethys

The restored Mesozoic succession of the Kyrenia Range documents Triassic rifting (Dikomo and Sikhari formations) (Fig. 22a), followed by Jurassic-Cretaceous passive margin development (Hilarion Formation) (Fig. 22b, 23), as throughout the Taurides. The Upper Permian shallow-water limestone blocks of the eastern range (Kantara Formation) are likely to document early-stage rifting, as in the Taurides (Poisson, 1977; Robertson and Woodcock,

1984; Mackintosh and Robertson, 2012; Şahin and Altner, 2019). The Kyrenia Range and the Alanya Massif could represent a single continental fragment (Robertson et al., 2016b; Barrier et al., 2018) (Fig. 23), or, alternatively, two separate rifted fragments could have existed (Robertson et al., 2012a). The relevant evidence is hidden beneath the deep-water Cilicia Basin.

#### 6.2. Late Cretaceous subduction of S Neotethys

A supra-subduction zone ophiolite, a possible metamorphic sole and OIB/E-type MORB lavas were tectonically emplaced over the Mesozoic Trypa Group carbonate platform during the post-early Cretaceous (i.e., the youngest confirmed palaeontological age of the underlying Hilarion Formation). The carbonate platform underwent greenschist facies metamorphism, whereas the mineralogy of the blocks of ophiolite-related metabasite and meta-chert suggests metamorphism at <450 °C, at burial pressure of 10–15 kbar (Glazer et al., 2021). Two options for the tectonic/metamorphic processes involved are: 1. the HP-LT rocks formed at depth, exhumed to the crustal level of the greenschist-metamorphosed Trypa Group, and were then all exhumed to the seafloor prior to Late Maastrichtian transgression; 2. the greenschist facies-metamorphosed Trypa Group and the HP-LT ophiolite-related melange exhumed

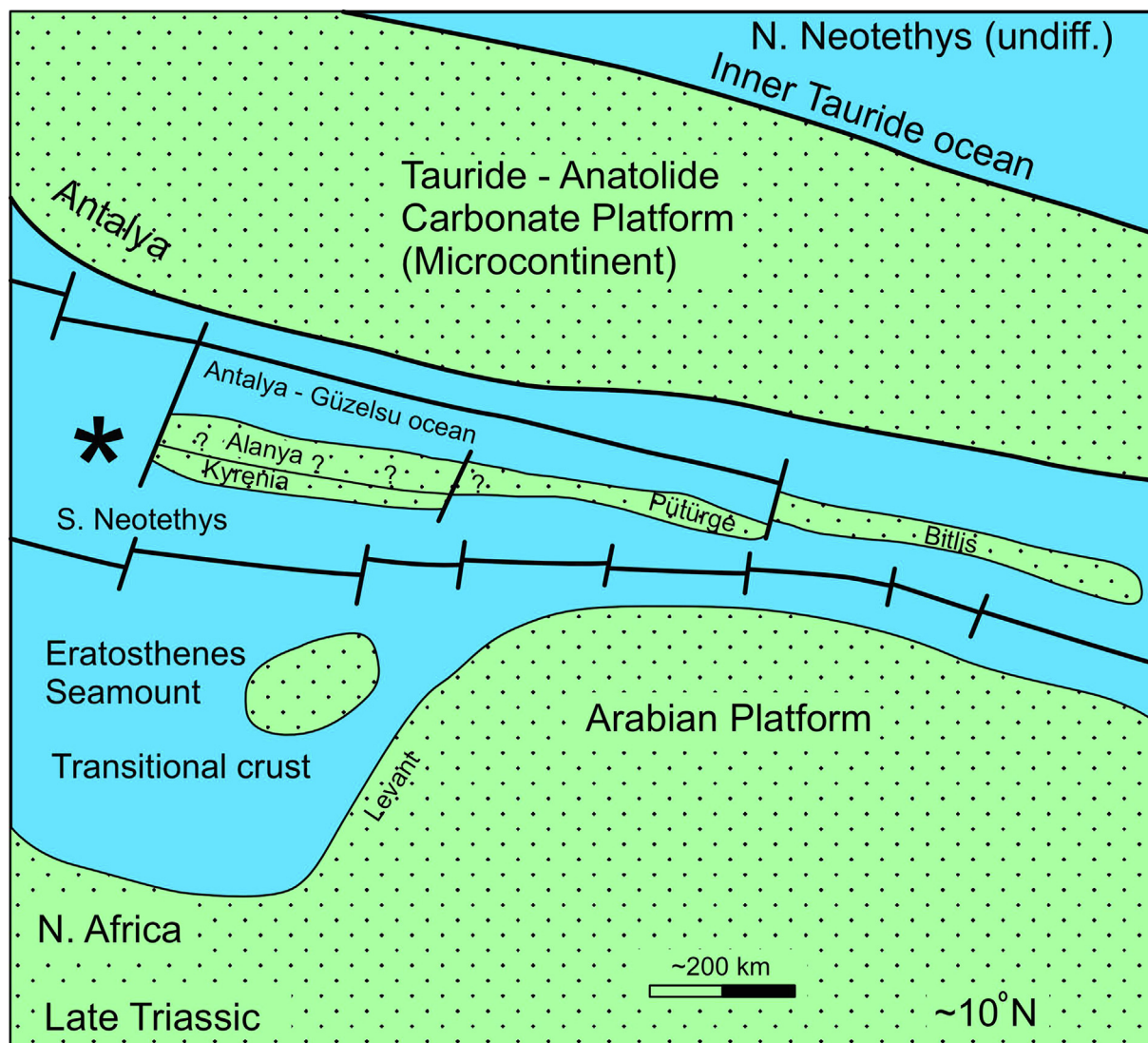


Fig. 23. Palaeogeographic sketch of the setting of the Kyrenia Range during the Late Triassic during the beginning of the passive margin subsidence phase. The Kyrenia Range and the Alanya Massif are shown as a single continental fragment; however, they could possibly also represent two separate fragments.



separately in different locations and the melange was then emplaced onto the Trypa Group as a whole, prior to the Late Maastriichtian (Fig. 22c).

The ophiolite-related melange could have originated in several alternative settings based on the limited available information. The first was a narrow oceanic basin to the north, between a small Mesozoic carbonate platform (Kyrenia Range) and a larger Mesozoic carbonate platform (Alanya Massif) farther north. However, the melange lithologies including SSZ-metabasalts and boninites are unlikely to have formed in a small intra-platform oceanic basin. This is mainly because of the necessary width of oceanic crust needing to subduct (100s km) before triggering supra-subduction spreading, based on comparisons with the Cenozoic of the NW Pacific region (e.g., Reagan et al., 2003). In a second option, the melange originated to the north of the Alanya Massif carbonate platform in a Mesozoic oceanic basin, for example related to the formation and emplacement of the Antalya Complex (Antalya nappes), as exposed within the Güzelsu Corridor and/or adjacent areas (Robertson et al., 2024). There is indeed evidence of southward emplacement of HP-LT ophiolite-related melange onto the Alanya Massif (Çetinkaplan et al., 2016; Robertson and Parlak, 2020; their Fig. 20f) in this area, although it is unclear whether or not these lithologies could have reached the Kyrenia Range.

### 6.3. Mid-Eocene emplacement of mass-transport unit

During the Late Maastriichtian-Early Eocene, pelagic carbonates accumulated, interspersed with Maastriichtian-Eocene basic volcanics of the Lapithos Group (Malounda and Ayios Nikolaos formations) (Fig. 22d). An incipient 'back-arc' setting is inferred during this time (Huang et al., 2007; Chen and Robertson, 2021). During the Middle Eocene, the Kalograia-Ardana Formation mass-transport unit formed and was emplaced southwards by gravity processes, associated with regional compressional deformation (Fig. 22e). The eastern range outcrop traces westwards to beneath the eastern part of the central range and so probably exists to the south of the entire range but was buried and concealed by the Late Miocene thrusting (Robertson et al., 2012a). Mass-flow accumulations along the northern margin of the central and western range were probably thicker and more extensive (100s m?) prior to pre-Late Eocene erosion.

The southward emplacement of the Eocene mass-transport unit was broadly contemporaneous with the southward emplacement of the Tauride nappes, notably the Hadim (Aladağ) nappe, which reached as far south as the Mediterranean coast north of Cyprus (near Silifke). The Eocene regional compression that emplaced the Tauride nappes could also have driven Eocene south-verging thrusting in the Kyrenia Range. Several thrust sheets were involved. One in the north (not now exposed) represented a thrust-top basin in which sedimentary melange (debris flows) accumulated on a substratum of Trypa-Lapithos group rocks. Structurally beneath this (farther south), a Trypa-Lapithos group thrust sheet shed debris into a flexurally controlled foreland basin to form the main mass-transport unit of the Kalograia-Ardana Formation (eastern range and Karpaz (Karpas) Peninsula).

The Upper Permian detached limestone blocks (Kantara Formation) are proposed to have formed along the distal rifted, northerly continental margin of the S Neotethys. Early rift facies were covered by deeper water later-rift and post-rift facies, including Triassic sandstone turbidites and radiolarian cherts that are not present in the Trypa Group. During the Eocene regional compression, the former rift basin stratigraphically inverted (uplifted) and was bulldozed ahead of the main Trypa-Lapithos group allochthon, leading to its collapse as detached blocks and debris-flows within the Middle Eocene Kalograia-Ardana Formation (Fig. 22e). One option is that, during the latest Cretaceous, unmetamorphosed ophiolite-

related rocks, including harzburgite, boninite and meta-chert, representing SSZ-ophiolitic rocks and accretionary melange were initially emplaced southwards from the Güzelsu oceanic basin (Antalya Complex) to the north of the Alanya Massif, and then finally emplaced farther southwards as part of the Middle Eocene mass-transport complex (Robertson et al., 2013).

The relative abundance of Carboniferous detrital zircons in the Kalograia-Ardana Formation (Chen et al., 2019, 2022a,b; Glazer et al., 2021) could be explicable by recycling from Upper Palaeozoic (mainly Carboniferous) units that were emplaced together with the Tauride thrust sheets during the Eocene. Potential source units include sandstones associated with the Upper Palaeozoic Konya Complex (Devonian-Carboniferous zircons) of the Anatolides, north of the Taurides (Löwen et al., 2020; Ustaömer et al., 2020). Other source candidates include the Upper Palaeozoic melange of the Karaburun Peninsula (Löwen et al., 2017; Ustaömer et al., 2020), the Upper Cretaceous Bornova Flysch (Okay and Kylander-Clark, 2023), and the adjacent Aegean region (Meinhold et al., 2008), all of which contain relatively high abundances of Carboniferous zircons. The Tauride platform succession in eastern Anatolia also contains significant abundances of Upper Palaeozoic basic extrusive igneous rocks (Robertson et al., 2021 and references), which might have contributed detrital zircons, although more magmatically evolved igneous rocks typically contain relatively greater proportions of detrital zircons. Many sandstone units in Turkey still lack detrital zircon data. Also, large areas of crust are concealed beneath both the Upper Cretaceous and Eocene thrust systems in the Taurides, such that options for detrital zircon provenance remain open.

### 6.4. Late Eocene-Late Miocene clastic accumulation and southward thrusting

During the Late Eocene-Late Miocene, northward underthrusting and/or late-stage subduction took place to the south of the range, and terrigenous turbidites accumulated in a subduction trench, transitional to a foreland basin (foredeep), as represented by the Kythrea Group (see McCay and Robertson, 2012) (Fig. 22f). Evidence from SE Turkey and more widely (e.g., Iran) suggests that the Mid-Late Eocene was the time of initial collision of the Arabian and Eurasian plates in this region, whereas more advanced collision took place during the Miocene (e.g., Boulton et al., 2006; Robertson et al., 2016a; Cavazza et al., 2018; Darren and Umhoefer, 2022).

Related to more advanced collisional deformation, the Kyrenia Range was thrust and folded mainly during later Messinian-earliest Pliocene time, although deformation continued locally into the Plio-Pleistocene. The Trypa and Lapithos groups were rotated to steeply dipping, as seen along the crest of the range. Slices of the Kythrea Group clastics were incorporated into the thrust stack in the western range. Eocene thrusts were extensively re-activated and over-steepened, associated with extensive northward back-thrusting (Fig. 22g).

### 6.5. Pleistocene tectonic uplift

Pleistocene coarse non-marine accumulations (e.g., terrace deposits) chart surface uplift of the Kyrenia Range, which was broadly coeval with surface uplift of both the Tauride Mountains to the north and the Troodos Massif to the south. The Pleistocene uplift of the Troodos Massif and the Kyrenia Range, together, relate to underthrusting of the Eratosthenes Seamount, which represents a promontory of the North African continental margin (e.g., Robertson et al., 1995; Kempler, 1998; Palamakumbura et al., 2016) (Fig. 22h). Farther north, the Pleistocene uplift of the central

Taurides has been attributed to post-collisional slab break-off (Schildgen et al., 2012).

## 7. Conclusions

1. Three contrasting tectonic models for the Late Palaeozoic–Pleistocene tectonic development of the Kyrenia Range have been tested based on new fieldwork. The best-fitting model is that the Kyrenia Range developed along the northern margin of the Southern Neotethys near its present relative position, rather than along the North African continental margin, or as a far-travelled allochthonous unit from outside the easternmost Mediterranean region.
2. A critical unit of lower Triassic low-grade-metamorphosed marls and meta-mudrocks (Dikomo Formation) is interpreted as rift-related sediments; these are interpreted as the base of the Kyrenia Range Mesozoic succession (Trypa Group). Similar Early Triassic rift-related facies are widely developed in the Taurides.
3. Fragmentary exposures of ophiolite-related melange occur between the Mesozoic platform succession (Trypa Group) and the overlying latest Cretaceous–Eocene deep-water carbonates and basic volcanics (Lapithos Group). The melange includes blocks of subduction-influenced meta-basalt (including boninite), E-MORB/OIB-meta-basalt, garnet amphibolite, diabase-gabbro meta-chert, marble and meta-clastic sediments, within a matrix of typically sheared meta-serpentinite (mainly meta-harzburgite). Meta-clastics and meta-basic igneous rocks are commonly seen to be overprinted by HP/LT metamorphism.
4. The ophiolite-related melange is interpreted as a supra-subduction zone ophiolite, potentially associated with a high-grade metamorphic sole (amphibolite) and deep-sea sediments (e.g., meta-chert).
5. Calcareous microfossil dating shows that the ophiolite-related melange exhumed prior to the Late Maastrichtian when breccias derived from underlying meta-platform and the melange began to accumulate.
6. A major mass-transport unit (olistostrome) developed during the Middle Eocene, comparable to sedimentary melanges along the Misis-Andırın-Engizek lineament in adjacent SE Turkey.
7. Thrusting and folding affected the Kyrenia Range during Mid-Late Eocene, as also documented throughout SE Turkey related to final southward emplacement of various Tauride nappes (e.g., Hadım (Aladağ) nappe). The driving force is likely to have been final closure of northern Neotethyan ocean to the north of the Tauride carbonate platform.
8. Following uplift and subaerial erosion, sedimentation resumed during the Late Eocene–Oligocene above a regionally important unconformity. Deepening upwards from subaerial, to shallow marine, to deep marine isolated the Kyrenia Range from clastic supply from the north as the Cilicia Basin formed.
9. Intense southward thrusting and folding took place mainly during the later Messinian–earliest Pliocene, related to advancing collision of the African and Eurasian plates.
10. Major surface uplift of the Kyrenia Range occurred during the Pleistocene, triggered by underthrusting/subduction of the Eratosthenes Seamount south of Cyprus.

## CRedit authorship contribution statement

**Alastair H.F. Robertson:** Conceptualization, Data curation, Formal analysis, Funding acquisition, Investigation, Methodology, Pro-

ject administration, Resources, Software, Supervision, Validation, Visualization, Writing – original draft, Writing – review & editing. **Osman Parlak:** Conceptualization, Data curation, Formal analysis, Investigation, Methodology, Resources, Software, Supervision, Validation, Visualization, Writing – original draft, Writing – review & editing. **Kemal Taslı:** Conceptualization, Data curation, Formal analysis, Investigation, Methodology, Resources, Software, Supervision, Validation, Visualization, Writing – original draft, Writing – review & editing.

## Declaration of competing interest

The authors declare that they have no known competing financial interests or personal relationships that could have appeared to influence the work reported in this paper.

## Acknowledgements

We thank Timur Ustaömer and Necdet Özgül for discussion. The fieldwork and chemical analyses were funded by the John Dixon Memorial Fund and the University of Edinburgh. We thank Yağız Demirtay for assistance with diagram drawing and Ayhan Zenginoglu for preparing the thin sections. The manuscript benefitted from comments by three reviewers and the Handling Editor A. Festa.

## Appendix A. Supplementary data

Supplementary data to this article can be found online at <https://doi.org/10.1016/j.jgr.2024.05.003>.

## References

- Akıncı, A.C., Ünlügenç, U.C., 2021. Neogene tectonic evolution of the Misis-Andırın-Engizek range: structural and sedimentary evidences from Bulgurkaya Sedimentary Mélange. *Arab. J. Geosci.* 14, 1–23.
- Akıncı, A.C., Robertson, A.H.F., Ünlügenç, U.C., 2016. Late Cretaceous–Cenozoic subduction–collision history of the Southern Neotethys: new evidence from the Çağlayançeri area, SE Turkey. *Int. J. Earth Sci.* 105, 315–337.
- Akıncı, A.C., Ünlügenç, U.C., 2020. Geodynamical evolution of the Misis structural high, Ceyhan (Adana), Turkey. *J. Afr. Earth Sci.* 166, 103828. <https://doi.org/10.1016/j.jafrearsci.2020.103828>.
- Aksu, A.E., Calon, T.J., Hall, J., Mansfield, S., Yaşar, D., 2005. The Cilicia-Adana basin complex, Eastern Mediterranean: Neogene evolution of an active fore-arc basin in an obliquely convergent margin. *Mar. Geol.* 221 (1–4), 121–159.
- Aldanmaz, E., Pearce, J.A., Thirlwall, M.F., Mitchell, J.G., 2000. Petrogenetic evolution of late Cenozoic, post-collision volcanism in western Anatolia. *Turkey. J. Volcanol. Geoth. Res.* 102, 67–95.
- Aldanmaz, E., van Hinsbergen, D.J., Yıldız-Yükseköl, Ö., Schmidt, M.W., McPhee, P.J., Meisel, T., Güçtekin, A., Mason, P.R., 2020. Effects of reactive dissolution of orthopyroxene in producing incompatible element depleted melts and refractory mantle residues during early fore-arc spreading: constraints from ophiolites in eastern Mediterranean. *Lithos* 360, 105438.
- Ali, M.Y., Watts, A.B., 2009. Subsidence history, gravity anomalies and flexure of the United Arab Emirates (UAE) foreland basin. *GeoArabia* 14, 17–44.
- Al-Riyami, K., Robertson, A., Dixon, J., Xenophontos, C., 2002. Origin and emplacement of the Late Cretaceous Baer-Bassit ophiolite and its metamorphic sole in NW Syria. *Lithos* 65, 225–260.
- Andrew, T., Robertson, A.H.F., 2002. The Beyşehir–Hoyran–Hadım Nappes: genesis and emplacement of Mesozoic marginal and oceanic units of the northern Neotethys in southern Turkey. *J. Geol. Soc. London* 159, 529–543.
- Artiaga, D., García-Veigas, J., Cendón, D.I., Atalar, C., Gibert, L., 2021. The Messinian evaporites of the Mesaoria basin (North Cyprus): A discrepancy with the current chronostratigraphic understanding. *Palaeogeog. Palaeoecol.* 584, 110681.
- Avigad, D., Abbo, A., Gerdes, A., 2016. Origin of the Eastern Mediterranean: Neotethys rifting along a cryptic Cadomian suture with Afro-Arabia. *Geol. Soc. Am. Bull.* 128, 1286–1296.
- Bağcı, U., Parlak, O., 2009. Petrology of the Tekirova (Antalya) ophiolite (Southern Turkey): evidence for diverse magma generations and their tectonic implications during Neotethyan-subduction. *Int. J. Earth Sci.* 98, 387–405.
- Bağcı, U., Parlak, O., Höck, V., 2008. Geochemistry and tectonic environment of diverse magma generations forming the crustal units of the Kızıldağ (Hatay) ophiolite. *Southern Turkey. Turk. J. Earth Sci.* 17, 43–71.

- Bağcı, U., Rızaoğlu, T., Önal, G., Parlak, O., 2020. Petrology of the late Triassic mafic volcanic rocks from the Antalya Complex, southern Turkey: evidence for mantle source characteristics during the Neotethyan rifting. *Turk. J. Earth Sci.* 29, 1049–1072.
- Baroz, F., 1979. Etude géologique dans le Pentadaktylos et la Mesaoria (Chypre Septentrionale). Université de Nancy. Ph.D. thesis.
- Baroz, F., 1980. Volcanism and continent-island arc collision in the Pentadaktylos range, Cyprus. In: Panayiotou, A. (Ed.), *Ophiolites: Proc. Int. Ophiolite Symp. Cyprus*, Geol. Surv. Dept. Nicosia, Cyprus, 73–85.
- Barrier, E., Vrielynck, B., Brouillet, J.F., Brunet, M.F., 2018. Paleotectonic reconstruction of the Central Tethyan Realm. Tectonono-sedimentary-palinspastic maps from Late Permian to Pliocene, CCGM/CGMW, Paris. <http://www.ccgm.org>.
- Beccaluva, L., Coltorti, M., Saccani, E., Siena, F., 2005. Magma generation and crustal accretion as evidenced by supra-subduction ophiolites of the Albanide-Hellenide Subpelagonian zone. *Isl. Arc* 14, 551–563.
- Boulton, S.J., Robertson, A.H., Ünlügenç, U.C., 2006. Tectonic and sedimentary evolution of the Cenozoic Hatay Graben, Southern Turkey: a two-phase model for graben formation. In: Robertson, A.H.F., Mountrakis, D. (Eds.), *Tectonic Development of the Eastern Mediterranean Region*. Geol. Soc. Lond. Spec. Publ. 260, 613–634.
- Burchette, T., Groves-Gidney, G., Karcz, K., 2023. Seismic stratigraphy of the southern Eratosthenes High, eastern Mediterranean Sea: growth, demise and deformation of three superposed carbonate platforms (Mesozoic–Cenozoic). *Petrol. Geosci.* 29 (3), petgeo2023-017.
- Calon, T.J., Aksu, A.E., Hall, J., 2005a. The Oligocene–Recent evolution of the Mesaoria Basin (Cyprus) and its western marine extension, Eastern Mediterranean. *Mar. Geol.* 221, 95–120.
- Calon, T.J., Aksu, A.E., Hall, J., 2005b. The neogene evolution of the outer Latakia Basin and its extension into the Eastern Mesaoria Basin (Cyprus), Eastern Mediterranean. *Mar. Geol.* 221, 61–94.
- Cavazza, W., Cattò, S., Zattin, M., Okay, A.I., Reiners, P., 2018. Thermochronology of the Miocene Arabia-Eurasia collision zone of southeastern Turkey. *Geosphere* 14, 2277–2293.
- Çelik, Ö.F., Delaloye, M., 2003. Origin of metamorphic sole rocks and their post-kinematic mafic dyke swarms in the Antalya and Lycian ophiolites, SW Turkey. *Geol. J.* 38, 235–256.
- Çelik, Ö.F., Delaloye, M., 2006. Characteristics of ophiolite-related metamorphic rocks in the Beyşehir ophiolitic melange (Central Taurides, Turkey), deduced from whole rock and mineral chemistry. *J. Asian Earth Sci.* 26, 461–476.
- Çetinkaplan, M., 2018. Anamur (Alanya Masifi, Mersin) Bölgesinde Yer Alan Prekambriyen Yaşlı Kayaçların Çok Evreli P-T-t Evrimi (Multi-Stage P-T-t Evolution of Precambrian Aged Rocks in Anamur (Alanya Massif, Mersin) Region). *Türk. Jeol. Bül.* 61, 91–130.
- Çetinkaplan, M., Pourteau, A., Candan, O., Koralay, O.E., Oberhänsli, R., Okay, A.I., Chen, F., Kozlu, H., Şengün, F., 2016. P-T-t evolution of eclogite/blueschist facies metamorphism in Alanya Massif: time and space relations with HP event in Bitlis Massif. *Turkey. Int. J. Earth Sci.* 105, 247–281.
- Chen, G., Robertson, A.H.F., Parlak, O., Wu, F.Y., 2021. Source to sink in the Easternmost Mediterranean: Insights from the provenance of Oligo-Miocene turbidites in the south Turkish basins (abstract and related poster presentation). AGU 2021 Fall Meeting, New Orleans, LA and Virtual, p. 1.
- Chen, G., Robertson, A.H.F., Parlak, O., Wu, F.Y., 2022. Provenance of sandstones related to pre, syn and post-rifting of N Gondwana: evidence from detrital zircon geochronology (Antalya Complex, E Mediterranean). 21st Int. Sedimentol. Congr. (Beijing 2022), p. 443 (ID:T2-50840).
- Chen, G., Robertson, A.H.F., Parlak, O., 2024. Zircon U-Pb and heavy mineral evidence for S Neotethyan closure and Arabia-Tauride collision from the Arabian foreland (Amanos Mountains), SE Türkiye. *Ann. Meet. Türk. Jeol. Soc., Ankara*, April, 2024, Abstr.
- Chen, G., Robertson, A.H.F., 2021. Evidence from Late Cretaceous–Paleogene volcanic rocks of the Kyrenia Range, Northern Cyprus for the northern, active continental margin of the Southern Neotethys. *Lithos* 380, 105835. <https://doi.org/10.1016/j.lithos.2020.105835>.
- Chen, G., Robertson, A.H.F., Wu, F.Y., 2022b. Detrital zircon geochronology and related evidence from clastic sediments in the Kyrenia Range, N Cyprus: Implications for the Mesozoic–Cenozoic erosional history and tectonics of southern Anatolia. *Earth Sci. Rev.* 233, 104167.
- Chen, C., Su, B.-X., Xiao, Y., Uysal, İ., Lin, W., Chu, Y., Jing, J.-J., Sakyi, P.A., 2020. Highly siderophile elements and Os isotope constraints on the genesis of peridotites from the Kızıldağ ophiolite, southern Turkey. *Lithos* 368–369, 105583.
- Cleintuar, M.R., Knox, G.J., Ealey, P.J., 1977. The geology of Cyprus and its place in the East Mediterranean framework. *Geol. Mijnb.* 56, 66–82.
- Crawford, A.J., Falloon, T.J., Green, D.H., 1989. Classification, petrogenesis and tectonic setting of boninites. In: Crawford, A.J. (Ed.), *Boninites and Related Rocks*. Unwin Hyman, London, pp. 1–49.
- Darin, M.H., Umhoefer, P.J., 2022. Diachronous initiation of Arabia-Eurasia collision from eastern Anatolia to the southeastern Zagros Mountains since middle Eocene time. *Int. Geol. Rev.* 64, 2653–2681.
- DeCelles, P.G., 2011. Foreland basin systems revisited: Variations in response to tectonic settings. *Recent advances, Tectonics of sedimentary basins*, pp. 405–426.
- Demirtaşlı, E., Erenler, F., Bilgin, A.Z., Çatal, E., Armağan, F., Serdaroğlu, M., Aksoy, S., Altuğ, S., Dirik, K., 1979. Toros kuşağının (Akseki yöresi) petrol olanakları. Türkiye Jeoloji Bilimsel ve Teknik Kongresi 5-6 Şubat, Ankara, 187–190.
- Dercourt, J., Zonenshain, L.P., Ricou, L.-E., Kazmin, V.G., Le Pichon, X., Knipper, A.L., Grandjaquet, C., Sbertshnikov, I.M., Geyssant, J., Lepvrier, C., Perchinsky, D.H., Boulin, J., Sibuet, J.-C., Savostin, L.A., Sorokhtin, O., Westphal, M., Bazhrnov, M.L., Lauer, J.-P., Biju-Duval, B., 1986. Geological evolution of the Tethys belt from the Atlantic to the Pamirs since the Lias. *Tectonophysics* 123, 241–315.
- Dilek, Y., Rowland, J.C., 1993. Evolution of a conjugate passive margin pair in Mesozoic southern Turkey. *Tectonics* 12, 954–970.
- Ducloz, C., 1963–1964. Geological map of the Central Kyrenia Range, Sheet 1. Geol. Surv. Depart., Cyprus.
- Ducloz, C., 1972. The geology of the Bellapais-Kythrea area of the Central Kyrenia Range, Cyprus. *Bull. Geol. Surv. Depart.*, No. p. 6.
- Duman, T.Y., Robertson, A.H.F., Elmaci, H., Kara, M., 2017. Palaeozoic–Recent geological development and uplift of the Amanos Mountains (S Turkey) in the critically located northwesternmost corner of the Arabian continent. *Geodinam. Acta* 29, 103–138.
- Evans, G., Morgan, P., Evans, W.E., Evans, T.R., Woodside, J.M., 1978. Faulting and halokinetics in the northeastern Mediterranean between Cyprus and Turkey. *Geology* 6, 392–396.
- Falloon, T.J., Crawford, A.J., 1991. The petrogenesis of high-Ca boninite lavas dredged from the northern Tonga ridge. *Earth Planet. Sci. Lett.* 102, 375–394.
- Feld, C., Mechie, J., Hübscher, C., Hall, J., Nicolaides, S., Gürbüz, C., Bauer, K., Loudon, K., Weber, M., 2017. Crustal structure of the Eratosthenes Seamount, Cyprus and S. Turkey from an amphibian wide-angle seismic profile. *Tectonophysics* 700, 32–59.
- Fitton, J.G., James, D., Leeman, W.P., 1991. Basic magmatism associated with the late Cenozoic extension in the western United States: compositional variation in space and time. *J. Geophys. Res.* 96, 13693–13711.
- Floyd, P.A., Winchester, J.A., 1975. Magma type and tectonic setting discrimination using immobile elements. *Earth Planet. Sci. Lett.* 27, 211–218.
- Floyd, P.A., Winchester, J.A., 1978. Identification and discrimination of altered and metamorphosed volcanic rocks using immobile elements. *Chem. Geol.* 21, 291–306.
- Gao, H., Wen, Z., Shi, B., Wang, Z., Song, C., 2020. Tectonic characteristics of the Eratosthenes Seamount and its periphery: implications for evolution of the eastern Mediterranean. *Mar. Geol.* 428, 106266.
- Garfunkel, Z., 1998. Constraints on the origin and history of the Eastern Mediterranean basin. *Tectonophysics* 298, 5–35.
- Glazer, A., Avigad, D., Morag, N., Güngör, T., Gerdes, A., 2021. The Kyrenia Terrane (Northern Cyprus): Detrital Zircon Evidence for Exotic Elements in the Southern Neotethys. *Tectonics* 40. <https://doi.org/10.1029/2021TC006763>. e2021TC006763.
- Gökçen, S.L., Kelling, G., Gökçen, N., Floyd, P.A., 1988. Sedimentology of a Late Cenozoic collisional sequence: the Misis Complex, Adana, southern Turkey. *Sediment. Geol.* 59, 205–235.
- Göncüoğlu, M.C., 2011. Kütahya Bolcardağ Kuşağının Jeolojisi. *MTA Bull.* 142, 227–282 (in Turkish with an English abstract).
- Gürsu, S., Möller, A., Göncüoğlu, M.C., Köksal, S., Demircan, H., Köksal, F.T., Kozlu, H., Sunal, G., 2015. Neoproterozoic continental arc volcanism at the northern edge of the Arabian Plate, SE Turkey. *Precamb. Res.* 258, 208–223.
- Gutnic, M.F., Monod, O., Poisson, A., Dumont, J., 1979. *Geologie des Taurides Occidentales (Turquie)*. Mem. Geol. Soc. France 137, 1–112.
- Hakyemez, Y., Turhan, N., Sönmez, İ., Sümenen, M., 2002. Kuzey Kıbrıs Türk Cumhuriyeti'nin Jeolojisi (Geology of the Turkish Republic of Northern Cyprus). Maden Tektik ve Arama (MTA) Genel Müdürlüğü, Ankara. Rapor No 10608, 69 pp (unpublished).
- Hall, J., Aksu, A.E., Calon, T.J., Yaşar, D., 2005. Varying tectonic control on basin development at an active microplate margin: Latakia Basin, Eastern Mediterranean. *Mar. Geol.* 221, 15–60.
- Harrison, R., Newell, W., Bathanlı, H., Panayides, I., McGeehin, J., Mahan, S., Özhür, A., Tsiolakis, E., Necdet, M., 2004. Tectonic framework and Late Cenozoic tectonic history of the northern part of Cyprus: implications for earthquake hazards and regional tectonics. *J. Asian Earth Sci.* 23, 191–210.
- Hart, S.R., Erlank, A.J., Kable, E.J.D., 1974. Sea floor basalt alteration: some chemical and Sr isotopic effects. *Contrib. Mineral. Petrol.* 44, 219–230.
- He, W., Zhang, K., Yang, T., Wu, S., 2014. Morphological Evolution of Claraia Species from the Late Permian (changhsingian) to the Early Triassic (induan) and the Response to the Permian-Triassic Stressed Environment. Springer International Publishing 1035–1038.
- Heller, P., Angevine, C., Winslow, N., Paola, C., 1998. 2-Phase Stratigraphic Model of Foreland-Basin Sequences. *Geology* 16. [https://doi.org/10.1130/0091-7613\(1988\)016<0501:TPSMOF>2.3.CO;2](https://doi.org/10.1130/0091-7613(1988)016<0501:TPSMOF>2.3.CO;2).
- Henson, F.R.S., Browne, R.V., McGinty, J., 1949. A synopsis of the stratigraphy and geological history of Cyprus. *Q.J.G.S. (London)* 105, 1–41.
- Huang, K., Malpas, J., Xenophontos, C., 2007. Geological studies of igneous rocks and their relationships along the Kyrenia Range. In: Moumiani, K., Shawabkeh, K., Al-Malabeh, A., Abdelghafoor, M. (Eds.), 6th Internat. Congr. Eastern Mediterranean Geology, 2–5 April, Amman, Jordan, p. 53.
- Humphris, S.E., Thompson, G., 1978. Trace element mobility during hydrothermal alteration of oceanic basalts. *Geochim. Cosmochim. Acta* 42, 127–136.
- Ishimaru, S., Saikawa, Y., Miura, M., Parlak, O., Arai, S., 2018. Decoding of Mantle Processes in the Mersin Ophiolite, Turkey, of End-Member Arc Type: Location of the Boninite Magma Generation. *Minerals* 8, 464. <https://doi.org/10.3390/min8100464>.
- Ishizuka, O., Tani, K., Reagan, M.K., 2014. Izu-Bonin-Mariana forearc crust as a modern ophiolite analogue. *Elements* 10 (2), 115–120. <https://doi.org/10.2113/gselements.10.2.115>.

- Ishizuka, O., Taylor, R.N., Umino, S., Kanayama, K., 2020. Geochemical evolution of arc and slab following subduction initiation: a record from the Bonin Islands. *Japan. J. Petrol.* 61 (5), egaa050. <https://doi.org/10.1093/ptrology/egaa050>.
- Karaođlan, F., Parlak, O., Klötzli, U., Thöni, M., Koller, F., 2013. U-Pb and Sm-Nd geochronology of the Kızıldağ (Hatay, Turkey) ophiolite: implications for the timing and duration of suprasubduction zone type oceanic crust formation in the southern Neotethys. *Geol. Mag.* 150, 283–299.
- Kelling, G., Gökçen, S.L., Floyd, P.A., Gökçen, N., 1987. Neogene tectonics and plate convergence in the Eastern Mediterranean: new data from southern Turkey. *Geology* 15, 425–429.
- Kempler, D., Garfunkel, Z., 1994. Structures and kinematics in the northeastern Mediterranean: a study of an irregular plate boundary. *Tectonophysics* 234, 19–32.
- Kempler, D., 1998. Eratosthenes Seamount: The possible spearhead of incipient continental collision in the Eastern Mediterranean. In: Robertson, A.H.F., Emeis, K.-C., Richter, C., Camerlenghi, A. (Eds.), *Proc. ODP, Scientific Results. College Station, TX, Ocean Drilling Program 160*, 709–721.
- Knup, P.E., Kluyver, H.M., 1969. Geological map of the Central Kyrenia Range (sheets 2 & 3). Republic of Cyprus, Geol. Surv. Dept.
- Kozlu, H., 1987. Misis-Andırın dolaylarının stratigrafisi ve yapısal evrimi. *Proc. 7<sup>th</sup> Petrol. Congr. Turkey*, 6–10 April, Ankara, 104–116.
- Lapierre, H., 1975. Les formations sédimentaires et éruptives des nappes de Mamonia et leurs relations avec le Massif du Troodos (Chypre occidentale). *Mem. Soc. Geol. France* 123, 1–127.
- Lapierre, H., Bosch, D., Narros, A., Mascle, G.H., Tardy, M., Demant, A., 2007. The Mamonia Complex (SW Cyprus) revisited: remnant of Late Triassic intra-oceanic volcanism along the Tethyan southwestern passive margin. *Geol. Mag.* 144, 1–19.
- Le Pichon, X., Şengör, A.C., İmren, C., 2019. A new approach to the opening of the eastern Mediterranean Sea and the origin of the Hellenic Subduction Zone. Part 1: The eastern Mediterranean Sea. *Can. J. Earth Sci.* 56, 1119–1143.
- Löwen, K., Meinhold, G., Güngör, T., Berndt, J., 2017. Palaeotethys-related sediments of the Karaburun Peninsula, western Turkey: constraints on provenance and stratigraphy from detrital zircon geochronology. *Int. J. Earth Sci.* 106, 2771–2796.
- Löwen, K., Meinhold, G., Arslan, A., Güngör, T., Berndt, J., 2020. Evolution of the Palaeotethys in the Eastern Mediterranean: a multi-method approach to unravel the age, provenance and tectonic setting of the Upper Palaeozoic Konya Complex and its Mesozoic cover sequence (south-central Turkey). *Int. Geol. Rev.* 62, 389–414.
- Mackintosh, P.W., Robertson, A.H.F., 2012. Late Devonian-Late Triassic sedimentary development of the central Taurides, S Turkey: Implications for the northern margin of Gondwana. *Gondwana Res.* 21, 1089–1114.
- Maffione, M., van Hinsbergen, D.J.J., de Gelder, G.L., van der Goes, F.C., Morris, A., 2017. Kinematics of Late Cretaceous subduction initiation in the Neo-Tethys Ocean reconstructed from ophiolites of Turkey, Cyprus, and Syria. *J. Geophys. Res.: Solid Earth* 122, 3953–3976.
- Maury, R.C., Lapierre, H., Bosch, D., Marcoux, J., Krystyn, L., Cotton, J., Buss, F., Brunet, P., Senebier, F., 2008. The alkaline intraplate volcanism of the Antalya nappes (Turkey): a Late Triassic remnant of the Neotethys. *Bull. Soc. Géol. France* 179, 397–410.
- McCay, G.A., 2011. Tectonic-sedimentary evolution of the Girne (Kyrenia) Range and the Mesarya (Mesaoria) Basin, North Cyprus, Unpub. Uni. Edinburgh PhD thesis.
- McCay, G.A., Robertson, A.H.F., 2013. Upper Miocene–Pleistocene deformation of the Girne (Kyrenia) Range and Dar Dere (Ovgos) lineaments, northern Cyprus: role in collision and tectonic escape in the easternmost Mediterranean region. In: Robertson, A.H.F., Parlak, O., Ünlügöç, U.C. (Eds.), *Geological Development of Anatolia and the Easternmost Mediterranean Region*. Geol. Soc. London Spec. Publ. 372, 421–445.
- McCay, G.A., Robertson, A.H.F., 2012. Late Eocene-Neogene sedimentary geology of the Girne (Kyrenia) Range, northern Cyprus: A case history of sedimentation related to progressive and diachronous continental collision. *Sediment. Geol.* 265, 30–55.
- McCay, G.A., Robertson, A.H., Kroon, D., Raffi, I., Ellam, R.M., Necdet, M., 2013. Stratigraphy of Cretaceous to Lower Pliocene sediments in the northern part of Cyprus based on comparative <sup>87</sup>Sr/<sup>86</sup>Sr isotopic, nannofossil and planktonic foraminiferal dating. *Geol. Mag.* 150, 333–359.
- McPhee, P.J., Van Hinsbergen, D.J., Maffione, M., Altner, D., 2018. Palinspastic Reconstruction Versus Cross-Section Balancing: How Complete Is the Central Taurides Fold-Thrust Belt (Turkey)? *Tectonics* 37, 4285–4310.
- McPhee, P.J., van Hinsbergen, D.J., 2019. Tectonic reconstruction of Cyprus reveals Late Miocene continental collision of Africa and Anatolia. *Gondwana Res.* 68, 158–173. <https://doi.org/10.1016/j.gr.2018.10.015>.
- Meinhold, G., Reischmann, T., Kostopoulos, D., Lehnert, O., Matukov, D., Sergeev, S., 2008. Provenance of sediments during subduction of Palaeotethys: Detrital zircon ages and olivolith analysis in Palaeozoic sediments from Chios Island, Greece. *Palaeogeog. Palaeoclimatol. Palaeoecol.* 263, 71–91.
- Monod, O., 1977. Recherches géologiques dans le Taurus occidental au Sud de Beyşehir (Turquie) (Thèse) [Geological investigations in the western Taurus at South of Beyşehir (Turkey)]. Université de Paris-Sud Orsay. Ph.D. thesis.
- Moore, T.A., 1960. The geology and mineral resources of the Astromeritis-Kormakiti area. *Geol. Surv. Depart., Mem. Nicosia, Cyprus*, p. 6.
- MTA, 2011. Geological Map of Turkey, 1:500,000, Maden Tektik ve Arama Genel Müdürlüğü (General Directorate of Mineral Research and Exploration), Ankara.
- Necdet, M., Anil, M., 2006. The geology and geochemistry of the gypsum deposits in Northern Cyprus. *Geosound (yerbilimleri)* 48–49, 11–49.
- Oberhänsli, R., Candan, O., Bousquet, R., Rimmele, G., Okay, A., Goff, J., 2010. Alpine high pressure evolution of the eastern Bitlis complex, SE Turkey. In: Sosson, M., Kaymakci, N., Stephenson, R.A., Bergerat, F., Starostenko, V. (Eds.), *Sedimentary Basin Tectonics from the Black Sea and Caucasus to the Arabian Platform*. Geol. Soc. London Spec. Publ. 340, 461–483.
- Oberhänsli, R., Koralay, E., Candan, O., Pourteau, A., Bousquet, R., 2013. Late Cretaceous eclogitic high-pressure relics in the Bitlis Massif. *Geodin. Acta* 26, 175–190.
- Okay, A.I., Özgül, N., 1984. HP/LT metamorphism and the structure of the Alanya Massif, Southern Turkey: an allochthonous composite tectonic sheet. In: Dixon, J.E., Robertson, A.H.F. (Eds.), *The Geological Evolution of the Eastern Mediterranean*. Geol. Soc. London, Spec. Publ. 17, 429–439.
- Okay, A.I., Tüysüz, O., 1999. Tethyan sutures of northern Turkey. In: Durand, B., Jolivet, Horváth, F., Séranne, M. (Eds.), *The Mediterranean basins: Tertiary extension within the Alpine orogen. The Geological Evolution of the Eastern Mediterranean*. Geol. Soc. London Spec. Publ. 156, 475–515.
- Okay, A.I., Kylander-Clark, A.R., 2023. No sediment transport across the Tethys ocean during the latest Cretaceous: detrital zircon record from the Pontides and the Anatolide-Tauride Block. *Int. J. Earth Sciences* 112, 999–1022.
- Özgül, N., 1976. Toroslann Bazı Temel Özellikleri. *TJK Bull.* 19, 5–78.
- Özgül, N., 1984a. Stratigraphy and tectonic evolution of the central Taurides. In: Tekeli, O., Gönçüođlu, M.C. (Eds.), *Proc. Internat. Symp. Geology of the Taurus Belt*, MTA, Ankara, pp. 77–90.
- Özgül, N., 1984b. Alanya Tektonik Penceresi ve Batı Kesiminin Jeolojisi (Alanya tectonic window and geology of its western part). *Ketin Symposium*, 1984. TJK Bull., Ankara, 97–120.
- Özgül, N., 1997. Stratigraphy of the tectonostratigraphical units around Hadım-Bozkır-Taşkent region, northern part of the Central Taurides. *MTA Bull.* 119, 113–174.
- Öztürk, E.M., Akdeniz, N., Bedi, Y., Sönmez, İ., Usta, D., Kuru, K., Erbay, G., 1995. Alanya Napının stratigrafisine farklı bir yaklaşım (A different approach to the stratigraphy of the Alanya nappe). *TJK Bull.* 10, 2–10.
- Palamakumbura, R.N., Robertson, A.H.F., 2016. Pleistocene terrace deposition related to tectonically controlled surface uplift: An example of the Kyrenia Range lineament in the northern part of Cyprus. *Sediment. Geol.* 339, 46–67.
- Palamakumbura, R.N., Robertson, A.H.F., 2018. Pliocene-Pleistocene sedimentary-tectonic development of the Mesaoria (Mesarya) Basin in an incipient, diachronous collisional setting: facies evidence from the north of Cyprus. *Geol. Mag.* 55, 997–1022.
- Palamakumbura, R.N., Robertson, A.H., Kinnaird, T.C., van Calsteren, P., Kroon, D., Tait, J.A., 2016. Quantitative dating of Pleistocene deposits of the Kyrenia Range, northern Cyprus: implications for timing, rates of uplift and driving mechanisms. *J. Geol. Soc. London Spec. Publ.* 173, 933–948.
- Parlak, O., 2016. The Tauride ophiolites of Anatolia (Turkey): A review. *J. Earth Sci.* 27, 901–934.
- Parlak, O., Delaloye, M., Bingöl, E., 1995. Origin of subophiolitic metamorphic rocks beneath the Mersin ophiolite, southern Turkey. *Ofoliti* 20, 97–110.
- Parlak, O., Delaloye, M., Bingöl, E., 1996. Mineral chemistry of ultramafic and mafic cumulates as an indicator of the arc-related origin of the Mersin ophiolite (southern Turkey). *Geol. Rundsch.* 85, 647–661.
- Parlak, O., Robertson, A.H.F., 2004. The ophiolite-related Mersin Melange, southern Turkey: its role in the tectonic-sedimentary setting of Tethys in the Eastern Mediterranean region. *Geol. Mag.* 141, 257–286.
- Parlak, O., Dunkl, I., Karaođlan, F., Kusky, T.M., Zhang, C., Wang, L., Koepke, J., Billor, Z., Hames, W.E., Şimşek, E., Şimşek, G., Şimşek, T., Öztürk, S.E., 2019. Rapid cooling history of a Neotethyan ophiolite: Evidence for contemporaneous subduction initiation and metamorphic sole formation. *Geol. Soc. Am. Bull.* 131, 2011–2038.
- Patton, T.L., O'Connor, S.J., 1988. Cretaceous flexural history of northern Oman mountain foredeep, United Arab Emirates. *Bull. Am. Ass. Petrol. Geol.* 72, 797–809.
- Pearce, J.A., 1975. Basalt geochemistry used to investigate past tectonic environments on Cyprus. *Tectonophysics* 25, 41–67.
- Pearce, J.A., 2008. Geochemical fingerprinting of oceanic basalts with applications to ophiolite classification and the search for Archean oceanic crust. *Lithos* 100, 14–48.
- Pearce, J.A., Cann, J.R., 1973. Tectonic setting of basaltic volcanic rocks determined using trace element analysis. *Earth Planet. Sci. Lett.* 19, 290–300.
- Pearce, J.A., Lippard, S.J., Roberts, S., 1984. Characteristics and tectonic significance of supra-subduction zone ophiolites. In: Kokelaar, B. P., Howells, M. F. (Eds.), *Marginal Basin Geology*. Geol. Soc., London Spec. Publ. 16, 77–94.
- Pearce, J.A., Norry, M.J., 1979. Petrogenetic implications of Ti, Zr, Y, and Nb variations in volcanic rocks. *Contrib. Mineral. Petrol.* 69, 33–47.
- Pearce, J.A., Robinson, P.T., 2010. The Troodos ophiolitic complex probably formed in a subduction initiation, slab edge setting. *Gondwana Res.* 18, 60–81.
- Pearce, J.A., 1996. A user's guide to basalt discrimination diagrams. In: Wyman, D.A. (Ed.), *Trace Element Geochemistry of Volcanic Rocks: Applications for Massive Sulphide Exploration*. Geological Association of Canada, Short Course Notes 12, 79–113.
- Poisson, A., 1977. Recherches Géologiques dans les Taurides Occidentales, Turquie. University of Paris-Sud, Orsay, France. Ph.D. thesis.
- Pourteau, A., Candan, O., Oberhänsli, R., 2010. High-pressure meta-sediments in central Turkey: Constraints on the Neotethyan closure history. *Tectonics* 29 (5). <https://doi.org/10.1029/2009TC002650>.

- Reagan, M.K., Pearce, J.A., Shervais, J., Christeson, G.L., 2023. Subduction initiation as recorded in the Izu-Bonin-Mariana forearc. *Earth Sci. Rev.* p. 104573.
- Regard, V., Faccenna, C., Martinod, J., Bellier, O., Thomas, J.C., 2003. From subduction to collision: Control of deep processes on the evolution of convergent plate boundary. *J. Geophys. Res.: Solid. Earth* 108 (B4), 16. <https://doi.org/10.1029/2002JB001943>.
- Ricou, L.E., Dercourt, J., Geysant, J., Grandjacquet, C., Lepvrier, C., Biju-Duval, B., 1986. Geological constraints on the Alpine evolution of the Mediterranean Tethys. *Tectonophysics* 123, 83–122.
- Robertson, A.H.F., 1987. The transition from a passive margin to an Upper Cretaceous foreland basin related to ophiolite emplacement in the Oman Mountains. *Geol. Soc. Am. Bull.* 99, 633–653.
- Robertson, A.H.F., 1998. Lithofacies evidence for the Cretaceous-Paleogene sedimentary history of Eratosthenes Seamount, Eastern Mediterranean, in its regional tectonic context (sites 966 and 967). *Proc. ODP, Scientific Results* 160, 403–417.
- Robertson, A.H.F., 1998. Tectonic significance of the Eratosthenes Seamount: a continental fragment in the process of collision with a subduction zone in the eastern Mediterranean (Ocean Drilling Program Leg 160). *Tectonophysics* 298, 63–82.
- Robertson, A.H.F., 2002. Overview of the genesis and emplacement of Mesozoic ophiolites in the Eastern Mediterranean Tethyan region. *Lithos* 65, 1–67.
- Robertson, A.H.F., Dixon, J.E., 1984. Introduction: aspects of the geological evolution of the Eastern Mediterranean. In: Dixon, J.E. and Robertson, A.H.F. (Eds.), *Geol. Soc., London Spec. Publ.* 17, 1–74.
- Robertson, A.H.F., Woodcock, N.H., 1984. The SW segment of the Antalya Complex, Turkey as a Mesozoic-Tertiary Tethyan continental margin. In: Robertson, A.H.F. and Dixon, J.E. (Eds.), *Geol. Soc., London Spec. Publ.* 17, 251–271.
- Robertson, A.H.F., Clift, P.D., Degnan, P.J., Jones, G., 1991a. Palaeogeographic and paleotectonic evolution of the Eastern Mediterranean Neotethys. *Palaeogeog. Palaeoclimatol. Palaeoecol.* 87, 289–343.
- Robertson, A.H.F., Eaton, S., Follows, E.J., McCallum, J.E., 1991b. The role of local tectonics versus global sea-level change in the Neogene evolution of the Cyprus active margin. In: David, I., Macdonald, M. (Eds.), *Sedimentation, Tectonics and Eustasy: Sea-Level Changes at Active Margins*. Wiley, pp. 331–369.
- Robertson, A.H.F., Parlak, O., Ustaömer, T., 2009. Melange genesis and ophiolite emplacement related to subduction of the northern margin of the Tauride-Anatolide continent, central and western Turkey. In: van Hinsbergen, D.J.J., Edwards, M.A., Govers, R. (Eds.), *Collision and Collapse at the Africa–Arabia–Eurasia Subduction Zone*. *Geol. Soc., London Spec. Publ.* 311, 9–66.
- Robertson, A.H.F., Kidd, R., Ivanov, M., Limonov, A., Woodside, J., Galindo-Zaldívar, J., Nieto, L., 1995. Eratosthenes Seamount: collisional processes in the easternmost Mediterranean in relation to the Plio-Quaternary uplift of southern Cyprus. *Terra Nova* 7, 254–264.
- Robertson, A.H.F., Boulton, S.J., Taslı, K., Yıldırım, N., İnan, N., Yıldız, A., Parlak, O., 2016a. Late Cretaceous-Miocene sedimentary development of the Arabian continental margin in SE Turkey (Adıyaman region): Implications for regional palaeogeography and the closure history of Southern Neotethys. *J. Asian Earth Sci.* 115, 571–616.
- Robertson, A.H.F., Kinnaird, T.C., 2016. Structural development of the central Kyrenia Range (north Cyprus) in its regional setting in the eastern Mediterranean region. *Int. J. Earth Sci.* 105, 417–437.
- Robertson, A.H.F., Parlak, O., Yıldırım, N., Dumitrica, P., Taslı, K., 2016b. Late Triassic rifting and Jurassic-Cretaceous passive margin development of the Southern Neotethys: evidence from the Adıyaman area. *SE Turkey. Int. J. Earth Sci.* 105, 167–201.
- Robertson, A.H.F., Parlak, O., 2020. Late Cretaceous-Palaeocene subduction-collision-exhumation of a microcontinent along the northern, active margin of the Southern Neotethys: Evidence from the Alanya Massif and the adjacent Antalya Complex (S Turkey). *J. Asian Earth Sci.* 201, 104467.
- Robertson, A.H., Parlak, O., Kinnaird, T.C., Taslı, K., Dumitrica, P., 2020. Cambrian-Eocene pre-rift, pulsed rift, passive margin and emplacement processes along the northern margin of the Southern Neotethys: evidence from the Antalya Complex in the Alanya Window (S Turkey). *J. Asian Earth Sci.* X 3, 100026.
- Robertson, A.H.F., Waldron, J.W.F., 1990. Geochemistry and tectonic setting of Late Triassic and Late Jurassic-Early Cretaceous basaltic extrusives from the Antalya Complex, SW Turkey. In: Savasçın, M.Y., Eronat, A.H. (Eds.), *Proc. Internat. Earth Sci. Congr.* 2, on Aegean Regions, Izmir, Turkey, pp. 279–299.
- Robertson, A.H.F., Necdet, M., Raffi, I., Chen, G., 2019. Early Mesinian manganese deposition in NE Cyprus related to cyclical redox changes in a silled hemipelagic basin prior to the Mediterranean salinity Crisis. *Sediment. Geol.* 385, 126–148.
- Robertson, A.H.F., Parlak, O., Ustaömer, T., 2021. Late Palaeozoic extensional volcanism along the northern margin of Gondwana in southern Turkey: implications for Palaeotethyan development. *Int. J. Earth Sci.* 110, 1961–1994.
- Robertson, A.H.F., Parlak, O., Dumitrica, P., 2022. Role of Late Cretaceous volcanic-sedimentary melanges, specifically the Aladağ melange, E Turkey, in the rift-drift-subduction-accretion-emplacement history of the Tethyan Inner Tauride ocean. *Int. Geol. Rev.* 64, 1139–1190.
- Robertson, A.H.F., Parlak, O., Taslı, K., Solak, C., Dumitrica, P., Danelian, T., 2024. Lower Palaeozoic-Paleogene geological development of a deep-water rift (Güzelsu Corridor) along the northern continental margin of the Southern Neotethys in the Eastern Mediterranean region: Evidence from the Antalya Complex and the adjacent Tauride Carbonate Platform. *Earth-Sci. Rev.* p. 104741.
- Robertson, A.H.F., Woodcock, N.H., 1979. Mamonía Complex, southwest Cyprus: Evolution and emplacement of a Mesozoic continental margin. *Geol. Soc. Amer. Bull.* 90, 651–665.
- Robertson, A.H.F., Woodcock, N.H., 1986. The role of the Kyrenia Range Lineament, Cyprus, in the geological evolution of the eastern Mediterranean area. *London Ser. A, Mathematical and Physical Sci.* 317 (1539), 141–177. *Phil. Trans. R. Soc.*
- Robertson, A.H.F., Ünüğenç, U.C., İnan, N., Taslı, K., 2004. The Misis-Andirin Complex: a Mid-Tertiary melange related to late-stage subduction of the Southern Neotethys in S Turkey. *J. Asian Earth Sci.* 22, 413–453.
- Robertson, A.H.F., Parlak, O., Ustaömer, T., 2012a. Overview of the Palaeozoic-Neogene evolution of Neotethys in the Eastern Mediterranean region (Southern Turkey, Cyprus, Syria). *Petrol. Geosci.* 18, 381–404.
- Robertson, A.H.F., Taslı, K., İnan, N., 2012b. Evidence from the Kyrenia Range, Cyprus, of the northerly active margin of the Southern Neotethys during Late Cretaceous-Early Cenozoic time. *Geol. Mag.* 149, 264–290.
- Robertson, A.H.F., McCay, G.A., Taslı, K., Yıldız, A., 2014. Eocene development of the northerly active continental margin of the Southern Neotethys in the Kyrenia Range, north Cyprus. *Geol. Mag.* 151, 692–731.
- Saccani, E., Photiades, A., 2004. Mid-ocean ridge and supra-subduction affinities in the Pindos Massif ophiolites (Greece): implications for magma genesis in a protoforearc setting. *Lithos* 73, 229–253.
- Saccani, E., Photiades, A., 2005. Petrogenesis and tectonomagmatic significance of volcanic and subvolcanic rocks in the Albanide-Hellenide ophiolitic mélanges. *Isl. Arc* 14, 494–516.
- Şahin, N., Altner, D., 2019. Testing of Permian-Lower Triassic stratigraphic data in a half-graben/tilt block system: evidence for the initial rifting phase in Antalya Nappes. *Can. J. Earth Sci.* 56, 1262–1283.
- Saka, S., Uysal, İ., Kapsiotis, A., Bağcı, U., Ersoy, E.Y., Su, B.-X., Seitz, H.M., Hegner, E., 2019. Petrological characteristics and geochemical compositions of the Neotethyan Mersin ophiolite (southern Turkey): Processes of melt depletion, refertilization, chromitite formation and oceanic crust generation. *J. Asian Earth Sci.* 176, 281–299.
- Schietecatte, J.P., 1971. Geology of the Misis Mountains. In: Campbell, M. (Ed.), *Geology and History of Turkey*. *Petrol. Explor. Soc. Tripoli*, pp. 305–312.
- Schildgen, T.F., Cosentino, D., Bookhagen, B., Niedermann, S., Yıldırım, C., Echter, H., Wittmann, H., Strecker, M.R., 2012. Multi-phased uplift of the southern margin of the Central Anatolian plateau, Turkey: A record of tectonic and upper mantle processes. *Earth Planet. Sci. Lett.* 317, 85–95.
- Şengör, A.M.C., Yılmaz, Y., 1981. Tethyan evolution of Turkey: a plate tectonic approach. *Tectonophysics* 75, 81–241.
- Shaanan, U., Avigad, D., Morag, N., Güngör, T., Gerdes, A., 2021. Drainage response to Arabia-Eurasia collision: Insights from provenance examination of the Cyprian Kythrea flysch (Eastern Mediterranean Basin). *Basin Res.* 33, 26–47. <https://doi.org/10.1111/bre.12452>.
- Shervais, J.W., 1982. Ti-V plots and the petrogenesis of modern ophiolitic lavas. *Earth Planet. Sci. Lett.* 59, 101–118.
- Shervais, J.W., Reagan, M.K., Godard, M., Prytulak, J., Ryan, J.G., Pearce, J.A., Almeev, R.R., Li, H., Haugen, E., Chapman, T., Kurz, W., 2021. Magmatic response to subduction initiation, Part II: boninites and related rocks of the Izu-Bonin Arc from IODP Expedition 352. *Geochem. Geophys. Geosyst.* 22 (1), p. e2020GC009093.
- Şimşek, E., Parlak, O., Robertson, A.H., 2023. Ion-probe (SIMS) U-Pb geochronology and geochemistry of the Upper Cretaceous Kızıldağ (Hatay) ophiolite: Implications for supra-subduction zone spreading in the Southern Neotethys. *Geosystems and Geoenvironment* 2 (3), 100165.
- Stampfli, G.M., Borel, G., 2002. A plate tectonic model for the Paleozoic and Mesozoic constrained by dynamic plate boundaries and restored synthetic oceanic isochrons. *Earth Planet. Sci. Lett.* 196, 17–33.
- Stern, R.J., Ali, K., 2020. Crustal evolution of the Egyptian Precambrian rocks. In: Hamimi, Z., El-Barkooky, A., Frías, J.M., Fritz, H., Abd El-Rahman, Y. (Eds.), *The Geology of Egypt*. Springer, Reg. Geol. Rev. pp. 131–151.
- Sun, S.-S., McDonough, W.F., 1989. Chemical and isotopic systematics of oceanic basalts: implications for mantle composition and processes. In: Saunders, A.D., Norry, M.J. (Eds.), *Magmatism in the Ocean Basins*. *Geol. Soc. London Spec. Publ.* 42, 313–345.
- Torley, J.M., Robertson, A.H.F., 2018. New evidence and interpretation of facies, provenance and geochemistry of late Triassic-early Cretaceous Tethyan deep-water passive margin-related sedimentary rocks (Ayios Photios Group), SW Cyprus in the context of eastern Mediterranean geodynamics. *Sediment. Geol.* 377, 82–110.
- Ustaömer, T., Ustaömer, P.A., Robertson, A.H.F., Gerdes, A., 2020. U-Pb-Hf isotopic data from detrital zircons in late Carboniferous and Mid-Late Triassic sandstones, and also Carboniferous granites from the Tauride and Anatolide continental units in S Turkey: implications for Tethyan palaeogeography. *Int. Geol. Rev.* 115, 1159–1186.
- Varol, B., Atalar, C., 2017. Messinian evaporites in the Mesaoria Basin, North Cyprus: facies and environmental interpretations. *Carbonate Evaporite* 32, 349–365.
- Varol, E., Tekin, U.K., Temel, A., 2007. Dating and geochemical properties of Middle to Late Carnian basalts from the Alakırçay Nappe of the Antalya Nappes, SW Turkey: implications for the evolution of southern branch of Neotethys. *Ophioliti* 32, 163–176.
- Vine, F.J., Poster, C.K., Gass, I.G., 1973. Aeromagnetic Survey of the Troodos Igneous Massif, Cyprus. *Nature Phys. Sci.* 244 (133), 34–38.
- Weiler, Y., 1970. Mode of occurrence of pelites in the Kythrea flysch basin (Cyprus). *J. Sediment. Res.* 40, 1255–1261.

Woelki, D., Regelous, M., Haase, K.M., Romer, R.H., Beier, C., 2018. Petrogenesis of boninitic lavas from the Troodos Ophiolite, and comparison with Izu–Bonin–Mariana fore-arc crust. *Earth Planet. Sci. Lett.* 498, 203–214. <https://doi.org/10.1016/j.epsl.2018.06.041>.

Yılmaz, Y., 1993. New evidence and model on the evolution of the southeast Anatolian orogen. *Geol. Soc. Amer. Bull.* 105, 251–271.

Yılmaz, Y., 2019. Southeast Anatolian Orogenic Belt revisited (geology and evolution). *Can. J. Earth Sci.* 56, 1163–1180.

Yılmaz, Y., Gürer, Ö.F., 1995. The geology and evolution of the Misis–Andırın Belt, around Andırın (Kahramanmaraş). *Turk. J. Earth Sci.* 5, 39–55.